

Massive MIMO Networks: Spectral, Energy, and Hardware Efficiency

Other titles in Foundations and Trends® in Signal Processing

Deep Learning in Object Recognition, Detection, and Segmentation

Xiaogang Wang

ISBN: 978-1-68083-116-0

Structured Robust Covariance Estimation

Ami Wiesel and Teng Zhang

ISBN: 978-1-68083-094-1

A Primer on Reproducing Kernel Hilbert Spaces

Jonathan H. Manton and Pierre-Olivier Amblard

ISBN: 978-1-68083-092-7

Deep Learning: Methods and Applications

Li Deng and Dong Yu

ISBN: 978-1-60198-814-0

Interactive Sensing and Decision Making in Social Networks

Vikram Krishnamurthy, Omid Namvar Gharehshiran and

Maziyar Hamdi

ISBN: 978-1-60198-812-6

Massive MIMO Networks: Spectral, Energy, and Hardware Efficiency

Emil Björnson

Linköping University
emil.bjornson@liu.se

Jakob Hoydis

Bell Labs, Nokia
jakob.hoydis@nokia.com

Luca Sanguinetti

University of Pisa
luca.sanguinetti@unipi.it

now

the essence of knowledge

Boston — Delft

Foundations and Trends[®] in Signal Processing

Published, sold and distributed by:

now Publishers Inc.
PO Box 1024
Hanover, MA 02339
United States
Tel. +1-781-985-4510
www.nowpublishers.com
sales@nowpublishers.com

Outside North America:

now Publishers Inc.
PO Box 179
2600 AD Delft
The Netherlands
Tel. +31-6-51115274

The preferred citation for this publication is

E. Björnson, J. Hoydis and L. Sanguinetti. *Massive MIMO Networks: Spectral, Energy, and Hardware Efficiency*. Foundations and Trends[®] in Signal Processing, vol. 11, no. 3-4, pp. 154–655, 2017.

ISBN: 978-1-68083-365-2

© 2017 E. Björnson, J. Hoydis and L. Sanguinetti

All rights reserved. No part of this publication may be reproduced, stored in a retrieval system, or transmitted in any form or by any means, mechanical, photocopying, recording or otherwise, without prior written permission of the publishers.

Photocopying. In the USA: This journal is registered at the Copyright Clearance Center, Inc., 222 Rosewood Drive, Danvers, MA 01923. Authorization to photocopy items for internal or personal use, or the internal or personal use of specific clients, is granted by now Publishers Inc for users registered with the Copyright Clearance Center (CCC). The 'services' for users can be found on the internet at: www.copyright.com

For those organizations that have been granted a photocopy license, a separate system of payment has been arranged. Authorization does not extend to other kinds of copying, such as that for general distribution, for advertising or promotional purposes, for creating new collective works, or for resale. In the rest of the world: Permission to photocopy must be obtained from the copyright owner. Please apply to now Publishers Inc., PO Box 1024, Hanover, MA 02339, USA; Tel. +1 781 871 0245; www.nowpublishers.com; sales@nowpublishers.com

now Publishers Inc. has an exclusive license to publish this material worldwide. Permission to use this content must be obtained from the copyright license holder. Please apply to now Publishers, PO Box 179, 2600 AD Delft, The Netherlands, www.nowpublishers.com; e-mail: sales@nowpublishers.com

Foundations and Trends[®] in Signal Processing

Volume 11, Issue 3-4, 2017

Editorial Board

Editor-in-Chief

Yonina Eldar

Technion
Israel

Editors

Pao-Chi Chang
*National Central
University*

Pamela Cosman
*University of California,
San Diego*

Michelle Effros
*California Institute of
Technology*

Yariv Ephraim
George Mason University

Alfonso Farina
Selex ES

Sadaoki Furui
*Tokyo Institute of
Technology*

Georgios Giannakis
University of Minnesota

Vivek Goyal
Boston University

Sinan Gunturk
Courant Institute

Christine Guillemot
INRIA

Robert W. Heath, Jr.
*The University of Texas at
Austin*

Sheila Hemami
Northeastern University

Lina Karam
Arizona State University

Nick Kingsbury
University of Cambridge

Alex Kot
*Nanyang Technical
University*

Jelena Kovacevic
*Carnegie Mellon
University*

Geert Leus
TU Delft

Jia Li
*Pennsylvania State
University*

Henrique Malvar
Microsoft Research

B.S. Manjunath
*University of California,
Santa Barbara*

Urbashi Mitra
*University of Southern
California*

Björn Ottersten
KTH Stockholm

Vincent Poor
Princeton University

Anna Scaglione
*University of California,
Davis*

Mihaela van der Shaar
*University of California,
Los Angeles*

Nicholas D. Sidiropoulos
*Technical University of
Crete*

Michael Unser
EPFL

P.P. Vaidyanathan
*California Institute of
Technology*

Ami Wiesel
*The Hebrew University of
Jerusalem*

Min Wu
University of Maryland

Josiane Zerubia
INRIA

Editorial Scope

Topics

Foundations and Trends[®] in Signal Processing publishes survey and tutorial articles in the following topics:

- Adaptive signal processing
- Audio signal processing
- Biological and biomedical signal processing
- Complexity in signal processing
- Digital signal processing
- Distributed and network signal processing
- Image and video processing
- Linear and nonlinear filtering
- Multidimensional signal processing
- Multimodal signal processing
- Multirate signal processing
- Multiresolution signal processing
- Nonlinear signal processing
- Randomized algorithms in signal processing
- Sensor and multiple source signal processing, source separation
- Signal decompositions, subband and transform methods, sparse representations
- Signal processing for communications
- Signal processing for security and forensic analysis, biometric signal processing
- Signal quantization, sampling, analog-to-digital conversion, coding and compression
- Signal reconstruction, digital-to-analog conversion, enhancement, decoding and inverse problems
- Speech/audio/image/video compression
- Speech and spoken language processing
- Statistical/machine learning
- Statistical signal processing
 - Classification and detection
 - Estimation and regression
 - Tree-structured methods

Information for Librarians

Foundations and Trends[®] in Signal Processing, 2017, Volume 11, 4 issues. ISSN paper version 1932-8346. ISSN online version 1932-8354. Also available as a combined paper and online subscription.

Contents

1	Introduction and Motivation	5
1.1	Cellular Networks	7
1.2	Definition of Spectral Efficiency	14
1.3	Ways to Improve the Spectral Efficiency	20
1.4	Summary of Key Points in Section 1	61
2	Massive MIMO Networks	63
2.1	Definition of Massive MIMO	63
2.2	Correlated Rayleigh Fading	69
2.3	System Model for Uplink and Downlink	73
2.4	Basic Impact of Spatial Channel Correlation	75
2.5	Channel Hardening and Favorable Propagation	78
2.6	Local Scattering Spatial Correlation Model	82
2.7	Summary of Key Points in Section 2	90
3	Channel Estimation	91
3.1	Uplink Pilot Transmission	91
3.2	MMSE Channel Estimation	95
3.3	Impact of Spatial Correlation and Pilot Contamination	101
3.4	Computational Complexity and Low-Complexity Estimators	111
3.5	Data-Aided Channel Estimation and Pilot Decontamination	118

3.6	Summary of Key Points in Section 3	121
4	Spectral Efficiency	122
4.1	Uplink Spectral Efficiency and Receive Combining	122
4.2	Alternative UL SE Expressions and Key Properties	148
4.3	Downlink Spectral Efficiency and Transmit Precoding	162
4.4	Asymptotic Analysis	183
4.5	Summary of Key Points in Section 4	198
5	Energy Efficiency	200
5.1	Motivation	201
5.2	Transmit Power Consumption	204
5.3	Definition of Energy Efficiency	209
5.4	Circuit Power Consumption Model	222
5.5	Tradeoff Between Energy Efficiency and Throughput	237
5.6	Network Design for Maximal Energy Efficiency	242
5.7	Summary of Key Points in Section 5	248
6	Hardware Efficiency	250
6.1	Transceiver Hardware Impairments	251
6.2	Channel Estimation with Hardware Impairments	260
6.3	Spectral Efficiency with Hardware Impairments	266
6.4	Hardware-Quality Scaling Law	286
6.5	Summary of Key Points in Section 6	296
7	Practical Deployment Considerations	298
7.1	Power Allocation	299
7.2	Spatial Resource Allocation	315
7.3	Channel Modeling	329
7.4	Array Deployment	347
7.5	Millimeter Wavelength Communications	369
7.6	Heterogeneous Networks	374
7.7	Case Study	384
7.8	Summary of Key Points in Section 7	393
	Acknowledgements	395

Appendices	396
A Notation and Abbreviations	397
B Standard Results	405
B.1 Matrix Analysis	405
B.2 Random Vectors and Matrices	410
B.3 Properties of the Lambert W Function	414
B.4 Basic Estimation Theory	414
B.5 Basic Information Theory	419
B.6 Basic Optimization Theory	422
C Collection of Proofs	426
C.1 Proofs in Section 1	426
C.2 Proofs in Section 3	438
C.3 Proofs in Section 4	440
C.4 Proofs in Section 5	456
C.5 Proofs in Section 6	459
References	468

Massive MIMO Networks: Spectral, Energy, and Hardware Efficiency

Emil Björnson¹, Jakob Hoydis² and Luca Sanguinetti³

¹*Linköping University; emil.bjornson@liu.se*

²*Bell Labs, Nokia; jakob.hoydis@nokia.com*

³*University of Pisa; luca.sanguinetti@unipi.it*

ABSTRACT

Massive multiple-input multiple-output (MIMO) is one of the most promising technologies for the next generation of wireless communication networks because it has the potential to provide game-changing improvements in spectral efficiency (SE) and energy efficiency (EE). This monograph summarizes many years of research insights in a clear and self-contained way and provides the reader with the necessary knowledge and mathematical tools to carry out independent research in this area. Starting from a rigorous definition of Massive MIMO, the monograph covers the important aspects of channel estimation, SE, EE, hardware efficiency (HE), and various practical deployment considerations.

From the beginning, a very general, yet tractable, canonical system model with spatial channel correlation is introduced. This model is used to realistically assess the SE and EE, and is later extended to also include the impact of hardware impairments. Owing to this rigorous modeling approach, a lot of classic “wisdom” about Massive MIMO, based on too simplistic system models, is shown to be questionable.

The monograph contains many numerical examples, which can be reproduced using Matlab code that is available online at https://dx.doi.org/10.1561/20000000093_supp.

Preface

Why We Wrote this Monograph

Massive multiple-input multiple-output (MIMO) is currently a buzzword in the evolution of cellular networks, but there is a great divide between what different people read into it. Some say Massive MIMO was conceived by Thomas Marzetta in a seminal paper from 2010, but the terminology cannot be found in that paper. Some say it is a reincarnation of space-division multiple access (SDMA), but with more antennas than in the field-trials carried out in the 1990s. Some say that any radio technology with at least 64 antennas is Massive MIMO. In this monograph, we explain what Massive MIMO is to us and how the research conducted in the past decades lead to a scalable multiantenna technology that offers great throughput and energy efficiency under practical conditions. We decided to write this monograph to share the insights and know-how that each of us has obtained through ten years of multiuser MIMO research. Two key differences from previous books on this topic are the spatial channel correlation and the rigorous signal processing design considered herein, which uncover fundamental characteristics that are easily overlooked by using more tractable but less realistic models and processing schemes. In our effort to provide a coherent description of the topic, we cover many details that cannot be found in the research literature, but are important to connect the dots.

This monograph is substantially longer than the average monograph published in *Foundations and Trends*, but we did not choose the publisher based on the format but the quality and openness that it offers. We want to reach a broad audience by offering printed books as well as open access to an electronic version. We have made the simulation code available online, to encourage reproducibility and continued research. This monograph is targeted at graduate students, researchers, and professors who want to learn the conceptual and analytical foundations of Massive MIMO, in terms of spectral, energy, and/or hardware efficiency, as well as channel estimation and practical considerations. We also cover some related topics and recent trends, but purposely in less detail, to focus on the unchanging fundamentals and not on the things that current research is targeting. Basic linear algebra, probability theory, estimation theory, and information theory are sufficient to read this monograph. The appendices contain detailed proofs of the analytical results and, for completeness, the basic theory is also summarized.

Structure of the Monograph

Section 1 introduces the basic concepts that lay the foundation for the definition and design of Massive MIMO. Section 2 provides a rigorous definition of the Massive MIMO technology and introduces the system and channel models that are used in the remainder of the monograph. Section 3 describes the signal processing used for channel estimation on the basis of uplink (UL) pilots. Receive combining and transmit precoding are considered in Section 4 wherein expressions for the spectral efficiency (SE) achieved in the UL and downlink (DL) are derived and the key insights are described and exemplified. Section 5 shows that Massive MIMO also plays a key role when designing highly energy-efficient cellular networks. Section 6 analyzes how transceiver hardware impairments affect the SE and shows that Massive MIMO makes more efficient use of the hardware. This opens the door for using components with lower resolution (e.g., fewer quantization bits) to save energy and cost. Section 7 provides an overview of important practical aspects, such as spatial resource allocation, channel modeling, array deployment, and the role of Massive MIMO in heterogeneous networks.

How to Use this Monograph

Researchers who want to delve into the field of Massive MIMO (e.g., for the purpose of performing independent research) can basically read the monograph from cover to cover. However, we stress that Sections 5, 6, and 7 can be read in any order, based on personal preferences.

Each section ends with a summary of key points. A professor who is familiar with the broad field of MIMO can read these summaries to become acquainted with the content, and then decide what to read in detail.

A graduate-level course can cover Sections 1–4 in depth or partially. Selected parts of the remaining sections may also be included in the course, depending on the background and interest of the students. An extensive slide set and homework exercises are made available for teachers who would like to give a course based on this monograph.

The authors, October 2017

1

Introduction and Motivation

Wireless communication technology has fundamentally changed the way we communicate. The time when telephones, computers, and Internet connections were bound to be wired, and only used at predefined locations, has passed. These communications services are nowadays wirelessly accessible almost everywhere on Earth, thanks to the deployment of cellular wide area networks (e.g., based on the GSM¹, UMTS², and LTE³ standards), local area networks (based on different versions of the WiFi standard IEEE 802.11), and satellite services. Wireless connectivity has become an essential part of the society—as vital as electricity—and as such the technology itself spurs new applications and services. We have already witnessed the streaming media revolution, where music and video are delivered on demand over the Internet. The first steps towards a fully networked society with augmented reality applications, connected homes and cars, and machine-to-machine communications have also been taken. Looking 15 years into the future, we will find new innovative wireless services that we cannot predict today.

¹Global System for Mobile Communications (GSM).

²Universal Mobile Telecommunications System (UMTS).

³Long Term Evolution (LTE).

The amount of wireless voice and data communications has grown at an exponential pace for many decades. This trend is referred to as *Cooper's law* because the wireless researcher Martin Cooper [91] noticed in the 1990s that the number of voice and data connections has doubled every two-and-a-half years, since Guglielmo Marconi's first wireless transmissions in 1895. This corresponds to a 32% annual growth rate. Looking ahead, the Ericsson Mobility Report forecasts a compound annual growth rate of 42% in mobile data traffic from 2016 to 2022 [109], which is even faster than Cooper's law. The demand for wireless data connectivity will definitely continue to increase in the foreseeable future; for example, since the video fidelity is constantly growing, since new must-have services are likely to arise, and because we are moving into a networked society, where all electronic devices connect to the Internet. An important question is how to evolve the current wireless communications technologies to meet the continuously increasing demand, and thereby avoid an imminent data traffic crunch. An equally important question is how to satisfy the rising expectations of service quality. Customers will expect the wireless services to work equally well anywhere and at any time, just as they expect the electricity grid to be robust and constantly available. To keep up with an exponential traffic growth rate and simultaneously provide ubiquitous connectivity, industrial and academic researchers need to turn every stone to design new revolutionary wireless network technologies. This monograph explains what the Massive multiple-input multiple-output (MIMO) technology is and why it is a promising solution to handle several orders-of-magnitude⁴ more wireless data traffic than today's technologies.

The cellular concept for wireless communication networks is defined in Section 1.1, which also discusses how to evolve current network technology to accommodate more traffic. Section 1.2 defines the spectral efficiency (SE) notion and provides basic information-theoretic results that will serve as a foundation for later analysis. Different ways to improve the SE are compared in Section 1.3, which motivates the design of Massive MIMO. The key points are summarized in Section 1.4.

⁴In communications, a factor ten is called one order-of-magnitude, while a factor 100 stands for two orders-of-magnitude and so on.

1.1 Cellular Networks

Wireless communication is based on radio, meaning that electromagnetic (EM) waves are designed to carry information from a transmitter to one or multiple receivers. Since the EM waves propagate in all possible directions from the transmitter, the signal energy spreads out and less energy reaches a desired receiver as the distance increases. To deliver wireless services with sufficiently high received signal energy over wide coverage areas, researchers at Bell Labs postulated in 1947 that a cellular network topology is needed [277]. According to this idea, the coverage area is divided into cells that operate individually using a fixed-location base station; that is, a piece of network equipment that facilitates wireless communication between a device and the network. The cellular concept was further developed and analyzed over the subsequent decades [291, 116, 204, 364] and later deployed in practice. Without any doubt, the cellular concept was a major breakthrough and has been the main driver to deliver wireless services in the last forty years (since the “first generation” of mobile phone systems emerged in the 1980s). In this monograph, a cellular network is defined as follows.

Definition 1.1 (Cellular network). A cellular network consists of a set of base stations (BSs) and a set of user equipments (UEs).⁵ Each UE is connected to one of the BSs, which provides service to it. The downlink (DL) refers to signals sent from the BSs to their respective UEs, while the uplink (UL) refers to transmissions from the UEs to their respective BSs.⁶

While this definition specifies the setup that we will study, it does not cover every aspect of cellular networks; for example, to enable efficient handover between cells, a UE can momentarily be connected to multiple BSs.

⁵The terms BS and UE stem from GSM and LTE standards, respectively, but are used in this monograph without any reference to particular standards.

⁶In a fully cooperative cellular network, called network MIMO [126] or cell-free system [240], all BSs are connected to a central processing site and are used to jointly serve all UEs in the network. In this case, the DL (UL) refers to signals transmitted from (to) all the BSs to (from) each UE. Such a cellular network is not the focus of this monograph, but cell-free systems are briefly described in Section 7.4.3 on p. 356.

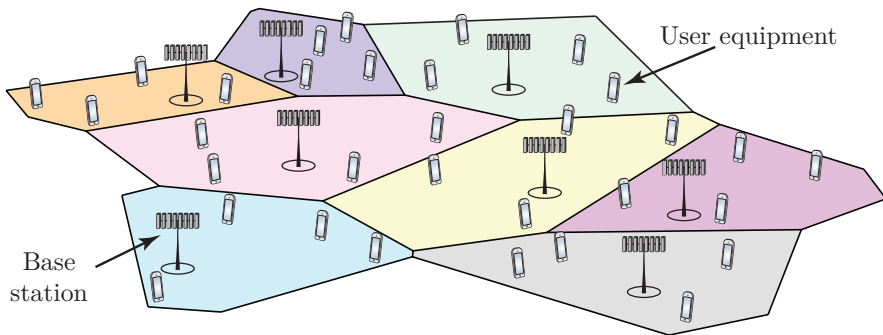


Figure 1.1: A basic cellular network, where each BS covers a distinct geographical area and provides service to all UEs in it. The area is called a “cell” and is illustrated with a distinct color. The cell may consist of all geographic locations where this BS provides the strongest DL signal.

An illustration of a cellular network is provided in Figure 1.1. This monograph focuses on the wireless communication links between BSs and UEs, while the remaining network infrastructure (e.g., fronthaul, backhaul, and core network) is assumed to function perfectly. There are several branches of wireless technologies that are currently in use, such as the IEEE 802.11 family for WiFi wireless local area networks (WLANs), the 3rd Generation Partnership Project (3GPP) family with GSM/UMTS/LTE for mobile communications [128], and the competing 3GPP2 family with IS-95/CDMA2000/EV-DO. Some standards within these families are evolutions of each other, optimized for the same use case, while others are designed for different use cases. Together they form a *heterogeneous network* consisting of two main tiers:

1. Coverage tier: Consisting of outdoor cellular BSs that provide wide-area coverage, mobility support, and are shared between many UEs;
2. Hotspot tier: Consisting of (mainly) indoor BSs that offer high throughput in small local areas to a few UEs.

The term “heterogeneous” implies that these two tiers coexist in the same area. In particular, the hotspot BSs are deployed to create *small cells (SCs)* within the coverage area of the cellular BSs, as illustrated in

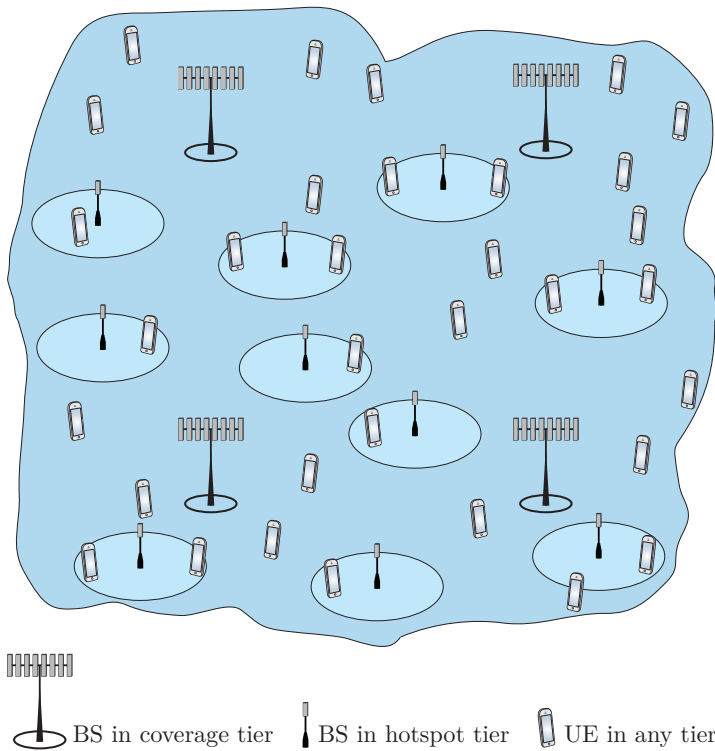


Figure 1.2: Current wireless networks are heterogeneous since a tier of SCs is deployed to offload traffic from the coverage tier. BSs in the coverage tier and in the hotspot tier are depicted differently, as shown in the figure. To improve the area throughput of the coverage tier, it is particularly important to increase the SE, because densification and the use of additional bandwidth at higher frequencies would degrade mobility support and coverage.

Figure 1.2. The two tiers may utilize the same frequency spectrum, but, in practice, it is common to use different spectrum to avoid inter-tier coordination; for example, the coverage tier might use LTE and operate in the 2.1 GHz band, while the hotspot tier might use WiFi in the 5 GHz band.

Cellular networks were originally designed for wireless voice communications, but it is wireless data transmissions that dominate nowadays [109]. Video on-demand accounts for the majority of traffic in wireless networks and is also the main driver of the predicted increase in traffic

demand [86]. The *area throughput* is thus a highly relevant performance metric of contemporary and future cellular networks. It is measured in bit/s/km² and can be modeled using the following high-level formula:

$$\text{Area throughput [bit/s/km}^2\text{]} = B \text{ [Hz]} \cdot D \text{ [cells/km}^2\text{]} \cdot \text{SE [bit/s/Hz/cell]} \quad (1.1)$$

where B is the bandwidth, D is the average cell density, and SE is the SE per cell. The SE is the amount of information that can be transferred per second over one Hz of bandwidth, and it is later defined in detail in Section 1.2.

These are the three main components that determine the area throughput, and that need to be increased in order to achieve higher area throughput in future cellular networks. This principle applies to the coverage tier as well as to the hotspot tier. Based on (1.1), one can think of the area throughput as being the volume of a rectangular box with sides B , D , and SE; see Figure 1.3. There is an inherent dependence between these three components in the sense that the choice of frequency band and cell density affects the propagation conditions; for example, the probability of having a line-of-sight (LoS) channel between the transmitter and receiver (and between out-of-cell interferers and the receiver), the average propagation losses, etc. However, one can treat these three components as independent as a first-order approximation to gain basic insights. Consequently, there are three main ways to improve the area throughput of cellular networks:

1. Allocate more bandwidth;
2. Densify the network by deploying more BSs;
3. Improve the SE per cell.

The main goal of this section is to demonstrate how we can achieve major improvements in SE. These insights are then utilized in Section 2 on p. 63 to define the Massive MIMO technology.

1.1.1 Evolving Cellular Networks for Higher Area Throughput

Suppose, for the matter of argument, that we want to design a new cellular network that improves the area throughput by a factor of 1000

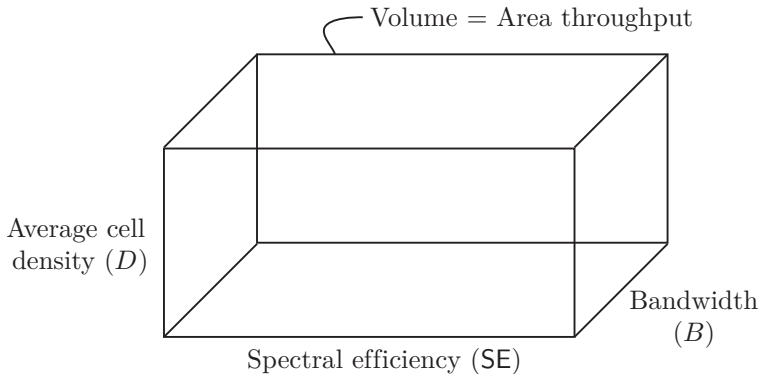


Figure 1.3: The area throughput can be computed according to (1.1) as the volume of a rectangular box where the bandwidth, average cell density, and SE are the length of each side.

over existing networks; that is, to solve “the $1000\times$ data challenge” posed by Qualcomm [271]. Note that such a network can handle the three orders-of-magnitude increase in wireless data traffic that will occur over the next 15–20 years, if the annual traffic growth rate continues to be in the range of 41%–59%. How can we handle such a huge traffic growth according to the formula in (1.1)?

One potential solution would be to increase the bandwidth B by $1000\times$. Current cellular networks utilize collectively more than 1 GHz of bandwidth in the frequency range below 6 GHz. For example, the telecom operators in Sweden have licenses for more than 1 GHz of spectrum [65], while the corresponding number in USA is around 650 MHz [30]. An additional 500 MHz of spectrum is available for WiFi [65]. This means that a $1000\times$ increase corresponds to using more than 1 THz of bandwidth in the future. This is physically impractical since the frequency spectrum is a global resource that is shared among many different services, and also because it entails using much higher frequency bands than in the past, which physically limits the range and service reliability. There are, however, substantial bandwidths in the millimeter wavelength (mmWave) bands (e.g., in the range 30–300 GHz) that can be used for short-range applications. These mmWave bands are attractive in the hotspot tier, but less so in the coverage tier since the signals at

those frequencies are easily blocked by objects and human bodies and thus cannot provide robust coverage.

Another potential solution would be to densify the cellular network by deploying $1000\times$ more BSs per km^2 . The inter-BS distances in the coverage tier are currently a few hundred meters in urban areas and the BSs are deployed at elevated locations to avoid being shadowed by large objects and buildings. This limits the number of locations where BSs can be deployed in the coverage tier. It is hard to densify without moving BSs closer to UEs, which leads to increased risks of being in deep shadow, thereby reducing coverage. Deploying additional hotspots is a more viable solution. Although WiFi is available almost everywhere in urban areas, the average inter-BS distance in the hotspot tier can certainly shrink down to tens of meters in the future. Reusing the spectrum from the coverage tier or using mmWave bands in these SCs can also bring substantial improvements to the area throughput [197]. Nevertheless, this solution is associated with high deployment costs, inter-cell interference issues [19], and is not suitable for mobile UEs, which would have to switch BS very often. Note that even under a substantial densification of the hotspot tier, the coverage tier is still required to support mobility and avoid coverage holes.

Higher cell density and larger bandwidth have historically dominated the evolution of the coverage tier, which explains why we are approaching a saturation point where further improvements are increasingly complicated and expensive. However, it might be possible to dramatically improve the SE of future cellular networks. This is particularly important for BSs in the coverage tier that, as explained above, can neither use mmWave bands nor rely on network densification. Increasing the SE corresponds to using the BSs and bandwidth that are already in place more efficiently by virtue of new modulation and multiplexing techniques. The principal goal is to select a rectangular box, as illustrated in Figure 1.4, where each side represents the multiplicative improvement in either B , D , or SE. As shown in the figure, there are different ways to choose these factors in order to achieve $1000\times$ higher area throughput. A pragmatic approach is to first investigate how much the SE can be improved towards the $1000\times$ goal and then jointly

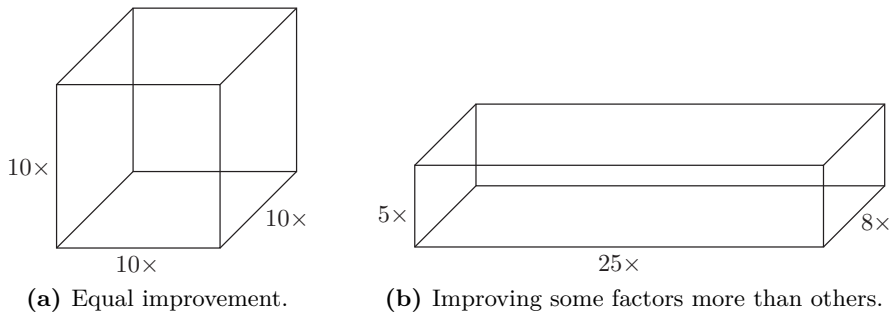


Figure 1.4: Examples of different ways to achieve a $1000\times$ improvement in area throughput. Each side of the rectangular box represents an improvement factor in either B , D , or SE in (1.1), and their multiplication (i.e., the volume) equals $1000\times$.

increase B and D to take care of the remaining part of the ambitious final goal. Section 4 on p. 122 shows why Massive MIMO is considered the most promising technology for improving the SE in future cellular networks.

Remark 1.1 (Massive MIMO versus SCs in mmWave bands). This monograph focuses on the coverage tier, which will remain the most challenging tier in the future since it should provide ubiquitous coverage, support mobility, and simultaneously deliver a uniform service quality within each cell. All of this must be achieved without any substantial densification or use of mmWave spectrum because that would inevitably result in patchy coverage. This is why major improvements in SE are needed. We will demonstrate that Massive MIMO can deliver that. In contrast, the main purpose of the hotspot tier is to reduce the pressure on the coverage tier by offloading a large portion of the traffic from low-mobility UEs. Since only short-range best-effort communications must be supported, this tier can be enhanced by straightforward cell densification and by using the large bandwidths available in mmWave bands. The use of Massive MIMO in mmWave bands will be discussed in Section 7.5 on p. 369, while the combination of Massive MIMO and SCs is considered in Section 7.6 on p. 374.

1.2 Definition of Spectral Efficiency

We now provide a definition of SE for a communication channel with a bandwidth of B Hz. The Nyquist-Shannon sampling theorem implies that the band-limited communication signal that is sent over this channel is completely determined by $2B$ real-valued equal-spaced samples per second [298]. When considering the complex-baseband representation of the signal, B complex-valued samples per second is the more natural quantity [314]. These B samples are the degrees of freedom available for designing the communication signal. The SE is the amount of information that can be transferred reliably per complex-valued sample.

Definition 1.2 (Spectral efficiency). The SE of an encoding/decoding scheme is the average number of bits of information, per complex-valued sample, that it can reliably transmit over the channel under consideration.

From this definition, it is clear that the SE is a deterministic number that can be measured in bit per complex-valued sample. Since there are B samples per second, an equivalent unit of the SE is bit per second per Hertz, often written in short-form as bit/s/Hz. For fading channels, which change over time, the SE can be viewed as the average number of bit/s/Hz over the fading realizations, as will be defined below. In this monograph, we often consider the SE of a channel between a UE and a BS, which for simplicity we refer to as the “SE of the UE”. A related metric is the *information rate* [bit/s], which is defined as the product of the SE and the bandwidth B . In addition, we commonly consider the sum SE of the channels from all UEs in a cell to the respective BS, which is measured in bit/s/Hz/cell.

The channel between a transmitter and a receiver at given locations can support many different SEs (depending on the chosen encoding/decoding scheme), but the largest achievable SE is of key importance when designing communication systems. The maximum SE is determined by the channel capacity, which was defined by Claude Shannon in his seminal paper [297] from 1948. The following theorem provides the capacity for the channel illustrated in Figure 1.5.



Figure 1.5: A general discrete memoryless channel with input x and output y .

Theorem 1.1 (Channel capacity). Consider a discrete memoryless channel with input x and output y , which are two random variables. Any SE smaller or equal to the channel capacity

$$C = \sup_{f(x)} (\mathcal{H}(y) - \mathcal{H}(y|x)) \quad (1.2)$$

is achievable with arbitrarily low error probability, while larger values cannot be achieved. The supremum is taken with respect to all feasible input distributions $f(x)$, while $\mathcal{H}(y)$ is the differential entropy of the output and $\mathcal{H}(y|x)$ is the conditional differential entropy of the output given the input.

The terminology of discrete memoryless channels and entropy is defined in Appendix B.5 on p. 419. We refer to [297] and textbooks on information theory, such as [94], for the proof of Theorem 1.1. The set of feasible input distributions depends on the application, but it is common to consider all distributions that satisfy a constraint on the input power. In wireless communications, we are particularly interested in channels where the received signal is the superposition of a scaled version of the desired signal and additive Gaussian noise. These channels are commonly referred to as additive white Gaussian noise (AWGN) channels. The channel capacity in Theorem 1.1 can be computed in closed form in the following canonical case from [298], which is also illustrated in Figure 1.6.

Corollary 1.2. Consider a discrete memoryless channel with input $x \in \mathbb{C}$ and output $y \in \mathbb{C}$ given by

$$y = hx + n \quad (1.3)$$

where $n \sim \mathcal{N}_{\mathbb{C}}(0, \sigma^2)$ is independent noise. The input distribution is power-limited as $\mathbb{E}\{|x|^2\} \leq p$ and the channel response $h \in \mathbb{C}$ is known at the output.

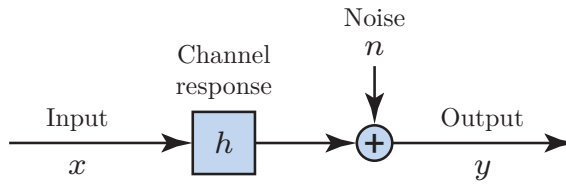


Figure 1.6: A discrete memoryless channel with input x and output $y = hx + n$, where h is the channel response and n is independent Gaussian noise.

If h is deterministic, then the channel capacity is

$$C = \log_2 \left(1 + \frac{p|h|^2}{\sigma^2} \right) \quad (1.4)$$

and is achieved by the input distribution $x \sim \mathcal{N}_{\mathbb{C}}(0, p)$.

If h is a realization of a random variable \mathbb{H} that is independent of the signal and noise, then the ergodic⁷ channel capacity is

$$C = \mathbb{E} \left\{ \log_2 \left(1 + \frac{p|h|^2}{\sigma^2} \right) \right\} \quad (1.5)$$

where the expectation is with respect to h . This is called a fading channel and the capacity is achieved by the input distribution $x \sim \mathcal{N}_{\mathbb{C}}(0, p)$.

Proof. The proof is available in Appendix C.1.1 on p. 426. □

The channel considered in Corollary 1.2 is called a single-input single-output (SISO) channel because one input signal is sent and results in one output signal. An average power constraint is assumed in the corollary and throughout this monograph, but other constraints also exist in practice; see Remark 7.1 on p. 307 for a further discussion. The practical meaning of the channel capacity can be described by considering the transmission of an information sequence with N scalar inputs, generated by an ergodic stochastic process, over the discrete

⁷The capacity of a fading channel requires that the transmission spans asymptotically many realizations of the random variable that describes the channel. This is referred to as the ergodic capacity since a stationary ergodic random fading process is required if the statistical properties shall be deducible from a single sequence of channel realizations. Each channel realization is used for a predetermined and finite number of input signals, then a new realization is taken from the random process.

memoryless channel in Corollary 1.2. If the scalar input has an SE smaller or equal to the capacity, the information sequence can be encoded such that the receiver can decode it with arbitrarily low error probability as $N \rightarrow \infty$. In other words, an infinite decoding delay is required to achieve the capacity. The seminal work in [267] quantifies how closely the capacity can be approached at a finite length of the information sequence. The SE is generally a good performance metric whenever data blocks of thousands of bits are transmitted [50].

The capacity expressions in (1.4) and (1.5) have a form that is typical for communications: the base-two logarithm of one plus the signal-to-noise ratio (SNR)-like expression

$$\frac{\overbrace{p|h|^2}^{\text{Received signal power}}}{\underbrace{\sigma^2}_{\text{Noise power}}}. \quad (1.6)$$

This is the actual measurable SNR for a deterministic channel response h , while it is the instantaneous SNR for a given channel realization when h is random. Since the SNR fluctuates in the latter case, it is more convenient to consider the average SNR when describing the quality of a communication channel. We define the average SNR as

$$\text{SNR} = \frac{p\mathbb{E}\{|h|^2\}}{\sigma^2} \quad (1.7)$$

where the expectation is computed with respect to the channel realizations. We call $\mathbb{E}\{|h|^2\}$ the average *channel gain* since it is the average scaling of the signal power incurred by the channel.

Transmissions in cellular networks are in general corrupted by interference from simultaneous transmissions in the same and other cells. By adding such interference to the channel in Figure 1.6, we obtain the discrete memoryless interference channel in Figure 1.7. The interference is not necessarily independent of the input x and the channel h . The exact channel capacity of interference channels is generally unknown, but convenient lower bounds can be obtained. Inspired by [36, 214], the following corollary provides the lower capacity bounds that will be used repeatedly in this monograph.

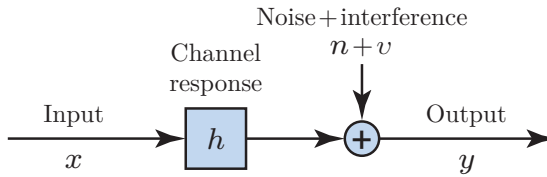


Figure 1.7: A discrete memoryless interference channel with input x and output $y = hx + v + n$, where h is the channel response, n is independent Gaussian noise, and v is the interference, which is uncorrelated with the input and the channel.

Corollary 1.3. Consider a discrete memoryless interference channel with input $x \in \mathbb{C}$ and output $y \in \mathbb{C}$ given by

$$y = hx + v + n \quad (1.8)$$

where $n \sim \mathcal{N}_{\mathbb{C}}(0, \sigma^2)$ is independent noise, the channel response $h \in \mathbb{C}$ is known at the output, and $v \in \mathbb{C}$ is random interference. The input is power-limited as $\mathbb{E}\{|x|^2\} \leq p$.

If h is deterministic and the interference v has zero mean, a known variance $p_v \in \mathbb{R}_+$, and is uncorrelated with the input (i.e., $\mathbb{E}\{x^*v\} = 0$), then the channel capacity C is lower bounded as

$$C \geq \log_2 \left(1 + \frac{p|h|^2}{p_v + \sigma^2} \right) \quad (1.9)$$

where the bound is achieved using the input distribution $x \sim \mathcal{N}_{\mathbb{C}}(0, p)$.

Suppose $h \in \mathbb{C}$ is instead a realization of the random variable \mathbb{H} and that \mathbb{U} is a random variable with realization u that affects the interference variance. The realizations of these random variables are known at the output. If the noise n is conditionally independent of v given h and u , the interference v has conditional zero mean (i.e., $\mathbb{E}\{v|h, u\} = 0$) and conditional variance denoted by $p_v(h, u) = \mathbb{E}\{|v|^2|h, u\}$, and the interference is conditionally uncorrelated with the input (i.e., $\mathbb{E}\{x^*v|h, u\} = 0$), then the ergodic⁸ channel capacity C is lower bounded as

$$C \geq \mathbb{E} \left\{ \log_2 \left(1 + \frac{p|h|^2}{p_v(h, u) + \sigma^2} \right) \right\} \quad (1.10)$$

⁸When transmitting an information sequence over this fading channel, a sequence of realizations of \mathbb{H} and \mathbb{U} is created, forming stationary ergodic random processes. Each set of realizations (h, u) is used for a predetermined and finite number of input signals, then a new set of realizations is taken from the random processes.

where the expectation is taken with respect to h and u , and the bound is achieved using the input distribution $x \sim \mathcal{N}_{\mathbb{C}}(0, p)$.

Proof. The proof is available in Appendix C.1.2 on p. 427. \square

Note that in Corollary 1.3, we use the shorthand notation $\mathbb{E}\{v|h, u\}$ for the conditional expectation $\mathbb{E}\{v|\mathbb{H} = h, \mathbb{U} = u\}$. For notational convenience, we will from now on omit the random variables in similar expressions and only write out the realizations.

The lower bounds on the channel capacity in Corollary 1.3 are obtained by treating the interference as an additional source of noise in the decoder, which might not be optimal from an information-theoretic point of view. For example, if an interfering signal is very strong, then one can potentially decode it and subtract the interference from the received signal, before decoding the desired signal. This is conceptually simple, but harder to perform in a practical cellular network, where the interfering signals change over time and the cells are not fully cooperating. In fact, there should not be any strongly interfering signal in a well-designed cellular network. In the low-interference regime, it is optimal (i.e., capacity-achieving) to treat interference as additional noise, as shown in [230, 296, 20, 21, 295].

We utilize SE expressions of the type in Corollary 1.3 throughout this monograph and stress that these might not be the highest achievable SEs, but SEs that can be achieved by low-complexity signal processing in the receiver, where interference is treated as noise. The SE expressions in (1.9) and (1.10) have a form typical for wireless communications: the base-two logarithm of one plus the expression

$$\text{SINR} = \frac{\overbrace{p|h|^2}^{\text{Received signal power}}}{\underbrace{p_v}_{\text{Interference power}} + \underbrace{\sigma^2}_{\text{Noise power}}} \quad (1.11)$$

that can be interpreted as the signal-to-interference-plus-noise ratio (SINR). Formally, this is only an SINR when h and p_v are deterministic; the expression is otherwise random. For simplicity, we will refer to any term a that appears as $\mathbb{E}\{\log_2(1 + a)\}$ in an SE expression as an *instantaneous SINR* (with slight abuse of terminology).

The SE expressions presented in this section are the fundamental building blocks for the theory developed in later sections. The capacity results consider discrete memoryless channels, which are different from practical continuous wireless channels. However, the bandwidth B can be divided into narrow subchannels (e.g., using orthogonal frequency-division multiplexing (OFDM)) that are essentially memoryless if the symbol time is much longer than the delay spread of the propagation environment [314].

1.3 Ways to Improve the Spectral Efficiency

There are different ways to improve the per-cell SE in cellular networks. In this section, we will compare different approaches to showcase which ones are the most promising. For simplicity, we consider a two-cell network where the average channel gain between a BS and every UE in a cell is identical, as illustrated in Figure 1.8. This is a tractable model for studying the basic properties of cellular communications, due to the small number of system parameters. It is an instance of the *Wyner model*, initially proposed by Aaron Wyner in [353] and studied for fading channels in [304]. It has been used extensively to study the fundamental information-theoretic properties of cellular networks; see the monograph [303] and references therein. More realistic, but less tractable, network models will be considered in later sections.

In the UL scenario shown in Figure 1.8, the UEs in cell 0 transmit to their serving BS, while the UL signals from the UEs in cell 1 leak into cell 0 as interference. The average channel gain from a UE in cell 0 to its serving BS is denoted by β_0^0 , while the interfering signals from UEs in cell 1 have an average channel gain of β_1^0 . Similarly, the average channel gain from a UE in cell 1 to its serving BS is denoted by β_1^1 , while the interfering signals from UEs in cell 0 have an average channel gain of β_0^1 . Notice that the superscript indicates the cell of the receiving BS and the subscript indicates the cell that the transmitting UE resides in. The average channel gains are positive dimensionless quantities that are often very small since the signal energy decays quickly with the propagation distance; values in the range from -70 dB to -120 dB are common within the serving cell, while even smaller values appear for

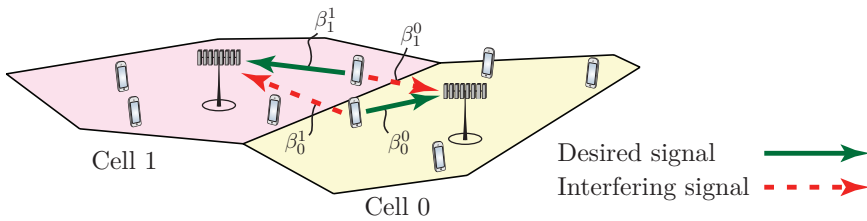


Figure 1.8: Illustration of the notion of desired and interfering UL signals in a two-cell network. In the Wyner model, every UE in cell 0 has the same value of the average channel gain β_0^0 from its serving BS and of the average channel gain β_0^1 to the other-cell BS, while every UE in cell 1 has the same value of β_1^0 and β_1^1 .

interfering signals. As shown later, it is not the absolute values that are of main importance when computing the SE, but the relative strength of the interference as compared to the desired signals. For simplicity, we assume that the intra-cell channel gains are equal (i.e., $\beta_0^0 = \beta_1^1$) and that the inter-cell channel gains are equal as well (i.e., $\beta_1^0 = \beta_0^1$); this is commonly assumed in the Wyner model. We can then define the ratio $\bar{\beta}$ between the inter-cell and intra-cell channel gains as

$$\bar{\beta} = \frac{\beta_1^0}{\beta_0^0} = \frac{\beta_0^1}{\beta_1^1} = \frac{\beta_1^0}{\beta_1^1} = \frac{\beta_0^1}{\beta_0^0}. \quad (1.12)$$

This ratio will be used in the analysis of both UL and DL. We typically have $0 \leq \bar{\beta} \leq 1$, where $\bar{\beta} \approx 0$ corresponds to a negligibly weak inter-cell interference and $\bar{\beta} \approx 1$ means that the inter-cell interference is as strong as the desired signals (which may happen for UEs at the cell edge). We will use this model in the remainder of Section 1, to discuss different ways to improve the SE per cell.

1.3.1 Increase the Transmit Power

The SE naturally depends on the strength of the received desired signal, represented by the average SNR, defined in (1.7). Using the Wyner model described above, the average SNR of a UE in cell 0 is

$$\text{SNR}_0 = \frac{p}{\sigma^2} \beta_0^0 \quad (1.13)$$

where p denotes the UE's transmit power and σ^2 is the noise power.

These power quantities are measured in Joule per time interval. Any type of time interval can be utilized as long as it is the same for both the signal and the noise, but common choices are “one second” or “one sample”. The parameter SNR_0 plays a key role in many of the expressions computed in this section.

Assume that there is one active UE per cell and that each BS and UE is equipped with a single antenna. Notice that with “antenna” we refer to a component with a size that is smaller than the wavelength (e.g., a patch antenna) and not the type of large high-gain antennas that are used at the BSs in conventional cellular networks. Antennas and antenna arrays are further discussed in Section 7.4 on p. 347.

Focusing on a flat-fading⁹ wireless channel, the symbol-sampled complex-baseband signal $y_0 \in \mathbb{C}$ received at the BS in cell 0 is

$$y_0 = \underbrace{h_0^0 s_0}_{\text{Desired signal}} + \underbrace{h_1^0 s_1}_{\text{Interfering signal}} + \underbrace{n_0}_{\text{Noise}} \quad (1.14)$$

where the additive receiver noise is modeled as $n_0 \sim \mathcal{N}_{\mathbb{C}}(0, \sigma^2)$. The scalars $s_0, s_1 \sim \mathcal{N}_{\mathbb{C}}(0, p)$ in (1.14) represent the information signals¹⁰ transmitted by the desired and interfering UEs, respectively. Moreover, their channel responses are denoted by $h_0^0 \in \mathbb{C}$ and $h_1^0 \in \mathbb{C}$, respectively. The properties of these channel responses depend on the propagation environment. In this section, we consider one model of LoS propagation and one model of non-line-of-sight (NLoS) propagation. In single-antenna LoS propagation, h_0^0 and h_1^0 are deterministic scalars corresponding to the square-root of the (average) channel gains:

$$h_i^0 = \sqrt{\beta_i^0} \quad \text{for } i = 0, 1. \quad (1.15)$$

In general, the channel response will also have a phase rotation, but it is neglected here since it does not affect the SE. The channel gain

⁹In flat-fading channels, the coherence bandwidth of the channel is larger than the signal bandwidth [314]. Therefore, all frequency components of the signal will experience the same magnitude of fading, resulting in a scalar channel response.

¹⁰The information signals are assumed to be complex Gaussian distributed since this maximizes the differential entropy of the signal (see Lemma B.21 on p. 421) and achieves the capacity in interference-free scenarios (see Corollary 1.2). In practice, quadrature amplitude modulation (QAM) schemes with finite number of constellation points are commonly used, which leads to a small shaping-loss as compared to having infinitely many constellation points from a Gaussian distribution.

β_i^0 can be interpreted as the macroscopic *large-scale fading* in LoS propagation, caused by distance-dependent pathloss. The impact of the transceiver hardware, including the antenna gains, is also absorbed into this parameter. The parameter is constant if the transmitter and receiver are fixed, while it changes if the transmitter and/or receiver move. Microscopic movements (at the order of the wavelength) can be modeled as phase-rotations in h_i^0 , while large movements (at the order of meters) lead to substantial changes in β_i^0 . We consider a fixed value of h_i^0 in order to apply the SE expression in Corollary 1.3 for deterministic channels.

In NLoS propagation environments, the channel responses are random variables that change over time and frequency. If there is sufficient scattering between the UEs and the BS, then h_0^0 and h_1^0 are well-modeled as

$$h_i^0 \sim \mathcal{N}_{\mathbb{C}}(0, \beta_i^0) \quad \text{for } i = 0, 1 \quad (1.16)$$

as validated by the channel measurements reported in [337, 177, 83, 365]. The transmitted signal reaches the receiver through many different paths and the superimposed received signals can either reinforce or cancel each other. When the number of paths is large, the central limit theorem motivates the use of a Gaussian distribution. This phenomenon is known as small-scale fading and is a microscopic effect caused by small variations in the propagation environment (e.g., movement of the transmitter, receiver, or other objects). In contrast, the variance β_i^0 is interpreted as the macroscopic large-scale fading, which includes distance-dependent pathloss, shadowing, antenna gains, and penetration losses in NLoS propagation. The channel model in (1.16) is called Rayleigh fading, because the magnitude $|h_i^0|$ is a Rayleigh distributed random variable.

Notice that the average channel gain is $\mathbb{E}\{|h_i^0|^2\} = \beta_i^0$, for $i = 0, 1$, in both propagation cases in order to make them easily comparable. Practical channels can contain a mix of a deterministic LoS component and a random NLoS component, but, by studying the differences between the two extreme cases, we can predict what will happen in the mixed cases as well. The following lemma provides closed-form SE expressions for the LoS and NLoS cases.

Lemma 1.4. Suppose the BS in cell 0 knows the channel responses. An achievable¹¹ UL SE for the desired UE in the LoS case is

$$SE_0^{\text{LoS}} = \log_2 \left(1 + \frac{1}{\bar{\beta} + \frac{1}{\text{SNR}_0}} \right) \quad (1.17)$$

with $\bar{\beta}$ and SNR_0 given by (1.12) and (1.13), respectively. In the NLoS case (with $\bar{\beta} \neq 1$), an achievable UL SE is

$$\begin{aligned} SE_0^{\text{NLoS}} &= \mathbb{E} \left\{ \log_2 \left(1 + \frac{p|h_0^0|^2}{p|h_1^0|^2 + \sigma^2} \right) \right\} \\ &= \frac{e^{\frac{1}{\text{SNR}_0}} E_1 \left(\frac{1}{\text{SNR}_0} \right) - e^{\frac{1}{\text{SNR}_0 \bar{\beta}}} E_1 \left(\frac{1}{\text{SNR}_0 \bar{\beta}} \right)}{\log_e(2) (1 - \bar{\beta})} \end{aligned} \quad (1.18)$$

where $E_1(x) = \int_1^\infty \frac{e^{-xu}}{u} du$ denotes the exponential integral and $\log_e(\cdot)$ denotes the natural logarithm.

Proof. The proof is available in Appendix C.1.3 on p. 429. \square

This lemma shows that the SE is fully characterized by the SNR of the desired signal, SNR_0 , and the relative strength of the inter-cell interference, $\bar{\beta}$. Note that the closed-form NLoS expression in (1.18) only applies for $\bar{\beta} \neq 1$. Recall that $0 \leq \bar{\beta} \leq 1$ is the typical range of $\bar{\beta}$. The pathological case $\bar{\beta} = 1$ represents a cell-edge scenario where the desired and interfering signals are equally strong. An alternative expression can be derived for $\bar{\beta} = 1$, using the same methodology as in the proof of Lemma 1.4, but it does not provide any further insights and is therefore omitted.

The SE is naturally an increasing function of the SNR, which is most easily seen from the LoS expression in (1.17), where the SE is the logarithm of the following SINR expression:

$$\frac{1}{\bar{\beta} + \frac{1}{\text{SNR}_0}} = \frac{\overbrace{p\beta_0^0}^{\text{Signal power}}}{\underbrace{p\beta_1^0}_{\text{Interference power}} + \underbrace{\sigma^2}_{\text{Noise power}}}. \quad (1.19)$$

¹¹Recall that an SE is achievable if there exists a sequence of codes such that the maximum probability of error in transmission for any message of length N converges to zero as $N \rightarrow \infty$ [94]. Any SE smaller or equal to the capacity is thus achievable.

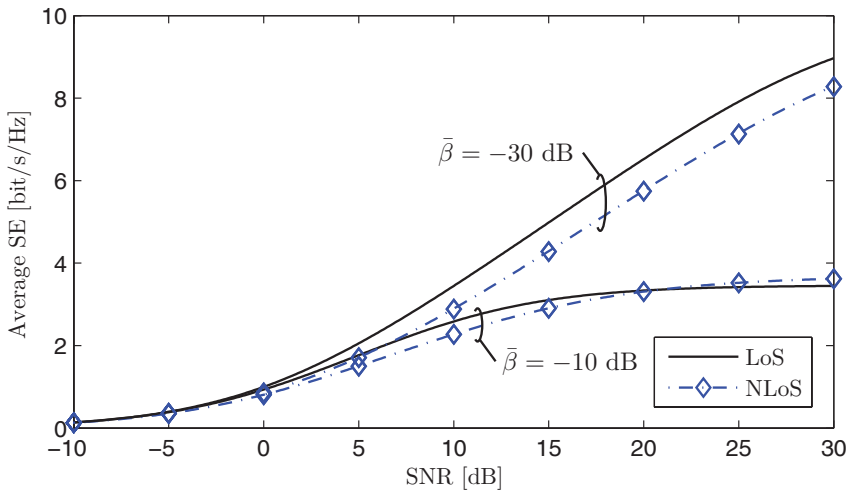


Figure 1.9: Average UL SE as a function of the SNR for different cases of inter-cell interference strength, $\bar{\beta} \in \{-10, -30\}$ dB, and different channel models.

One can improve the SE by increasing the transmit power p . However, the SE will not increase indefinitely with p . In the LoS case, we have

$$SE_0^{\text{LoS}} \rightarrow \log_2 \left(1 + \frac{1}{\bar{\beta}} \right) \quad \text{as } p \rightarrow \infty \quad (1.20)$$

where the limit is completely determined by the strength of the interference. This is due to the fact that the desired UE and the interfering UE both increase their transmit powers, which is the case of interest in cellular networks since good service quality should be guaranteed in all cells. The corresponding limit in the NLoS case is

$$SE_0^{\text{NLoS}} \rightarrow \frac{1}{1 - \bar{\beta}} \log_2 \left(\frac{1}{\bar{\beta}} \right) \quad \text{as } p \rightarrow \infty \quad (1.21)$$

which can be proved by expanding the exponential integrals in (1.18) using the identity in [3, Eq. (5.1.11)] and then taking the limit $p \rightarrow \infty$.

To exemplify these behaviors, Figure 1.9 shows the SE as a function of the SNR, where an SNR increase is interpreted as increasing the transmit power p . We consider two different strengths of the inter-cell interference: $\bar{\beta} = -10$ dB and $\bar{\beta} = -30$ dB. The SE converges quickly to the LoS limit $\log_2(1 + 1/\bar{\beta}) \approx 3.46$ bit/s/Hz and the NLoS

limit $\log_2(1/\bar{\beta})/(1 - \bar{\beta}) \approx 3.69$ bit/s/Hz in the former case, since the interference is only 10 dB weaker than the desired signal. In the case of $\bar{\beta} = -30$ dB, the convergence to the LoS limit 9.97 bit/s/Hz and NLoS limit 9.98 bit/s/Hz is less visible in the considered SNR range, since the interference is weaker and the logarithm makes the SE grow slowly. Nevertheless, we notice that going from $\text{SNR}_0 = 10$ dB to $\text{SNR}_0 = 30$ dB only doubles the SE, though 100 times more transmit power is required. The NLoS case provides slightly lower SE than the LoS case for most SNRs, due to the random fluctuations of the squared magnitude $|h_0^0|^2$ of the channel. However, the randomness turns into a small advantage at high SNR, where the limit is slightly higher in NLoS because the interference can be much weaker than the signal for some channel realizations. This behavior is seen for $\bar{\beta} = -10$ dB in Figure 1.9, while it occurs at higher SNRs for $\bar{\beta} = -30$ dB.

In summary, increasing the SNR by using more transmit power improves the SE, but the positive effect quickly pushes the network into an interference-limited regime where no extraordinary SEs can be obtained. This is basically because of the lack of *degrees of freedom* at the BS, which cannot separate the desired signal from the interference from a single observation.¹² This interference-limited regime is where the coverage tier operates in current networks, while the situation for the hotspot tier depends on how the BSs are deployed. For example, the signals at mmWave frequencies are greatly attenuated by walls and other objects. A mmWave SC will typically cover a very limited area, but on the other hand the cell might be noise-limited since the interfering signals from SCs in other rooms are also attenuated by walls. The SE range in Figure 1.9 is comparable to what contemporary networks deliver (e.g., 0–5 bit/s/Hz in LTE [144]). Hence, a simple power-scaling approach cannot contribute much to achieving higher SE in cellular networks.

Remark 1.2 (Increasing cell density). Another way to increase the SNR is to keep the transmit power fixed and increase the cell density D

¹²The transmission scheme considered in this example is not optimal. The UEs could take turns in transmitting, thereby achieving an SE that grows without bound, but with a pre-log factor of 1/2 if each UE is active 50% of the time. More generally, interference alignment methods can be used to handle the interference [70].

instead. It is commonly assumed in channel modeling that the average channel gain is inversely proportional to the propagation distance to some fixed “pathloss” exponent. Under such a basic propagation model, the power of the received desired signal and the inter-cell interference increase at roughly the same pace when D is increased, since both the distance to the desired BS and the interfering BSs are reduced. This implies that the interference-limited SE limit is obtained also when D increases. While D cannot be much increased in the coverage tier, cell densification is a suitable way to improve the hotspot tier [198]; the area throughput in (1.1) increases linearly with D as long as the basic propagation model holds true. At some point, this model will, however, become invalid since the pathloss exponent will also reduce with the distance and approach the free-space propagation scenario with an exponent of two [19]. Cell densification is no longer desired in this extreme short-range scenario since the sum power of the interfering signals increase faster than the desired signal power.

1.3.2 Obtain an Array Gain

Instead of increasing the UL transmit power, the BS can deploy multiple receive antennas to collect more energy from the EM waves. This concept has at least been around since the 1930s [257, 117], with the particular focus on achieving spatial diversity; that is, to combat the channel fading in NLoS propagation by deploying multiple receive antennas that observe different fading realizations. The related idea of using multiple transmit antennas to increase the received signal power was described as early as 1919 [10]. Having multiple receive antennas also allows the receiver to distinguish between signals with different spatial directivity by using spatial filtering/processing [324]. Implementations of these methods have been referred to as “adaptive” or “smart” antennas [16, 350]. In general, it is more convenient to equip the BSs with multiple antennas than the UEs, because the latter are typically compact commercial end-user products powered by batteries and relying on low-cost components.

Suppose the BS in cell 0 is equipped with an array of M antennas. The channel responses from the desired and interfering UEs can then be represented by the vectors $\mathbf{h}_0^0 \in \mathbb{C}^M$ and $\mathbf{h}_1^0 \in \mathbb{C}^M$, respectively. The

m th element of each vector is the channel response observed at the m th BS antenna, for $m = 1, \dots, M$. The scalar received UL signal in (1.14) is then extended to a received vector $\mathbf{y}_0 \in \mathbb{C}^M$, modeled as

$$\mathbf{y}_0 = \underbrace{\mathbf{h}_0^0 s_0}_{\text{Desired signal}} + \underbrace{\mathbf{h}_1^0 s_1}_{\text{Interfering signal}} + \underbrace{\mathbf{n}_0}_{\text{Noise}} \quad (1.22)$$

where $\mathbf{n}_0 \sim \mathcal{N}_{\mathbb{C}}(\mathbf{0}_M, \sigma^2 \mathbf{I}_M)$ is the receiver noise over the BS array and the transmit signals s_0 and s_1 are defined as in (1.14).

To analyze the SE of this UL single-input multiple-output (SIMO) channel with inter-cell interference, we need to extend the propagation models to the multiple antenna case. In the LoS case, we consider a horizontal uniform linear array (ULA) with antenna spacing d_H , which is measured in the number of wavelengths between adjacent antennas. Hence, if λ denotes the wavelength at the carrier frequency, then the antenna spacing is λd_H meters. Channel models for other array geometries are considered in Section 7.3 on p. 329. We further assume that the UEs are located at fixed locations in the far-field of the BS array, which leads to the following deterministic channel response [254]:

$$\mathbf{h}_i^0 = \sqrt{\beta_i^0} \left[1 \ e^{2\pi j d_H \sin(\varphi_i^0)} \ \dots \ e^{2\pi j d_H (M-1) \sin(\varphi_i^0)} \right]^T \quad \text{for } i = 0, 1 \quad (1.23)$$

where $\varphi_i^0 \in [0, 2\pi)$ is the azimuth angle to the UE, relative to the boresight of the array at the BS in cell 0, and β_i^0 describes the macroscopic large-scale fading. The channel response in (1.23) can also have a common phase rotation of all elements, but it is neglected here since it does not affect the SE. The LoS propagation model is illustrated in Figure 1.10, where a plane wave reaches the array from a generic azimuth angle φ . When comparing two adjacent antennas, one of them observes a signal that has traveled $d_H \sin(\varphi)$ longer than the other one. This leads to the array response in (1.23) with phase rotations that are multiples of $d_H \sin(\varphi)$, as also illustrated in Figure 1.10.

In the NLoS case, we assume for now that the channel response is spatially uncorrelated over the array. This yields

$$\mathbf{h}_i^0 \sim \mathcal{N}_{\mathbb{C}}(\mathbf{0}_M, \beta_i^0 \mathbf{I}_M) \quad \text{for } i = 0, 1 \quad (1.24)$$

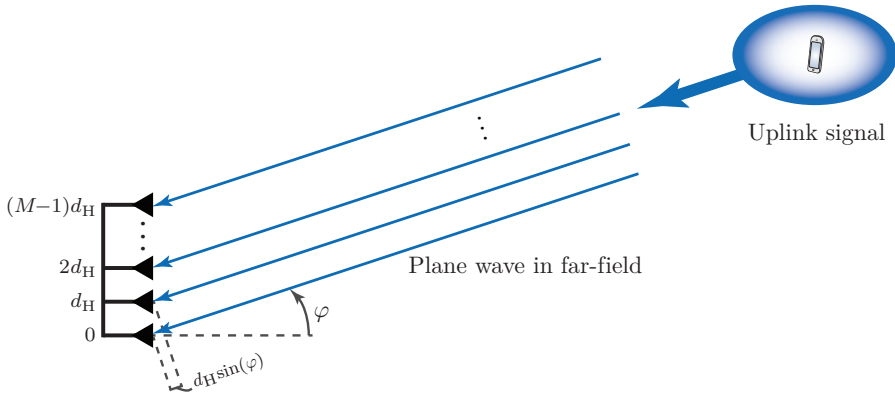


Figure 1.10: LoS propagation between a transmitting single-antenna UE and a BS equipped with a ULA with M antennas. The antenna spacing is d_H wavelengths, the azimuth angle to the UE is φ , and the UE is located in the far-field of the array, so that a plane wave reaches it. Note that the setup is illustrated from above.

where β_i^0 describes the macroscopic large-scale fading, while the randomness and Gaussian distribution account for the small-scale fading. This channel model is called *uncorrelated Rayleigh fading* or independent and identically distributed (i.i.d.) Rayleigh fading, since the elements in \mathbf{h}_i^0 are uncorrelated (and also independent) and have Rayleigh distributed magnitudes. Uncorrelated Rayleigh fading is a tractable model for rich scattering conditions, where the BS array is surrounded by many scattering objects, as compared to the number of antennas. We will use it to describe the basic properties in this section, while a more general and realistic model is introduced in Section 2.2 on p. 69 and then used in the remainder of the monograph. Channel modeling is further discussed in Section 7.3 on p. 329. The NLoS propagation model with uncorrelated Rayleigh fading is illustrated in Figure 1.11. Notice that the average channel gain β_i^0 is, for simplicity, assumed to be the same for all BS antennas. This is a reasonable approximation when the distance between the BS and UE is much larger than the distance between the BS antennas. However, in practice, there can be several decibels of channel gain variations between the antennas [122]. This fact is neglected in this section, but has a strong impact on the SE when M is large; see Section 4.4 on p. 183 for further details.

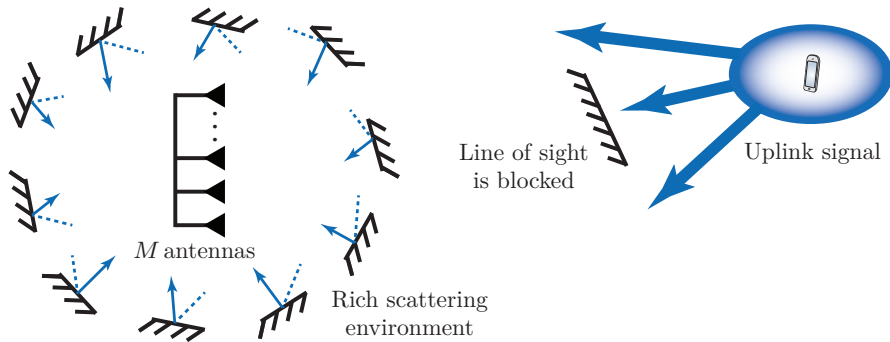


Figure 1.11: NLoS propagation with uncorrelated Rayleigh fading between a transmitting single-antenna UE and a BS equipped with an array of M antennas. The LoS path is blocked, but the signal finds multiple other paths via scattering objects. The BS is surrounded by many scattering objects so that the UE location has no impact on the spatial directivity of the received signal.

The benefits of having multiple antennas at the BS appear when the BS knows the channel response of the desired UE. This knowledge enables the BS to coherently combine the received signals from all antennas. Estimation of the channel response is thus a key aspect in multi-antenna systems and will be further discussed in Section 1.3.5 and later analyzed in detail in Section 3 on p. 91. For now, we assume that the channel responses are known at the BS and can be used to select a *receive combining vector* $\mathbf{v}_0 \in \mathbb{C}^M$. This vector is multiplied with the received signal in (1.22) to obtain

$$\mathbf{v}_0^H \mathbf{y}_0 = \underbrace{\mathbf{v}_0^H \mathbf{h}_0^0 s_0}_{\text{Desired signal}} + \underbrace{\mathbf{v}_0^H \mathbf{h}_1^0 s_1}_{\text{Interfering signal}} + \underbrace{\mathbf{v}_0^H \mathbf{n}_0}_{\text{Noise}}. \quad (1.25)$$

Receive combining is a linear projection, which transforms the SIMO channel into an effective SISO channel that may support higher SEs than in the single-antenna case, if the combining vector is selected judiciously. There are many different combining schemes, but a simple and popular one is *maximum ratio (MR) combining*, defined as

$$\mathbf{v}_0 = \mathbf{h}_0^0. \quad (1.26)$$

This is a vector that maximizes the ratio $|\mathbf{v}_0^H \mathbf{h}_0^0|^2 / \|\mathbf{v}_0\|^2$ between the power of the desired signal and the squared norm of the combining

vector [172, 68].¹³ The following lemma gives closed-form SE expressions for the case of MR combining.

Lemma 1.5. Suppose the BS in cell 0 knows the channel responses and applies MR combining to the received signal in (1.22). An achievable UL SE for the desired UE in the LoS case is

$$SE_0^{\text{LoS}} = \log_2 \left(1 + \frac{M}{\bar{\beta} g(\varphi_0^0, \varphi_1^0) + \frac{1}{\text{SNR}_0}} \right) \quad (1.27)$$

where the function $g(\varphi, \psi)$ is defined as

$$g(\varphi, \psi) = \begin{cases} \frac{\sin^2(\pi d_{\text{H}} M (\sin(\varphi) - \sin(\psi)))}{M \sin^2(\pi d_{\text{H}} (\sin(\varphi) - \sin(\psi)))} & \text{if } \sin(\varphi) \neq \sin(\psi) \\ M & \text{if } \sin(\varphi) = \sin(\psi). \end{cases} \quad (1.28)$$

Similarly, an achievable UL SE for the desired UE in the NLoS case (with $\bar{\beta} \neq 1$) is

$$SE_0^{\text{NLoS}} = \left(\frac{1}{\left(1 - \frac{1}{\bar{\beta}}\right)^M} - 1 \right) \frac{e^{\frac{1}{\text{SNR}_0 \bar{\beta}} E_1\left(\frac{1}{\text{SNR}_0 \bar{\beta}}\right)}}{\log_e(2)} + \sum_{m=1}^M \sum_{l=0}^{M-m} \frac{(-1)^{M-m-l+1}}{\left(1 - \frac{1}{\bar{\beta}}\right)^m} \frac{\left(e^{\frac{1}{\text{SNR}_0} E_1\left(\frac{1}{\text{SNR}_0}\right)} + \sum_{n=1}^l \frac{1}{n} \sum_{j=0}^{n-1} \frac{1}{j! \text{SNR}_0^j} \right)}{(M-m-l)! \text{SNR}_0^{M-m-l} \bar{\beta} \log_e(2)} \quad (1.29)$$

where $n!$ denotes the factorial function and $E_1(x) = \int_1^\infty \frac{e^{-xu}}{u} du$ denotes the exponential integral.

Proof. The proof is available in Appendix C.1.4 on p. 430. \square

This lemma shows that the SE is characterized by the SNR of the desired signal, SNR_0 , the strength of the inter-cell interference, $\bar{\beta}$, and the number of BS antennas, M . Notice that by having M receive antennas, the array collects M times more energy from the desired

¹³The Cauchy-Schwartz inequality can be used to prove that $\mathbf{v}_0 = \mathbf{h}_0^0$ maximizes the ratio $|\mathbf{v}_0^H \mathbf{h}_0^0|^2 / \|\mathbf{v}_0\|^2$.

and interfering signals, and also from the noise. In the LoS case in (1.27), the gain of the desired signal scales as M . The linear scaling with the number of antennas is called *array gain*. It shows that MR coherently combines all the received energy from the desired signal, because the combining vector is matched to the channel response of the desired UE. In contrast, MR combines the noise and the interfering signal components non-coherently over the array since \mathbf{v}_0 is independent of \mathbf{h}_1^0 and \mathbf{n}_0 . As a consequence, the interference power $\bar{\beta}g(\varphi_0^0, \varphi_1^0)$ in (1.27) can be upper bounded as

$$\bar{\beta}g(\varphi_0^0, \varphi_1^0) \leq \frac{\bar{\beta}}{M} \frac{1}{\sin^2(\pi d_H(\sin(\varphi_0^0) - \sin(\varphi_1^0)))} \quad (1.30)$$

when $\sin(\varphi_0^0) \neq \sin(\varphi_1^0)$, which decreases as $1/M$ when more receive antennas are added. The basic reason that MR combining rejects the interfering signal is that the M antennas provide the BS with M spatial degrees of freedom, which can be used to separate the desired signal from the interfering signal. In particular, the directions of the LoS channel responses \mathbf{h}_0^0 and \mathbf{h}_1^0 gradually become orthogonal as M increases. This property is called (asymptotically) *favorable propagation* [245], since UEs with orthogonal channels can communicate with the BS simultaneously without causing mutual interference. We will further discuss this property in Section 1.3.3 and also in Section 2.5.2 on p. 80.

The equation $\sin(\varphi_0^0) = \sin(\varphi_1^0)$ has two unique solutions: $\varphi_0^0 = \varphi_1^0$ and the mirror reflection $\varphi_0^0 = \pi - \varphi_1^0$. Hence, the ULA can only uniquely resolve angles either in the interval $[-\pi/2, \pi/2]$ or in the interval $[\pi/2, 3\pi/2]$ at the other side of the array. The discussion above does not apply when $\sin(\varphi_0^0) = \sin(\varphi_1^0)$, because then $g(\varphi_0^0, \varphi_1^0) = M$ instead. It is natural that both the desired and the interfering signal scale linearly with M in this case, because the two signals arrive from exactly the same angle (or its mirror reflection). This will most likely never happen in practice, but we can infer from (1.28) that the interference is stronger when the UEs' angles are similar to each other. For example,

we can utilize the fact that $\sin(\pi z) \approx \pi z$ for $|z| < 0.2$ to show that

$$\begin{aligned} g(\varphi, \psi) &= \frac{\sin^2(\pi d_{\text{H}} M (\sin(\varphi) - \sin(\psi)))}{M \sin^2(\pi d_{\text{H}} (\sin(\varphi) - \sin(\psi)))} \\ &\approx \frac{(\pi d_{\text{H}} M (\sin(\varphi) - \sin(\psi)))^2}{M (\pi d_{\text{H}} (\sin(\varphi) - \sin(\psi)))^2} = M \end{aligned} \quad (1.31)$$

if $d_{\text{H}} M |\sin(\varphi) - \sin(\psi)| < 0.2$. The angular interval for which this holds becomes smaller as the aperture $d_{\text{H}} M$ of the ULA increases, but it exists for any finite-sized array. Since it is $d_{\text{H}} M$ that determines the angular resolution, the interference is reduced by either increasing the number of antennas M and/or using a larger antenna spacing d_{H} . This is in contrast to the signal term, which is proportional only to the number of antennas. For a given array aperture, it is therefore beneficial to have many antennas rather than widely separated antennas. Note that we have considered a two-dimensional LoS model in this section where only the azimuth angle can differ between the UEs. In practice, UEs can also have different elevation angles to the BS array and this can be exploited to separate the UEs. These aspects will be discussed in more detail in Section 7.4.2 on p. 350.

To illustrate these behaviors, the function $g(\varphi_0^0, \varphi_1^0)$ is shown in Figure 1.12 for a desired UE at the fixed angle $\varphi_0^0 = 30^\circ$, while the angle of the interfering UE is varied between -180° and 180° . The antenna-spacing is $d_{\text{H}} = 1/2$. In the single-antenna case, we have $g(\varphi_0^0, \varphi_1^0) = 1$ irrespective of the angles, which is in line with Lemma 1.4. When the BS has multiple antennas, $g(\varphi_0^0, \varphi_1^0)$ depends strongly on the individual UE angles. There are interference peaks when the two UEs have the same angle (i.e., $\varphi_1^0 = 30^\circ$) and when the angles are each others' mirror reflections (i.e., $\varphi_1^0 = 180^\circ - 30^\circ = 150^\circ$). The function is equal to M at these peaks, because the interfering signal is coherently combined by the MR combining (just as the desired signal). When the ULA can resolve the individual UEs, the interference level instead decreases rapidly (notice the logarithmic vertical scale) and gets generally smaller as M increases. In these cases, the interference level oscillates as the interfering UE's angle is varied, but is approximately $1/M$ times weaker than in the single-antenna case. Hence, the multiple BS antennas help to

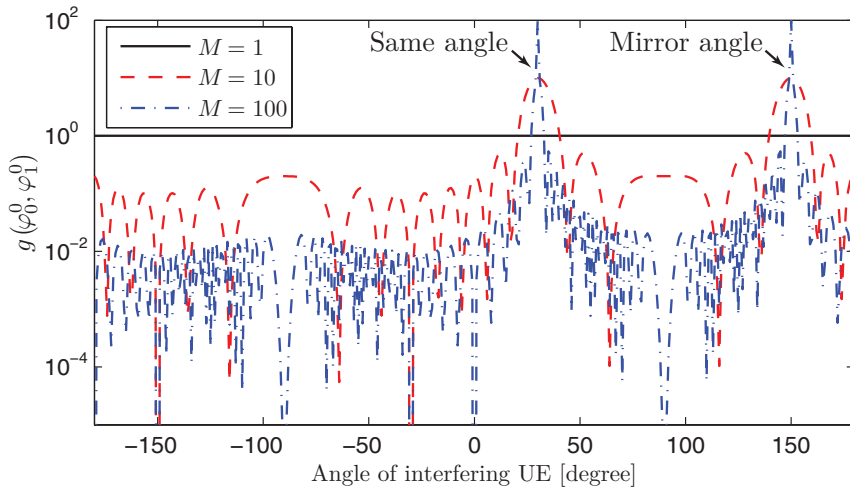


Figure 1.12: The function $g(\varphi_0^0, \varphi_1^0)$ in (1.28) that determines the interference level in an LoS scenario. The desired UE is at the fixed angle $\varphi_0^0 = 30^\circ$ and the interfering UE has a varying angle $\varphi_1^0 \in [-180^\circ, 180^\circ]$.

suppress interference, as long as the UE angles are sufficiently different.

The SE in the NLoS case is harder to interpret since the closed-form expression in (1.29) has a complicated structure with several summations and special functions. Fortunately, we can obtain the following convenient lower bound that is very tight for $M \gg 1$ (see Figure 1.14 for a comparison).

Corollary 1.6. A lower bound on the UL SE in (1.29) for NLoS channels is

$$\text{SE}_0^{\text{NLoS}} = \mathbb{E} \left\{ \log_2 \left(1 + \frac{p \|\mathbf{h}_0^0\|^2}{p \frac{|\langle \mathbf{h}_0^0, \mathbf{h}_1^0 \rangle|^2}{\|\mathbf{h}_0^0\|^2} + \sigma^2} \right) \right\} \geq \log_2 \left(1 + \frac{M-1}{\bar{\beta} + \frac{1}{\text{SNR}_0}} \right). \quad (1.32)$$

Proof. The proof is available in Appendix C.1.5 on p. 433. \square

The SE expression above can be interpreted similarly to the LoS expression in (1.27); it is the logarithm of one plus an SINR expression where the signal power increases as $(M-1)$. A linear array gain is thus obtained for both LoS and NLoS channels. It is the lower-bounding

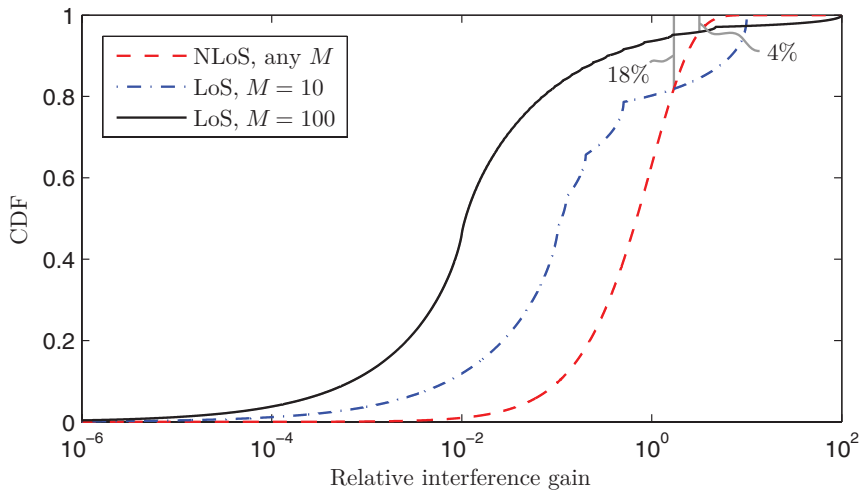


Figure 1.13: CDF of the relative interference gain in (1.33), using logarithmic scale on the horizontal axis. The randomness in the NLoS case is due to Rayleigh fading, while it is due to random UE angles in the LoS cases. The percentages of realizations when LoS gives higher interference gain than NLoS are indicated.

technique used in Corollary 1.6 that made the desired signal scale as $(M - 1)$, instead of M which is the natural array gain obtained with MR combining. However, the difference is negligible when M is large. The interference power in (1.32) is independent of M , in contrast to the LoS case in (1.27) where it decays as $1/M$. This scaling behavior suggests that NLoS channels provide less favorable propagation than LoS channels, but the reality is more complicated. To exemplify this, Figure 1.13 shows the cumulative distribution function (CDF) of the relative interference gain

$$\frac{1}{\beta_1^0} \frac{|(\mathbf{h}_0^0)^H \mathbf{h}_1^0|^2}{\|\mathbf{h}_0^0\|^2} \quad (1.33)$$

which determines how well interference is suppressed by MR combining.

For NLoS channels, (1.33) can be shown to have an $\text{Exp}(1)$ distribution, irrespectively of the value of M . In contrast, (1.33) equals $g(\varphi_0^0, \varphi_1^0)$ in (1.28) for LoS channels, which is a function of M and the UE angles. Figure 1.13 considers the LoS case with $M = 10$ and $M = 100$, and shows the CDF over different uniformly distributed UE angles between

0 and 2π (with $d_H = 1/2$). The CDF of the small-scale fading with NLoS channels is also shown. Figure 1.13 shows that LoS channels often provide several orders-of-magnitude lower interference gains than NLoS channels, but this only applies to the majority of random angle realizations. There is a small probability that the interference gain is larger in LoS than in NLoS; it happens in 18% of the realizations with $M = 10$ and 4% of the realizations with $M = 100$. This corresponds to cases when $\sin(\varphi_0^0) \approx \sin(\varphi_1^0)$ so that the array cannot resolve and separate the UE angles. As discussed earlier, this occurs approximately when $d_H M |\sin(\varphi_0^0) - \sin(\varphi_1^0)| < 0.2$. This happens less frequently for random angles as M increases (for fixed d_H), since the array aperture grows and thus obtains a better spatial resolution. Nevertheless, for any finite M , there will be a small angular interval around φ_0^0 where incoming interference will be amplified just as the desired signal. Since the array is unable to separate UEs with such small angle differences, time-frequency scheduling might be needed to separate them; see Section 7.2.2 on p. 321 for further guidelines for scheduling.

The favorable propagation concept provides a way to quantify the ability to separate UE channels at a BS with many antennas [245]. The channels \mathbf{h}_i^0 and \mathbf{h}_k^0 are said to provide asymptotically favorable propagation if

$$\frac{(\mathbf{h}_i^0)^H \mathbf{h}_k^0}{\sqrt{\mathbb{E}\{\|\mathbf{h}_i^0\|^2\} \mathbb{E}\{\|\mathbf{h}_k^0\|^2\}}} \rightarrow 0 \quad \text{as } M \rightarrow \infty. \quad (1.34)$$

For fading channels, different types of convergence can be considered in (1.34). Herein, we consider almost sure convergence, also known as convergence with probability one, but the literature also contains definitions that build on weaker types of convergence (e.g., convergence in probability). The interpretation of (1.34) is that the channel directions $\mathbf{h}_i^0 / \sqrt{\mathbb{E}\{\|\mathbf{h}_i^0\|^2\}}$ and $\mathbf{h}_k^0 / \sqrt{\mathbb{E}\{\|\mathbf{h}_k^0\|^2\}}$ becomes asymptotically orthogonal. The condition in (1.34) is satisfied for LoS channels as well as for NLoS channels with uncorrelated Rayleigh fading [245]. One can show that the superposition of LoS and NLoS components also satisfies (1.34). Channel measurements with large BS arrays have also confirmed that the UE channels decorrelate as more antennas are added [120, 150]; see

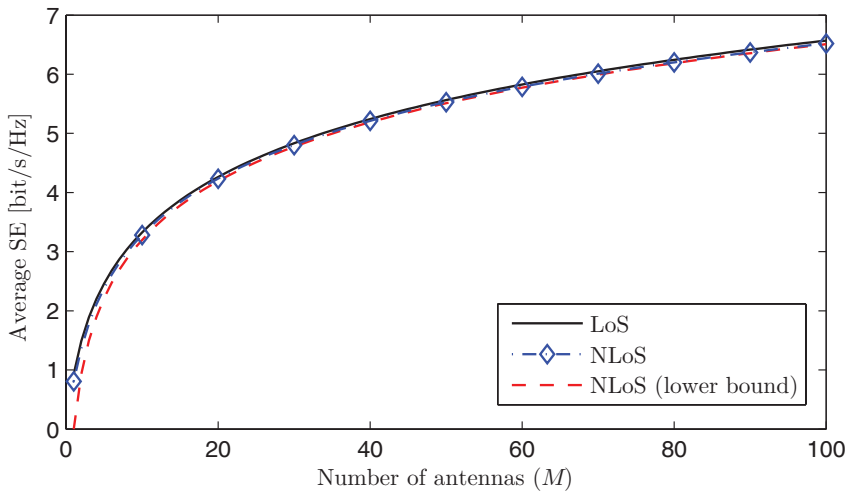


Figure 1.14: Average UL SE as a function of the number of BS antennas M for different channel models. The SNR is $\text{SNR}_0 = 0$ dB and the strength of the inter-cell interference is $\bar{\beta} = -10$ dB.

Section 7.3.4 on p. 342 for further details on channel measurements. Note that (1.34) does not imply that channel responses become orthogonal, in the sense that $(\mathbf{h}_i^0)^H \mathbf{h}_k^0 \rightarrow 0$. We later provide a general definition of asymptotically favorable propagation in Section 2.5.2 on p. 80.

Figure 1.14 shows the average SE as a function of the number of BS antennas when the SNR of the desired UE is fixed at $\text{SNR}_0 = 0$ dB and the strength of the inter-cell interference is $\bar{\beta} = -10$ dB. The LoS case considers a ULA with $d_H = 1/2$ and the results are averaged over different independent UE angles, all being uniformly distributed from 0 to 2π . Despite the rather poor SNR and interference conditions, Figure 1.14 shows that, by going from $M = 1$ to $M = 10$ antennas, one can improve the SE from 0.8 bit/s/Hz to 3.3 bit/s/Hz. This is achieved thanks to the array gain provided by MR combining. We notice that the lower bound on the SE with NLoS propagation in Corollary 1.6 is very tight for $M > 10$. The SE is a monotonically increasing function of M and grows without limit as $M \rightarrow \infty$, in contrast to the power-scaling case analyzed in Section 1.3.2 where the SE saturated in the high-SNR regime. This is once again due to MR combining, which selectively collects more signal energy from the array, without collecting

more interference energy. The difference between LoS and NLoS is negligible in Figure 1.14 because the channel fading has a gradually smaller impact on the mutual information between the transmitted and received signal as more antennas are added [142]. This is attributed to the spatial diversity from having multiple receive antennas that observe independent fading realizations, which are unlikely to all be nearly zero simultaneously. This phenomenon has been known for a long time; in fact, the early works [257, 117] on multiantenna reception focused on combating channel fading. The term *channel hardening* was used in [142] to describe a fading channel that behaves almost deterministically due to spatial diversity.

In the Massive MIMO literature [243], a channel \mathbf{h}_i^0 is said to provide asymptotic channel hardening if

$$\frac{\|\mathbf{h}_i^0\|^2}{\mathbb{E}\{\|\mathbf{h}_i^0\|^2\}} \rightarrow 1 \quad (1.35)$$

almost surely as $M \rightarrow \infty$. The essence of this result is that the channel variations reduce as more antennas are added, in the sense that the normalized instantaneous channel gain converges to the deterministic average channel gain. It is no surprise that deterministic LoS channels provide channel hardening. More importantly, in NLoS propagation,

$$\frac{\|\mathbf{h}_i^0\|^2}{\mathbb{E}\{\|\mathbf{h}_i^0\|^2\}} = \frac{\|\mathbf{h}_i^0\|^2}{M\beta_i^0} \rightarrow 1 \quad (1.36)$$

almost surely as $M \rightarrow \infty$. This is an example of the strong law of large numbers (see Lemma B.12 on p. 411) and can be interpreted as the variations of $\|\mathbf{h}_i^0\|^2/M$ becoming increasingly concentrated around its mean value $\mathbb{E}\{\|\mathbf{h}_i^0\|^2\}/M = \beta_i^0$ as more antennas are added. This does not mean that $\|\mathbf{h}_i^0\|^2$ becomes deterministic; in fact, its standard deviation grows as \sqrt{M} , while the standard deviation of $\|\mathbf{h}_i^0\|^2/M$ goes asymptotically to zero as $1/\sqrt{M}$. Asymptotic channel hardening can be also proved for other channel distributions, as will be further discussed in Section 2.5.1 on p. 78.

The channel hardening effect for the M -dimensional channel $\mathbf{h} \sim \mathcal{N}_{\mathbb{C}}(\mathbf{0}_M, \mathbf{I}_M)$ is illustrated in Figure 1.15. The mean value of the normalized instantaneous channel gain $\|\mathbf{h}\|^2/\mathbb{E}\{\|\mathbf{h}\|^2\}$ and the 10% and 90%

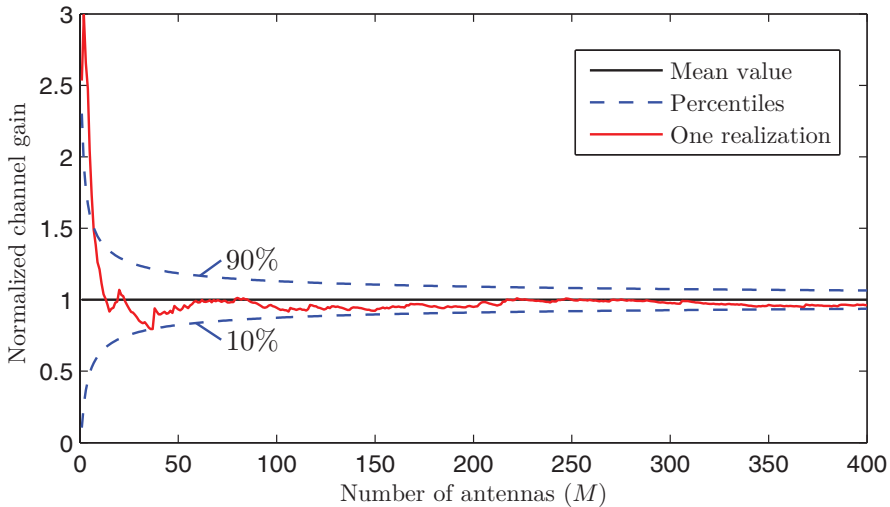


Figure 1.15: Illustration of the channel hardening phenomenon for an M -dimensional channel $\mathbf{h} \sim \mathcal{N}_{\mathbb{C}}(\mathbf{0}_M, \mathbf{I}_M)$. The normalized instantaneous channel gain $\|\mathbf{h}\|^2/\mathbb{E}\{\|\mathbf{h}\|^2\}$ approaches its average value 1 and the standard deviations reduces as $1/\sqrt{M}$.

percentiles are shown for different numbers of antennas. One random realization is also shown. As expected, we have $\|\mathbf{h}\|^2/\mathbb{E}\{\|\mathbf{h}\|^2\} \approx 1$ when M is large. The convergence towards this limit is gradual, but the approximation is reasonably tight for $M \geq 50$.

In summary, increasing the number of BS antennas improves the SE, which even grows without bound when $M \rightarrow \infty$. This is because the BS can process its received signal over the array to selectively increase the signal gain without collecting more interference. In contrast, increasing the transmit power will increase both the signal and interference equally much and give an upper SE limit. Nevertheless, the SE grows only logarithmically with the number of antennas, as $\log_2(M)$, which does not provide sufficient scalability to achieve any order-of-magnitude improvement in SE in future cellular networks.

Remark 1.3 (Physical limits of large arrays). The scaling behavior obtained by the asymptotic analysis above has been validated experimentally for practical antenna numbers [120, 150]. However, it is important to note that the physics prevent us from letting the size of the array grow

indefinitely as $M \rightarrow \infty$, since the propagation environment is enclosed by a finite volume [281]. Ideally, we can cover the surface of this volume with antennas, and neglect any absorption, to collect all signal energy, but we can never collect more energy than was transmitted. This is not an issue when we deal with hundreds or thousands of antennas since a “large” channel gain of -60 dB in cellular communications implies that we need one million antennas to collect all the transmitted energy. In conclusion, the limit $M \rightarrow \infty$ is not physically achievable, but asymptotic analysis can still be suitable for investigating the system behavior at practically large antenna numbers. Other channel distributions than uncorrelated Rayleigh fading are, however, needed to get reliable results; see Section 2.2 on p. 69 and Section 7.3 on p. 329 for further details.

1.3.3 Uplink Space-Division Multiple Access

Increasing the transmit power or using multiple BS antennas can only bring modest improvements to the UL SE, as previously shown. This is because these methods improve the SINR, which appears inside the logarithm of the SE expression, thus the SE increases slowly. We would like to identify a way that improves the SE at the outside of the logarithm instead. Since the logarithmic expressions in Lemmas 1.4 and 1.5 describe the SE of the channel between a particular UE and its serving BS, we can potentially serve multiple UEs, say K UEs, simultaneously in each cell and achieve a sum SE that is the summation of K SE expressions of the types in Lemmas 1.4 and 1.5. An obvious bottleneck of such multiplexing of UEs is the co-user interference that increases with K and now appears also within each cell. The intra-cell interference can be much stronger than the inter-cell interference and needs to be suppressed if a K -fold increase in SE is actually to be achieved.

Space-division multiple access (SDMA) was conceived in the late 1980s and early 1990s [349, 308, 17, 280, 125, 373] to handle the co-user interference in a cell by using multiple antennas at the BS to reject interference by spatial processing. Multiple field-trials were carried out in the 1990s, using (at least) up to ten antennas [15, 96, 16]. The

information-theoretic capacity¹⁴ of these systems was characterized in the early 2000s and described in [74, 129, 335, 342, 366, 127] for single-cell systems, where the terminology “multiuser MIMO” was used. Note that the K UEs are the multiple inputs and the M BS antennas are the multiple outputs, thus the MIMO terminology is used irrespective of how many antennas each UE is equipped with.¹⁵ Extensions of multiuser MIMO to cellular networks have been developed and surveyed in papers such as [276, 33, 294, 46, 126, 208], but the exact capacity is hard to obtain in this case.

We will now analyze a cellular network with UL SDMA transmission by assuming that there are K active UEs in each cell, as previously illustrated in Figure 1.8. The channel response between the k th desired UE in cell 0 and the serving BS is denoted by $\mathbf{h}_{0k}^0 \in \mathbb{C}^M$ for $k = 1, \dots, K$, while the channel responses from the interfering UEs in cell 1 to the BS in cell 0 are denoted by $\mathbf{h}_{1i}^0 \in \mathbb{C}^M$ for $i = 1, \dots, K$. Notice that the subscript still indicates the identity of the UE, while the superscript is the index of the receiving BS. The received multiantenna UL signal in (1.22) is then generalized to

$$\mathbf{y}_0 = \underbrace{\sum_{k=1}^K \mathbf{h}_{0k}^0 s_{0k}}_{\text{Desired signals}} + \underbrace{\sum_{k=1}^K \mathbf{h}_{1k}^0 s_{1k}}_{\text{Interfering signals}} + \underbrace{\mathbf{n}_0}_{\text{Noise}} \quad (1.37)$$

where $s_{jk} \sim \mathcal{N}_{\mathbb{C}}(0, p)$ is the signal transmitted by the k th UE in cell j and the receiver noise $\mathbf{n}_0 \sim \mathcal{N}_{\mathbb{C}}(\mathbf{0}_M, \sigma^2 \mathbf{I}_M)$ is the same as before.

We consider the same LoS and NLoS propagation models as before. More precisely, the LoS channel response for UE k in cell j is

$$\mathbf{h}_{jk}^0 = \sqrt{\beta_j^0} \left[1 \quad e^{2\pi j d_H \sin(\varphi_{jk}^0)} \quad \dots \quad e^{2\pi j d_H (M-1) \sin(\varphi_{jk}^0)} \right]^T \quad (1.38)$$

¹⁴When there are K UEs in the network, the conventional one-dimensional capacity notion generalizes to a K -dimensional capacity region that represents the set of capacities that the K UEs can achieve simultaneously. The sum capacity represents one point in this region and has gained particular traction since it is the one-dimensional metric that describes the aggregate capacity of the network. This and other operating points are further described in Section 7.1 on p. 299.

¹⁵The terminology “multiuser SIMO” was used in the 1990s for the case of SDMA with single-antenna UEs [254], but nowadays the information-theoretic multiuser MIMO terminology dominates and it is adopted in this monograph.

where $\varphi_{jk}^0 \in [0, 2\pi)$ is the azimuth angle relative to the boresight of the BS array in cell 0. In the NLoS case, the corresponding channel response between UE k in cell j and the BS in cell 0 is defined as

$$\mathbf{h}_{jk}^0 \sim \mathcal{N}_{\mathbb{C}}\left(\mathbf{0}_M, \beta_j^0 \mathbf{I}_M\right) \quad (1.39)$$

and assumed to be statistically independent between UEs. Recall that we use the Wyner model in which, for simplicity, the average channel gain β_j^0 is assumed to be the same for all UEs in cell j .

Since the BS in cell 0 receives a superposition of the signals transmitted by its K desired UEs, it needs to process the received signal in (1.37) to separate the UEs in the spatial domain—simply speaking, by directing its hearing towards the location of each desired UE. The separation of UEs is more demanding in SDMA than in conventional time-frequency multiplexing of UEs, because it requires the BS to have knowledge of the channel responses [127]. For example, the BS in cell 0 can use knowledge of its k th UE's channel response to tailor a receive combining vector $\mathbf{v}_{0k} \in \mathbb{C}^M$ to this UE channel. This vector is multiplied with the received signal in (1.37) to obtain

$$\mathbf{v}_{0k}^H \mathbf{y}_0 = \underbrace{\mathbf{v}_{0k}^H \mathbf{h}_{0k}^0 s_{0k}}_{\text{Desired signal}} + \underbrace{\sum_{\substack{i=1 \\ i \neq k}}^K \mathbf{v}_{0k}^H \mathbf{h}_{0i}^0 s_{0i}}_{\text{Intra-cell interference}} + \underbrace{\sum_{i=1}^K \mathbf{v}_{0k}^H \mathbf{h}_{1i}^0 s_{1i}}_{\text{Inter-cell interference}} + \underbrace{\mathbf{v}_{0k}^H \mathbf{n}_0}_{\text{Noise}}. \quad (1.40)$$

The purpose of the receive combining is to make the desired signal much stronger than the sum of interfering signals and noise. MR combined with

$$\mathbf{v}_{0k} = \mathbf{h}_{0k}^0 \quad (1.41)$$

is a popular suboptimal choice since it maximizes the relative power $|\mathbf{v}_{0k}^H \mathbf{h}_{0k}^0|^2 / \|\mathbf{v}_{0k}\|^2$ of the desired signal, but it is not the optimal choice when there are interfering signals [28, 348, 349]. The receive combining design for multiuser MIMO is analytically similar to multiuser detection in code-division multiple access (CDMA) [202, 205, 106] and the key methods were developed at roughly the same time. In Section 4.1 on p. 122, we will show that it is the *multicell minimum mean-squared*

error (*M*-MMSE) combining vector

$$\mathbf{v}_{0k} = p \left(p \sum_{i=1}^K \mathbf{h}_{0i}^0 (\mathbf{h}_{0i}^0)^H + p \sum_{i=1}^K \mathbf{h}_{1i}^0 (\mathbf{h}_{1i}^0)^H + \sigma^2 \mathbf{I}_M \right)^{-1} \mathbf{h}_{0k}^0 \quad (1.42)$$

that maximizes the UL SE in cellular networks. This combining scheme has received its name from the fact that it also minimizes the mean-squared error (MSE) $\mathbb{E}\{|s_{0k} - \mathbf{v}_{0k}^H \mathbf{y}_0|^2\}$ between the desired signal s_{0k} and the receive combined signal $\mathbf{v}_{0k}^H \mathbf{y}_0$, where the expectation is with respect to the transmit signals (while the channels are considered deterministic). Interfering signals from all cells are taken into account in *M*-MMSE combining and the matrix inverse in (1.42) has a role similar to that of a whitening filter in classic signal processing [175]. *M*-MMSE combining maximizes the SINR by finding the best balance between amplifying the desired signal and suppressing interference in the spatial domain. The price to pay is the increased computational complexity from inverting a matrix and the need to learn the matrix that is inverted in (1.42).

The next lemma provides closed-form SE expressions for the case of MR combining. *M*-MMSE combining will be studied by simulations.

Lemma 1.7. If the BS in cell 0 knows the channel responses of all UEs and applies MR combining to detect the signals from each of its K desired UEs, then an achievable UL sum SE [bit/s/Hz/cell] in the LoS case is

$$\text{SE}_0^{\text{LoS}} = \sum_{k=1}^K \log_2 \left(1 + \frac{M}{\sum_{\substack{i=1 \\ i \neq k}}^K g(\varphi_{0k}^0, \varphi_{0i}^0) + \bar{\beta} \sum_{i=1}^K g(\varphi_{0k}^0, \varphi_{1i}^0) + \frac{1}{\text{SNR}_0}} \right) \quad (1.43)$$

with $g(\cdot, \cdot)$ being defined in (1.28).

With NLoS channels, an achievable UL sum SE [bit/s/Hz/cell] and

a closed-form lower bound are

$$\begin{aligned} \text{SE}_0^{\text{NLoS}} &= \sum_{k=1}^K \mathbb{E} \left\{ \log_2 \left(1 + \frac{p \|\mathbf{h}_{0k}^0\|^2}{\sum_{\substack{i=1 \\ i \neq k}}^K p \frac{|(\mathbf{h}_{0k}^0)^H \mathbf{h}_{0i}^0|^2}{\|\mathbf{h}_{0k}^0\|^2} + \sum_{i=1}^K p \frac{|(\mathbf{h}_{0k}^0)^H \mathbf{h}_{1i}^0|^2}{\|\mathbf{h}_{0k}^0\|^2} + \sigma^2} \right) \right\} \\ &\geq K \log_2 \left(1 + \frac{M-1}{(K-1) + K\bar{\beta} + \frac{1}{\text{SNR}_0}} \right). \end{aligned} \quad (1.44)$$

Proof. The proof is available in Appendix C.1.6 on p. 434. \square

The sum SE expressions in Lemma 1.7 have similar forms as the ones in Lemma 1.5 and Corollary 1.6, but are more complicated due to the addition of intra-cell interference and the greater amount of inter-cell interference. In the LoS case, SDMA results in the summation of K SE expressions, one per desired UE. The desired signal gains inside the logarithms increase linearly with M and thus every UE experiences the full array gain when using MR combining. The drawback of SDMA is seen from the denominator, where the interference terms contain contributions from $K-1$ intra-cell UEs and K inter-cell UEs. Each interference term has the same form as in the single-user case in Lemma 1.5, thus one can expect the interference to be the lowest when the UEs have well-separated angles (to avoid the worst cases illustrated in Figure 1.12). Recall from (1.30) that the function $g(\varphi, \psi)$ decreases as $1/M$ for any $\sin(\varphi) \neq \sin(\psi)$. In conjunction with the array gain of the desired signal, we can thus serve multiple UEs and still maintain roughly the same SINR per UE if M is increased proportionally to \sqrt{K} to counteract the increased interference.¹⁶

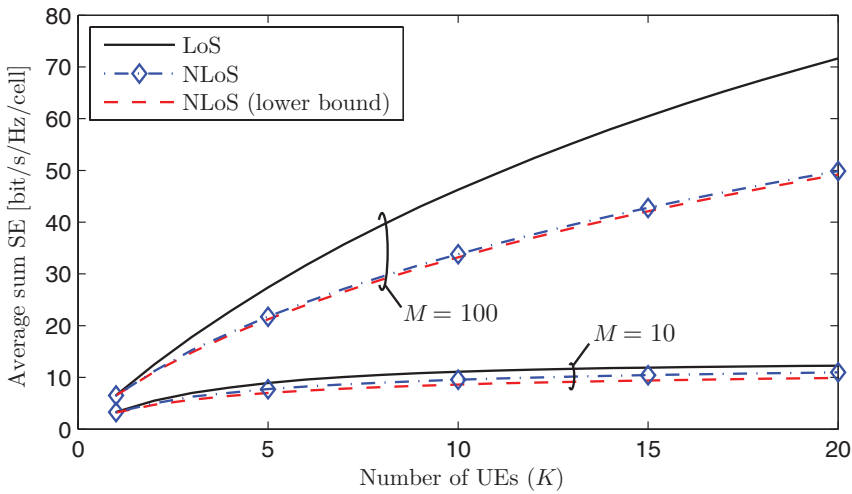
The NLoS case in Lemma 1.7 generalizes the lower bound in Corollary 1.6 to $K \geq 1$ and the bound is tight for $M \gg 1$. An exact closed-form expression similar to (1.29) can also be obtained, but it contains many summations and is omitted since it does not provide

¹⁶To obtain this scaling behavior, we notice that the desired signal power grows as M and the interference power is proportional to K/M , due to the bound in (1.30). The signal-to-interference ratio becomes M^2/K and thus it is sufficient to scale M proportionally to \sqrt{K} to achieve a constant signal-to-interference ratio as K grows.

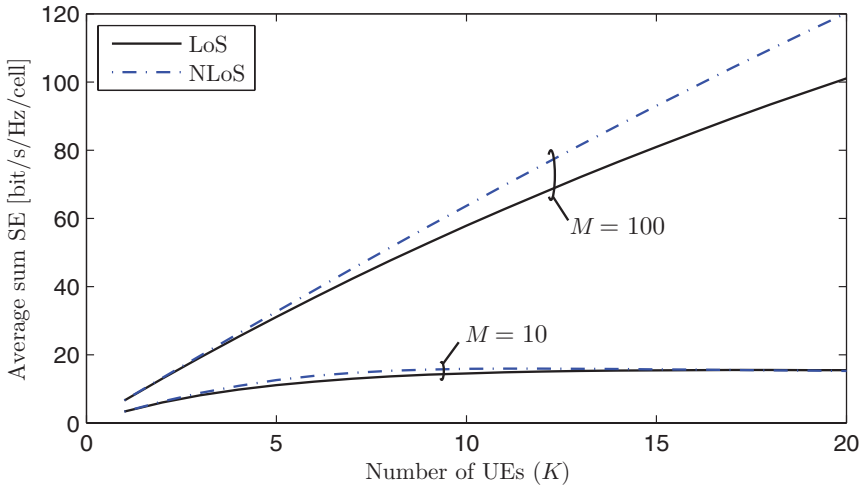
any additional insight. The gain from SDMA is easily seen from (1.44); there is a factor K in front of the logarithm that shows that the sum SE increases proportionally to the number of UEs. This multiplicative factor is known as the *multiplexing gain* and achieving this gain is the main point with SDMA. Inside the logarithm, the desired signal power increases linearly with M , while the intra-cell interference power $K - 1$ and the inter-cell interference power $K \bar{\beta}$ increase linearly with K . This means that, as we add more UEs, we can counteract the increasing interference by adding a proportional amount of additional BS antennas; more precisely, we can maintain roughly the same SINR per UE by increasing M jointly with K to keep the antenna-UE ratio M/K fixed. Interestingly, this means that more antennas are needed to suppress interference with MR combining in the NLoS case than in the LoS case, where M only needs to increase as \sqrt{K} . The explanation is that all interfering UEs cause substantial interference in the NLoS case, while only the ones with sufficiently similar angles to the desired UE does that in the LoS case (and the angular interval where this happens decreases with M).

To exemplify these behaviors, Figure 1.16 shows the average sum SE as a function of the number of UEs per cell, for either $M = 10$ or $M = 100$ antennas. The sum SE with MR combining is shown in Figure 1.16a based on the analytic formulas from Lemma 1.7, while Monte-Carlo simulations are used for M-MMSE combining in Figure 1.16b. In both cases, the SNR is fixed at $\text{SNR}_0 = 0$ dB and the strength of the inter-cell interference is $\bar{\beta} = -10$ dB. The antenna spacing is $d_H = 1/2$ in the LoS case and the results are averaged over different independent UE angles, all being uniformly distributed from 0 to 2π .

Figure 1.16 shows that the sum SE is a slowly increasing function of K in the case of $M = 10$, because the BS does not have enough spatial degrees of freedom to separate the UEs—neither by MR nor by M-MMSE combining. The behavior is completely different when $M = 100$ antennas are used since the channel response of each UE is then a 100-dimensional vector but there are only up to 20 UEs per cell so the UE channels only span a small portion of the spatial dimensions that the BS can resolve. Consequently, the sum SE increases almost



(a) MR combining.



(b) M-MMSE combining.

Figure 1.16: Average UL sum SE as a function of the number of UEs per cell for different combining schemes, different channel models, and either $M = 10$ or $M = 100$ BS antennas. The SNR is $\text{SNR}_0 = 0$ dB and the strength of the inter-cell interference is $\bar{\beta} = -10$ dB. The sum SE grows linearly with K as long as M/K remains large. M-MMSE rejects interference more efficiently than MR.

linearly with the number of UEs and we can achieve a roughly K -fold improvement in sum SE over a single-user scenario. For example, we achieve an SE of 3.3 bit/s/Hz/cell with $(M, K) = (10, 1)$ using MR/M-MMSE combining and can increase it to 71.6 bit/s/Hz/cell with MR and 101 bit/s/Hz/cell with M-MMSE for $(M, K) = (100, 20)$. This corresponds to $21\times$ and $31\times$ gains in SE, respectively. These numbers were selected from the LoS curves, because the NLoS case shows some interesting behaviors that deserve further discussion. The sum SE is considerably lower with NLoS than with LoS when using MR combining, while we get the opposite result when using M-MMSE combining. The reason for this is that each UE is affected by interference from many UEs in the NLoS case, while only a few UEs with similar angles cause strong interference in the LoS case. If the interference is ignored, as with MR combining, the SE is lower in the NLoS case due to the larger sum interference power. However, it is easier for M-MMSE combining to reject interference in NLoS than in LoS, where there might be a few UEs with channels that are nearly parallel to the desired UE's channel. That is why the SE is higher in the NLoS when using M-MMSE.

We now consider cases wherein M is increased proportionally to K , to suppress the inter-user interference that increases with K . The proportionality constant M/K is called *antenna-UE ratio*. Figure 1.17 shows the sum SE obtained by M-MMSE combining, as a function of K for different antenna-UE ratios: $M/K \in \{1, 2, 4, 8\}$. The SE grows almost linearly with K in all four cases, as expected from Lemma 1.7. The steepness of the curves increases as M/K increases, since it becomes easier to suppress the interference when $M \gg K$. Looking at the NLoS case with $K = 10$, the first doubling of the number of antennas (from $M/K = 1$ to $M/K = 2$) gives a 94% gain in SE, while the second doubling gives another 51% gain and the third doubling gives yet another 29% gain. Since the relative improvements are decaying, we say that $M/K \geq 4$ is the preferred operating regime for multiuser MIMO.¹⁷ The LoS and NLoS cases once again provide comparable results.

¹⁷We will revisit this statement in Section 7.2.2 on p. 321, where scheduling is discussed. By taking the channel estimation overhead into account, we will show that for a given M there is a particular K that maximizes the sum SE.

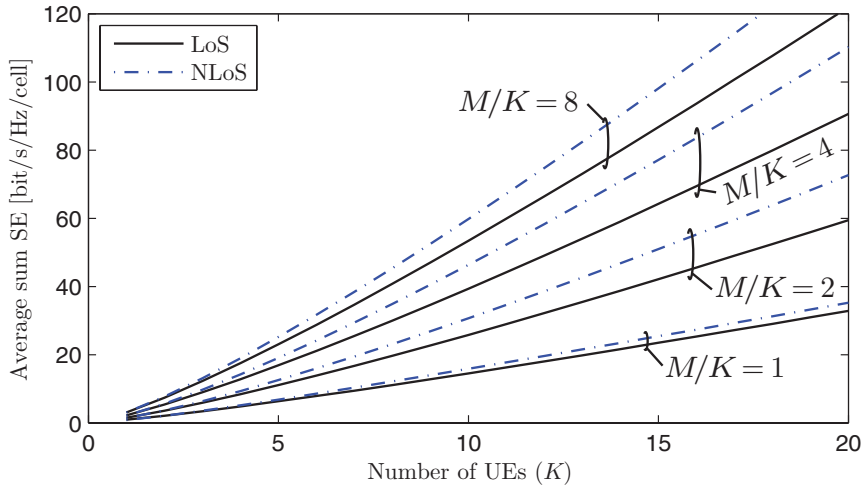


Figure 1.17: Average UL sum SE with M-MMSE combining as a function of the number of UEs per cell, when the number of antennas increases with K with different fixed antenna-UE ratios M/K . The SNR is $\text{SNR}_0 = 0$ dB and the strength of the inter-cell interference is $\bar{\beta} = -10$ dB. The sum SE grows as M/K increases.

M-MMSE is the linear receive combining scheme that maximizes the SE. The basic characteristic of linear schemes is that they treat interference as spatially colored noise. From a channel capacity perspective, this is only optimal when the interference between each pair of UEs is sufficiently small [230, 296, 20, 21, 295]. The information theory for interference channels proves that strong interference sources should be canceled using non-linear receiver processing schemes, such as successive interference cancellation, before the desired signals are decoded [314]. However, such schemes are rather impractical, since one needs to store large blocks of received signals and then decode the UEs' data sequentially, leading to high complexity, large memory requirements, and latency issues. If we would limit ourselves to linear receiver processing schemes, how large is the performance loss?

Figure 1.18 quantifies the performance loss of linear receiver processing as compared to non-linear receiver processing, as a function of the number of UEs. The figure shows the ratio between the average UL sum SE achieved by M-MMSE combining and by successive interfer-

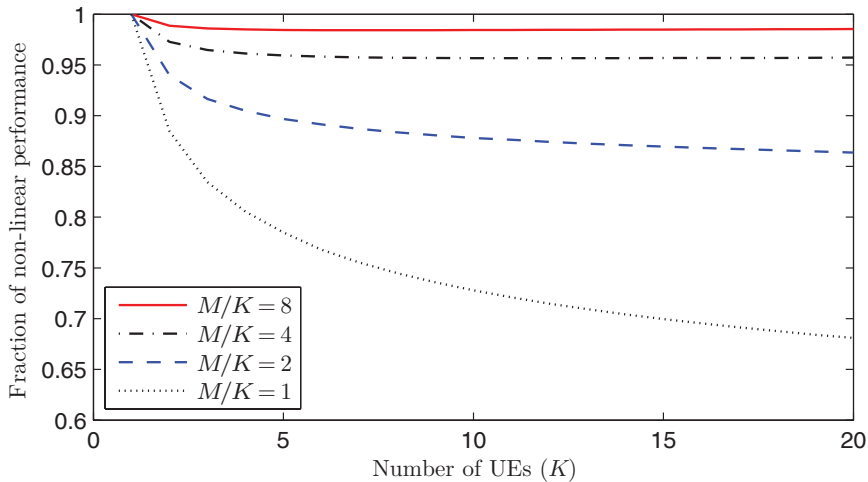


Figure 1.18: Ratio between the average UL sum SE achieved with M-MMSE combining and with non-linear receiver processing, as a function of the number of UEs per cell. The number of antennas M increases with K for different fixed antenna-UE ratios: $M/K \in \{1, 2, 4, 8\}$. The SNR is $\text{SNR}_0 = 0$ dB and the strength of the inter-cell interference is $\bar{\beta} = -10$ dB.

ence cancellation, where the intra-cell signals are decoded sequentially while treating inter-cell interference as noise [314]. The setup is the same as in the previous figure, but we only consider NLoS propagation for simplicity. The non-linear scheme performs much better for $M/K = 1$, in which case M-MMSE only achieves 70%–80% of its sum SE. The performance difference reduces quickly as M/K increases. For $M/K = 4$ and $M/K = 8$, we only lose a few percentages in sum SE by using M-MMSE instead of the non-linear scheme, even if there is as much as 20 UEs. The interpretation is that the favorable propagation, achieved by having many BS antennas, makes the interference between each pair of UEs sufficiently small to make linear receiver processing nearly optimal. When there are many active UEs, the total interference caused to a UE can indeed be large, but nevertheless, linear processing performs well since the interference between each pair of UEs is small. Similar observations have been made in the overview articles [50, 209, 210].

In summary, UL SDMA transmission can increase the sum SE per cell by more than one order-of-magnitude. This is achieved by serving K UEs simultaneously and increasing the number of BS antennas to achieve an array gain that counteracts the increased interference. This leads to an operating regime with antenna-UE ratio $M/K \geq c$, for some preferably large value c , where we can provide K -fold gains in sum SE. This is the type of highly scalable SE improvements that are needed to handle much higher data volumes in the coverage tier of future cellular networks. Note that the SE per UE is not dramatically changed, thus the use of more spectrum is still key to improving the throughput per UE. The sum SE gains are achievable with both LoS and NLoS channels, using either MR combining that maximizes the array gain or M-MMSE combining that also suppresses interference to maximize the SE. Non-linear processing schemes can only bring minor performance improvements in the preferable operating regime and are therefore not considered in the remainder of this monograph.

Remark 1.4 (Multiantenna UEs). We have shown above that SDMA transmission with many single-antenna UEs and an even larger number of BS antennas achieves high sum SE. What would happen if the UEs were also equipped with multiple antennas? The cost, size, and complexity of each UE will certainly increase. The positive effect is that a UE with N_{UE} antennas can transmit up to N_{UE} simultaneous data streams to its serving BS. From the BS's perspective, each stream can be treated as a signal from a separate "virtual" UE and the signal can only be distinguished if it has a different spatial directivity than the other signals. This means that the vector that describes the channel response from the BS to the n th antenna of a particular UE should be nearly orthogonal to the other antennas' channel responses (for $n = 1, \dots, N_{\text{UE}}$). In NLoS propagation, this is achieved when the UE antennas observe nearly uncorrelated random channel realizations, which is possible in a rich scattering environment with an adequate antenna spacing. Channel orthogonality is much harder to achieve in LoS propagation since the angle between the BS and a UE in the far-field is roughly the same for all the antennas at the UE; recall from (1.28) that the inner product $g(\varphi, \psi)$ between LoS channel responses with angles φ

and ψ is large whenever $\varphi \approx \psi$. Hence, the benefit of sending multiple data signals cannot be exploited in propagation environments with only a dominating LoS path. The UE can, however, achieve an additional array gain proportional to N_{UE} by coherently combining the signals over N_{UE} antennas, if it knows the channel responses. This monograph focuses on single-antenna UEs, but the results can be readily applied to N_{UE} -antenna UEs by viewing them as N_{UE} virtual UEs that transmit N_{UE} separate signals, representing different data streams. The paper [194] considers multi-antenna UEs and shows that the SE is maximized when a particular number of data streams are received/transmitted per cell (see Section 7.2.2 on p. 321 for a further discussion). Suppose this number of streams is K_{stream}^* and that each UE is allocated as many streams as it has antennas. The analysis in [194] indicates that roughly the same sum SE is achieved when having K UEs that are equipped with N_{UE} antennas and when having $N_{\text{UE}}K$ single-antenna UEs. Hence, the distinct advantage of having multiple UE antennas occurs at low user load, $K < K_{\text{stream}}^*$, where the only way to send all K_{stream}^* streams is to allocate multiple streams per UE.

1.3.4 Downlink Space-Division Multiple Access

This section has so far focused on the UL, where we have identified SDMA as a suitable way to improve the SE by an order-of-magnitude or more. We will now describe how SDMA is applied in the DL. We continue to use the Wyner model, which is illustrated in Figure 1.19 for the DL. The main difference from the UL in Figure 1.8 is that the signals are transmitted from BSs instead of from UEs. There are K active UEs in each cell and the serving BS sends a separate signal to each of them using linear transmit precoding from an array of M antennas. Precoding means that each data signal is sent from all antennas, but with different amplitude and phase to direct the signal spatially. This is also called beamforming, but we refrain from using this terminology since it can give the misleading impression that a signal beam is always formed in a particular angular direction and that analog phase-shifters are used. In contrast, precoding means that each antenna's transmit signal is generated separately in the digital baseband, which gives full

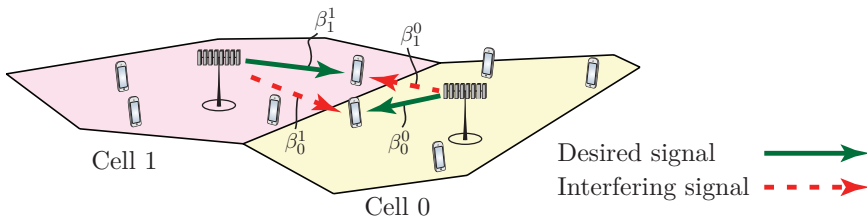


Figure 1.19: Illustration of the notion of desired and interfering DL signals in a two-cell network. In the Wyner model, every UE in cell 0 has the same value of the average channel gains β_0^0 and β_1^0 , while every UE in cell 1 has the same value of β_0^1 and β_1^1 .

flexibility in the signal generation.¹⁸ Angular beams are a special case of precoding that is useful in LoS propagation, but for NLoS channels the transmitted signal might not have a distinct angular directivity, but can still be precoded such that the multipath components are received coherently at the UE.

Similar to the UL, the DL channel response between the BS in cell 0 and its k th desired UE is denoted by $(\mathbf{h}_{0k}^0)^H$ for $k = 1, \dots, K$. The DL channel response between the BS in cell 1 and the k th UE in cell 0 is denoted by $(\mathbf{h}_{0k}^1)^H$. The transpose represents the fact that we are now looking at the channel from the opposite direction, while the complex conjugate is added for notational convenience. There is no such conjugation in practice, but it simplifies the notation and does not change the SE.

The received DL signal $z_{0k} \in \mathbb{C}$ at UE k in cell 0 is modeled as

$$\begin{aligned}
 z_{0k} = & \underbrace{(\mathbf{h}_{0k}^0)^H \mathbf{w}_{0k} s_{0k}}_{\text{Desired signal}} + \underbrace{\sum_{\substack{i=1 \\ i \neq k}}^K (\mathbf{h}_{0k}^0)^H \mathbf{w}_{0i} s_{0i}}_{\text{Intra-cell interference}} \\
 & + \underbrace{\sum_{i=1}^K (\mathbf{h}_{0k}^1)^H \mathbf{w}_{1i} s_{1i}}_{\text{Inter-cell interference}} + \underbrace{n_{0k}}_{\text{Noise}} \quad (1.45)
 \end{aligned}$$

where $s_{jk} \sim \mathcal{N}_{\mathbb{C}}(0, p)$ is the signal transmitted to the k th UE in cell j

¹⁸An animation of precoding is found at <https://youtu.be/XBb481RNqGw>.

and $\mathbf{w}_{jk} \in \mathbb{C}^M$ is the corresponding unit-norm precoding vector (i.e., $\|\mathbf{w}_{jk}\| = 1$) that determines the spatial directivity of the signal. The receiver noise at this UE is denoted by $n_{0k} \sim \mathcal{N}_{\mathbb{C}}(0, \sigma^2)$.

We consider the same LoS and NLoS propagation models as before. In the LoS case, we have the multiple-input single-output (MISO) channel response

$$\mathbf{h}_{jk}^l = \sqrt{\beta_j^l} \left[1 \ e^{2\pi j d_H \sin(\varphi_{jk}^l)} \ \dots \ e^{2\pi j d_H (M-1) \sin(\varphi_{jk}^l)} \right]^T \quad (1.46)$$

between UE k in cell j and the BS in cell l , where $\varphi_{jk}^l \in [0, 2\pi)$ is the azimuth angle relative to the boresight of the transmitting BS array. In the NLoS case, the corresponding channel response is

$$\mathbf{h}_{jk}^l \sim \mathcal{N}_{\mathbb{C}} \left(\mathbf{0}_M, \beta_j^l \mathbf{I}_M \right) \quad (1.47)$$

and is assumed to be independent between UEs. Recall from (1.12) that we use the same notation, $\bar{\beta} = \beta_0^1 / \beta_0^0$, for the relative strength of inter-cell interference in the DL as in the UL.

The precoding vectors \mathbf{w}_{jk} , for $k = 1, \dots, K$ and $j = 0, 1$, can be selected in a variety of ways. As seen from the received signal in (1.45), each UE is affected by all the precoding vectors; the own precoding vector is multiplied with the channel response from the serving BS, while the other ones cause interference and are multiplied with the channel response from the corresponding transmitting BSs. Hence, the precoding vectors should be selected carefully in the DL, based on knowledge of the channel responses. We will study this in detail in Section 4.3 on p. 162, but for now we consider MR precoding with

$$\mathbf{w}_{jk} = \frac{\mathbf{h}_{jk}^j}{\|\mathbf{h}_{jk}^j\|}. \quad (1.48)$$

This precoding vector focuses the DL signal at the desired UE to achieve the maximum array gain, similar to MR combining in the UL. Note that $\|\mathbf{w}_{jk}\|^2 = 1$, which implies that the total transmit power of the BS is constant, irrespective of the number of antennas. Consequently, the transmit power per BS antenna decreases roughly as $1/M$. The following lemma provides SE expressions for MR precoding.

Lemma 1.8. If the BSs use MR precoding and the UEs in cell 0 know their respective effective channels $(\mathbf{h}_{0k}^0)^H \mathbf{w}_{0k}$ and the interference variance, then an achievable DL sum SE [bit/s/Hz/cell] in the LoS case is

$$\text{SE}_0^{\text{LoS}} = \sum_{k=1}^K \log_2 \left(1 + \frac{M}{\sum_{\substack{i=1 \\ i \neq k}}^K g(\varphi_{0i}^0, \varphi_{0k}^0) + \bar{\beta} \sum_{i=1}^K g(\varphi_{1i}^1, \varphi_{0k}^1) + \frac{1}{\text{SNR}_0}} \right). \quad (1.49)$$

With NLoS channels, a DL sum SE [bit/s/Hz/cell] and a closed-form lower bound are

$$\begin{aligned} \text{SE}_0^{\text{NLoS}} &= \sum_{k=1}^K \mathbb{E} \left\{ \log_2 \left(1 + \frac{p \|\mathbf{h}_{0k}^0\|^2}{\sum_{\substack{i=1 \\ i \neq k}}^K p \frac{|\mathbf{h}_{0k}^0\|^2 \|\mathbf{h}_{0i}^0\|^2}{\|\mathbf{h}_{0i}^0\|^2} + \sum_{i=1}^K p \frac{|\mathbf{h}_{0k}^1\|^2 \|\mathbf{h}_{1i}^1\|^2}{\|\mathbf{h}_{1i}^1\|^2} + \sigma^2} \right) \right\} \\ &\geq K \log_2 \left(1 + \frac{(M-1)}{(K-1) \frac{M-1}{M} + K \bar{\beta} + \frac{1}{\text{SNR}_0}} \right). \end{aligned} \quad (1.50)$$

Proof. The proof is available in Appendix C.1.7 on p. 435. \square

The DL sum SE in this lemma is very similar to the UL sum SE in Lemma 1.7. The NLoS case only differs in the extra multiplicative term $\frac{M-1}{M}$ in the denominator of (1.50), which is almost one for large M . The LoS case only differs in the angles that appear in each expression; all angles in the UL are from UEs to the BS in cell 0, while the DL includes both the angles from the desired UE to all transmitting BSs and the angles from the other UEs that these BSs are transmitting to (representing the directivity of each DL signal). Some of the similarities are induced by the Wyner model since we have assumed that the inter-cell interference is equally strong in the UL and DL (i.e., $\beta_0^0 = \beta_1^0$); in general, there are also differences in the average channel gains, as we elaborate on in Section 4.3.2 on p. 167. Nonetheless, when using the Wyner model, the UL simulations in Figures 1.16–1.17 are representative

for the DL performance as well—no additional simulations are needed to uncover the basic behaviors.

The array gain is M with MR processing in both UL and DL, but it is obtained differently. In the UL, the BS makes M observations of the desired signal over its M receive antennas, each being corrupted by an independent noise term. By coherently combining the M signal components, the signal power grows proportionally to M while the noise realizations add incoherently so that the noise variance is unchanged. In the DL, the M transmit antennas have different channels to the receiving UE. Since the total transmit power is fixed, the signal power per antenna is reduced as $1/M$ and the signal amplitude as $1/\sqrt{M}$. With precoding that makes the M transmitted signal components add coherently at the UE, the received signal's amplitude grows as $M/\sqrt{M} = \sqrt{M}$ and the received signal power therefore grows as M .

1.3.5 Acquiring Channel State Information

The channel responses, \mathbf{h}_{jk}^j , are utilized by BS j to process the UL and DL signals. We have assumed so far that the channel responses are known perfectly, but in practice, these vectors need to be estimated regularly. More precisely, the channel responses are typically only constant for a few milliseconds and over a bandwidth of a few hundred kHz. A random distribution is commonly used to model the channel variations. The current set of channel response realizations is called the *channel state* and the knowledge that the BSs have of them is referred to as the *channel state information (CSI)*. Full statistical CSI regarding the distributions¹⁹ of random variables is assumed to be available anywhere in the network, while instantaneous CSI regarding the current channel realizations need to be acquired at the same pace as the channels change. The main method for CSI acquisition is pilot signaling, where a predefined pilot signal is transmitted from an antenna. As illustrated in Figure 1.20, any other antenna in the network can simultaneously receive the transmission and compare it with the known pilot signal to

¹⁹It is in many cases sufficient to know the first- and second-order moments of the random variables, but for simplicity we assume that the full distributions are available.

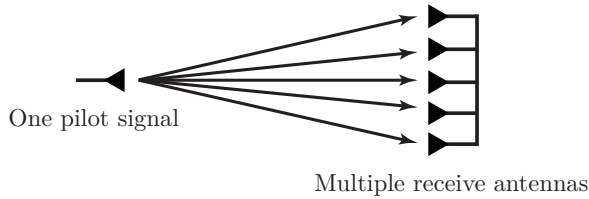


Figure 1.20: When an antenna is transmitting a pilot signal, any number of receive antennas can simultaneously receive the pilot signal and use it to estimate their respective channels to the transmitter.

estimate the channel from the transmitting antenna. If we instead need to estimate the channel response from two transmitting antennas, two orthogonal pilot signals are generally required to separate the signals from the two antennas [182, 195, 38]. The orthogonality is achieved by spending two samples on the transmission, as further explained in Section 3.1 on p. 91. The number of orthogonal pilot signals is proportional to the number of transmit antennas, while any number of receive antennas can “listen” to the pilots simultaneously and estimate their individual channels to the transmitters.

Every pilot signal that is transmitted could have been a signal that carried payload data, thus we want to minimize this overhead caused by pilot signaling. In SDMA, there are key differences between UL and DL in terms of the overhead for channel acquisition. There are K single-antenna UEs per cell and thus K pilot signals are required to estimate the channels in the UL. Similarly, there are M antennas at the BS and thus M pilot signals are required to estimate the channels in the DL. Since having an antenna-UE ratio $M/K \geq 4$ is the preferable operating regime in SDMA, the overhead from sending DL pilots is typically much larger than that from UL pilots. A BS antenna is only useful if we know the channel response, which limits the number of BS antennas that we can utilize in practice, unless we can find a workaround.

The UL and DL can be separated in either time or frequency; see Figure 1.21. If the UL and DL are separated in time, using a time-division duplex (TDD) protocol, then the channel responses are *reciprocal*²⁰ [254].

²⁰The physical propagation channels are reciprocal, but the transceiver chains are

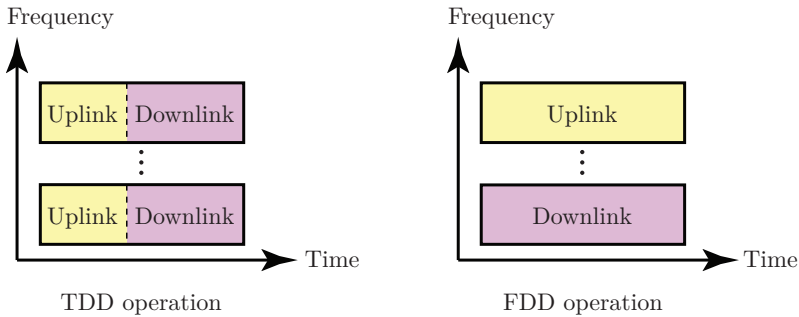


Figure 1.21: Illustration of two ways to divide a block of time/frequency resources between UL and DL. Each solid box represents a time-frequency block where the channel responses are constant and need to be estimated.

This means that the channel response is the same in both directions and can be estimated at the BS using only K UL pilots. Only the BS in cell j needs to know the complete channel response \mathbf{h}_{jk}^j to its k th UE, while the corresponding UE only needs to know the effective scalar channel $g_{jk} = (\mathbf{h}_{jk}^j)^H \mathbf{w}_{jk}$ that is obtained after precoding. Since the value of g_{jk} is constant as long as the channels are constant, it can be estimated blindly from the DL payload data signals, irrespective of the channel distribution [243].²¹ For example, the BS can use its CSI to adjust the phase of \mathbf{w}_{jk} so that the phase of g_{jk} becomes (nearly) deterministic, thereby mainly the magnitude $|g_{jk}|$ needs to be estimated. Channel hardening improves the estimation quality since the relative variations in $|g_{jk}|/\mathbb{E}\{|g_{jk}|\}$ becomes smaller. Consequently, a TDD protocol only requires K pilots, independently of the number of antennas, M .

If the UL and DL are instead separated in frequency, using a frequency-division duplex (FDD) protocol, then the UL and DL channels are always different and we cannot rely on reciprocity. Hence, we need to send pilots in both UL and DL. In addition, the estimates of the DL channel responses need to be fed back to the BS, to enable DL precoding computation. The feedback overhead is approximately the

generally not fully reciprocal. This is further discussed in Section 6.4.4 on p. 292.

²¹DL pilot signals can be utilized to improve the estimation quality, but this does not necessarily improve the SE since the overhead for channel estimation increases [243].

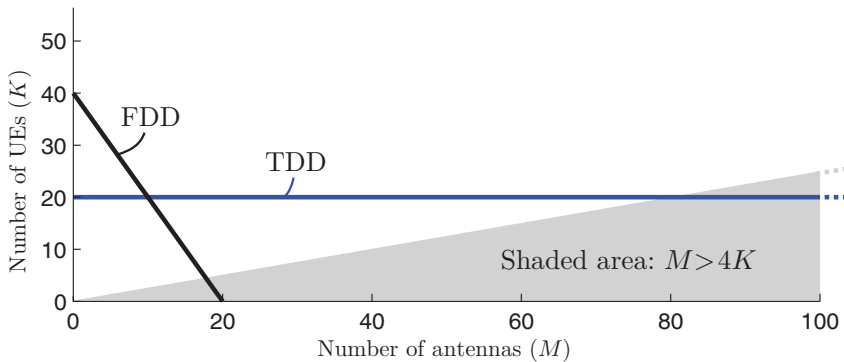


Figure 1.22: Illustration of the operating points (M, K) that are supported by using $\tau_p = 20$ pilots, for TDD and FDD protocols. The shaded area corresponds to the preferable operating points for SDMA systems. The TDD protocol is scalable with respect to the number of antennas and the number of UEs that can be supported is only limited by τ_p .

same as that of sending M additional UL pilot signals.²² The precoded channels $g_{jk} = (\mathbf{h}_{jk}^j)^H \mathbf{w}_{jk}$ can be estimated from the DL signals, as described for TDD above. Hence, an FDD protocol has a pilot/feedback overhead that is equivalent to sending $M + K$ pilots in the UL and M pilots in the DL. To compare this with TDD, suppose the frequency resources in FDD are divided equally between UL and DL. The average pilot overhead of the FDD protocol is then $\frac{M+K+M}{2} = M + \frac{K}{2}$.

We will now illustrate the important difference in pilot dimensionality between TDD and FDD operation. Consider an SDMA system that can afford τ_p pilots. This value determines the combinations of M and K that can be supported. The TDD protocol supports up to $K = \tau_p$ UEs and an arbitrary M . The FDD protocol supports any M and K such that $M + \frac{K}{2} \leq \tau_p$. The operating points supported by these protocols are illustrated in Figure 1.22 for $\tau_p = 20$. The shaded area indicates $M \geq 4K$, which are the operating points attractive for SDMA as discussed in Section 1.3.3 (see for example the results in Figure 1.17). The tradeoff between antennas and UEs caused by the FDD protocol

²²This approximation assumes analog CSI feedback, where UE k sends the value of each element in \mathbf{h}_{jk}^j as a real-valued data symbol and this feedback is multiplexed using SDMA. Quantized digital feedback is another option, but it gives roughly the same overhead if the feedback accuracy should be the same [73].

leads to a very limited intersection with the shaded area. In contrast, the TDD protocol is entirely scalable with respect to M and the number of pilots only limits how many UEs can be supported. Any number of antennas can be used, but preferably we select one of the many operating points that lie in the shaded area.

In summary, SDMA systems should ideally be combined with TDD, by exploiting the reciprocity between UL and DL channels. This is because the required channel acquisition overhead in TDD is K , while it is $M + \frac{K}{2}$ in FDD. The FDD overhead is around 50% larger when $M \approx K$, while it is much larger for $M \gg K$, which is the preferable operating regime for SDMA. Note that it is the channel acquisition needed for DL precoding that differs between TDD and FDD, while the UL works essentially the same.

Remark 1.5 (Channel parameterizations). In some propagation scenarios, the set of possible M -dimensional channel responses can be parameterized using much less than M parameters. A key example is LoS propagation where the model that we used in (1.38) mainly depends on the angle φ_{jk}^0 between the BS and the UE. Instead of transmitting M DL pilots, we can in the LoS case select a set of equally spaced angles between 0 and π and send precoded DL pilot signals only in these directions. If the number of such angles is much smaller than M , then this method can enable FDD operation with reduced pilot overhead and can still give good estimation quality [50]. However, LoS channel parameterizations require the array geometry to be predefined and that the antennas are phase-calibrated, in the sense that the phase drifts incurred by the radio frequency (RF) hardware are known and can be compensated for. In particular, the model in (1.38) is only valid for phase-calibrated ULAs. There are several drawbacks with building a system that strictly relies on channel parameterizations. One is that even if some UE channels can be parameterized efficiently, there might not exist a single low-dimensional parameterization model that applies to all channels—it is sufficient that one part of the cell provides approximately uncorrelated Rayleigh fading to discourage the use of channel parametrization for simplified DL estimation. Another drawback is that practical channels are not bound to follow a particular channel model.

NLoS channels can consist of various multipath components that arrive from different angles and with different phase-rotations, while practical LoS channels contain random reflections and scattering, in addition to the deterministic LoS path. TDD operation is generally preferred because we want to design a network that can operate efficiently in any kind of propagation environment, with any array geometry, and without inter-antenna phase-calibration. However, TDD also has its own specific challenges: *i*) the SNR is slightly lower than in FDD since the power amplifier is only turned on part of the time; *ii*) the transmitter and receiver hardware of an antenna must be calibrated to maintain channel reciprocity (see Section 6.4.4 on p. 292 for a further discussion).

1.4 Summary of Key Points in Section 1

- Users of future networks will demand wireless connectivity with uniform service quality, anywhere at any time.
- The demand for data traffic increases rapidly and calls for higher area throughput in future cellular networks. This can be achieved by cell densification, allocating more frequency spectrum, and/or improving the SE [bit/s/Hz/cell].
- Current and future network infrastructure consists of two key parts: the coverage tier and the hotspot tier. The area throughput needs to be improved in both tiers.
- The coverage tier takes care of coverage, mobility, and guarantees a minimum service quality. To increase the area throughput of this tier, it is preferred to increase the SE, since densification or the use of spectrum at higher frequencies degrade the mobility support and coverage.
- The hotspot tier offloads traffic from the coverage tier, for example, from low-mobility indoor UEs. Densification and the use of new spectrum at higher frequencies are attractive ways to increase the area throughput of this tier, but the SE can be also improved by an array gain.
- The SE of a single UE is a slowly increasing, logarithmic function of the SINR. Only modest SE gains are possible by increasing the SINR (e.g., by using higher transmit power or deploying multiple antennas at the BS).
- A K -fold SE gain is achievable by serving K UEs per cell, on the same time/frequency resources, using SDMA. The number of BS antennas is preferably increased with K to get an array gain that compensates for the increased interference.

- Each BS should have more antennas, M , than UEs, leading to an antenna-UE ratio $M/K > 1$. This makes linear UL receive combining and DL transmit precoding nearly optimal since each interfering UE contributes with relatively little interference.
- When the number of BS antennas is large, the effective channels to the desired UEs are almost deterministic after combining/precoding, although the channel responses are random. This phenomenon is called channel hardening.
- CSI is used by the BS to spatially separate the UEs in UL and DL. The channels are most efficiently estimated with a TDD protocol that utilizes channel reciprocity, since only UL pilot signals are required and no feedback is needed.

References

- [1] 3GPP TR 36.873. 2015. “Study on 3D channel model for LTE”. *Tech. rep.*
- [2] 3GPP TS 25.213. 2006. “Universal Mobile Telecommunications System (UMTS); Spreading and modulation (FDD)”. *Tech. rep.*
- [3] Abramowitz, M. and I. Stegun. 1965. *Handbook of mathematical functions*. Dover Publications.
- [4] Adachi, F., M. T. Feeney, J. D. Parsons, and A. G. Williamson. 1986. “Crosscorrelation between the envelopes of 900 MHz signals received at a mobile radio base station site”. *IEE Proc. F - Commun., Radar and Signal Process.* 133(6): 506–512.
- [5] Ademaj, F., M. Taranetz, and M. Rupp. 2016. “3GPP 3D MIMO channel model: A holistic implementation guideline for open source simulation tools”. *EURASIP J. Wirel. Commun. Netw.* (55): 1–14.
- [6] Adhikary, A., A. Ashikhmin, and T. L. Marzetta. 2017. “Uplink interference reduction in Large Scale Antenna Systems”. *IEEE Trans. Commun.* 65(5): 2194–2206.
- [7] Adhikary, A., J. Nam, J.-Y. Ahn, and G. Caire. 2013. “Joint spatial division and multiplexing—The large-scale array regime”. *IEEE Trans. Inf. Theory.* 59(10): 6441–6463.

- [8] Adhikary, A., E. A. Safadi, M. K. Samimi, R. Wang, G. Caire, T. S. Rappaport, and A. F. Molisch. 2014. "Joint spatial division and multiplexing for mm-wave channels". *IEEE J. Sel. Areas Commun.* 32(6): 1239–1255.
- [9] Adhikary, A., H. S. Dhillon, and G. Caire. 2015. "Massive-MIMO meets HetNet: Interference coordination through spatial blanking". *IEEE J. Sel. Areas Commun.* 33(6): 1171–1186.
- [10] Alexanderson, E. F. W. 1919. "Transatlantic radio communication". *Trans. American Institute of Electrical Engineers.* 38(2): 1269–1285.
- [11] Alkhateeb, A., O. El Ayach, G. Leus, and R. W. Heath. 2013. "Hybrid precoding for millimeter wave cellular systems with partial channel knowledge". In: *Proc. IEEE ITA*. IEEE. 1–5.
- [12] Almers, P., E. Bonek, A. Burr, N. Czink, M. Debbah, V. Degli-Esposti, H. Hofstetter, P. Kyösti, D. Laurenson, G. Matz, *et al.* 2007. "Survey of channel and radio propagation models for wireless MIMO systems". *EURASIP J. Wirel. Commun. Netw.* (1): 1–19.
- [13] Amari, S. V. and R. B. Misra. 1997. "Closed-form expressions for distribution of sum of exponential random variables". *IEEE Trans. Rel.* 46(4): 519–522.
- [14] Anderson, N. 2009. "Paired and unpaired spectrum". In: *LTE - The UMTS Long Term Evolution: From Theory to Practice*. Ed. by S. Sesia, I. Toufik, and M. Baker. Wiley. Chap. 23. 551–583.
- [15] Anderson, S., U. Forssen, J. Karlsson, T. Witzschel, P. Fischer, and A. Krug. 1996. "Ericsson/Mannesmann GSM field-trials with adaptive antennas". In: *Proc. IEE Colloquium on Advanced TDMA Techniques and Applications*.
- [16] Anderson, S., B. Hagerman, H. Dam, U. Forssen, J. Karlsson, F. Kronestedt, S. Mazur, and K. J. Molnar. 1999. "Adaptive antennas for GSM and TDMA systems". *IEEE Personal Commun.* 6(3): 74–86.
- [17] Anderson, S., M. Millnert, M. Viberg, and B. Wahlberg. 1991. "An adaptive array for mobile communication systems". *IEEE Trans. Veh. Technol.* 40(1): 230–236.

- [18] Andrews, J. G., F. Baccelli, and R. K. Ganti. 2011. "A tractable approach to coverage and rate in cellular networks". *IEEE Trans. Commun.* 59(11): 3122–3134.
- [19] Andrews, J. G., X. Zhang, G. D. Durgin, and A. K. Gupta. 2016. "Are we approaching the fundamental limits of wireless network densification?" *IEEE Commun. Mag.* 54(10): 184–190.
- [20] Annapureddy, V. S. and V. V. Veeravalli. 2011a. "Gaussian interference networks: Sum capacity in the low-interference regime and new outer bounds on the capacity region". *IEEE Trans. Inf. Theory.* 55(7): 3032–3050.
- [21] Annapureddy, V. S. and V. V. Veeravalli. 2011b. "Sum capacity of MIMO interference channels in the low interference regime". *IEEE Trans. Inf. Theory.* 57(5): 2565–2581.
- [22] ApS, M. 2016. *MOSEK optimization suite release 8.0.0.42*. URL: <http://docs.mosek.com/8.0/intro.pdf>.
- [23] Ashikhmin, A. and T. Marzetta. 2012. "Pilot contamination precoding in multi-cell large scale antenna systems". In: *IEEE International Symposium on Information Theory Proceedings (ISIT)*. 1137–1141.
- [24] Ashraf, I., F. Boccardi, and L. Ho. 2011. "SLEEP mode techniques for small cell deployments". *IEEE Commun. Mag.* 49(8): 72–79.
- [25] Asplund, H., J.-E. Berg, F. Harrysson, J. Medbo, and M. Riback. 2007. "Propagation characteristics of polarized radio waves in cellular communications". In: *Proc. IEEE VTC-Fall*. 839–843.
- [26] Auer, G., O. Blume, V. Giannini, I. Godor, M. Imran, Y. Jading, E. Katranaras, M. Olsson, D. Sabella, P. Skillermark, and W. Wajda. 2012. *D2.3: Energy efficiency analysis of the reference systems, areas of improvements and target breakdown*. INFSO-ICT-247733 EARTH, ver. 2.0.
- [27] Auer, G., V. Giannini, C. Desset, I. Godor, P. Skillermark, M. Olsson, M. A. Imran, D. Sabella, M. J. Gonzalez, O. Blume, and A. Fehske. 2011. "How much energy is needed to run a wireless network?" *IEEE Wireless Commun.* 18(5): 40–49.

- [28] Baird, C. A. and C. L. Zahm. 1971. "Performance criteria for narrowband array processing". In: *Proc. IEEE Conf. Decision and Control*. 564–565.
- [29] Baumert, L. D. and M. Hall. 1965. "Hadamard matrices of the Williamson type". *Math. Comp.* 19(6): 442–447.
- [30] Bazelon, C. and G. McHenry. 2015. "Mobile broadband spectrum: A vital resource for the U.S. economy". *Tech. rep.* The Brattle Group.
- [31] Bengtsson, E., P. Karlsson, F. Tufvesson, J. Vieira, S. Malkowsky, L. Liu, F. Rusek, and O. Edfors. 2016. "Transmission Schemes for Multiple Antenna Terminals in real Massive MIMO systems". In: *Proc. IEEE GLOBECOM*.
- [32] Bengtsson, E., F. Tufvesson, and O. Edfors. 2015. "UE antenna properties and their influence on massive MIMO system performance". In: *Proc. EuCAP*.
- [33] Bengtsson, M. and B. Ottersten. 2001. "Optimal and suboptimal transmit beamforming". In: *Handbook of Antennas in Wireless Communications*. Ed. by L. C. Godara. CRC Press.
- [34] Bertsekas, D. 1999. *Nonlinear programming*. 2nd edition. Athena Scientific.
- [35] Bethanabhotla, D., O. Y. Bursalioglu, H. C. Papadopoulos, and G. Caire. 2016. "Optimal user-cell association for massive MIMO wireless networks". *IEEE Trans. Wireless Commun.* 15(3): 1835–1850.
- [36] Biglieri, E., J. Proakis, and S. Shamai. 1998. "Fading channels: Information-theoretic and communications aspects". *IEEE Trans. Inf. Theory*. 44(6): 2619–2691.
- [37] Biguesh, M. and A. Gershman. 2004. "Downlink channel estimation in cellular systems with antenna arrays at base stations using channel probing with feedback". *EURASIP J. Appl. Signal Process.* (9): 1330–1339.
- [38] Björnson, E. and B. Ottersten. 2010. "A framework for training-based estimation in arbitrarily correlated Rician MIMO channels with Rician disturbance". *IEEE Trans. Signal Process.* 58(3): 1807–1820.

- [39] Björnson, E., M. Bengtsson, and B. Ottersten. 2012. “Pareto characterization of the multicell MIMO performance region with simple receivers”. *IEEE Trans. Signal Process.* 60(8): 4464–4469.
- [40] Björnson, E., M. Bengtsson, and B. Ottersten. 2014a. “Optimal multiuser transmit beamforming: A difficult problem with a simple solution structure”. *IEEE Signal Process. Mag.* 31(4): 142–148.
- [41] Björnson, E., E. de Carvalho, J. H. Sørensen, E. G. Larsson, and P. Popovski. 2017a. “A random access protocol for pilot allocation in crowded massive MIMO systems”. *IEEE Trans. Wireless Commun.* 16(4): 2220–2234.
- [42] Björnson, E., J. Hoydis, M. Kountouris, and M. Debbah. 2014b. “Massive MIMO systems with non-ideal hardware: Energy efficiency, estimation, and capacity limits”. *IEEE Trans. Inf. Theory.* 60(11): 7112–7139.
- [43] Björnson, E., J. Hoydis, and L. Sanguinetti. 2017b. “Massive MIMO has Unlimited Capacity”. *CoRR*. abs/1705.00538. URL: <http://arxiv.org/abs/1705.00538>.
- [44] Björnson, E., J. Hoydis, and L. Sanguinetti. 2017c. “Pilot contamination is not a fundamental asymptotic limitation in massive MIMO”. In: *Proc. IEEE ICC*.
- [45] Björnson, E., N. Jaldén, M. Bengtsson, and B. Ottersten. 2011. “Optimality properties, distributed strategies, and measurement-based evaluation of coordinated multicell OFDMA transmission”. *IEEE Trans. Signal Process.* 59(12): 6086–6101.
- [46] Björnson, E. and E. Jorswieck. 2013. “Optimal resource allocation in coordinated multi-cell systems”. *Foundations and Trends in Communications and Information Theory.* 9(2-3): 113–381.
- [47] Björnson, E., E. Jorswieck, M. Debbah, and B. Ottersten. 2014c. “Multi-objective signal processing optimization: The way to balance conflicting metrics in 5G systems”. *IEEE Signal Process. Mag.* 31(6): 14–23.

- [48] Björnson, E. and E. G. Larsson. 2015. “Three practical aspects of massive MIMO: Intermittent user activity, pilot synchronism, and asymmetric deployment”. In: *Proc. IEEE GLOBECOM Workshops*.
- [49] Björnson, E., E. G. Larsson, and M. Debbah. 2016a. “Massive MIMO for maximal spectral efficiency: How many users and pilots should be allocated?” *IEEE Trans. Wireless Commun.* 15(2): 1293–1308.
- [50] Björnson, E., E. G. Larsson, and T. L. Marzetta. 2016b. “Massive MIMO: Ten myths and one critical question”. *IEEE Commun. Mag.* 54(2): 114–123.
- [51] Björnson, E., M. Kountouris, and M. Debbah. 2013a. “Massive MIMO and small cells: Improving energy efficiency by optimal soft-cell coordination”. In: *Proc. IEEE ICT*.
- [52] Björnson, E., M. Kountouris, M. Bengtsson, and B. Ottersten. 2013b. “Receive combining vs. multi-stream multiplexing in downlink systems with multi-antenna users”. *IEEE Trans. Signal Process.* 61(13): 3431–3446.
- [53] Björnson, E., M. Matthaiou, and M. Debbah. 2015a. “Massive MIMO with non-ideal arbitrary arrays: Hardware scaling laws and circuit-aware design”. *IEEE Trans. Wireless Commun.* 14(8): 4353–4368.
- [54] Björnson, E., M. Matthaiou, A. Pitarokoilis, and E. G. Larsson. 2015b. “Distributed massive MIMO in cellular networks: Impact of imperfect hardware and number of oscillators”. In: *Proc. EUSIPCO*.
- [55] Björnson, E. and B. Ottersten. 2008. “Post-user-selection quantization and estimation of correlated Frobenius and spectral channel norms”. In: *Proc. IEEE PIMRC*.
- [56] Björnson, E., P. Zetterberg, M. Bengtsson, and B. Ottersten. 2013c. “Capacity limits and multiplexing gains of MIMO channels with transceiver impairments”. *IEEE Commun. Lett.* 17(1): 91–94.

- [57] Björnson, E., L. Sanguinetti, and M. Debbah. 2016c. “Massive MIMO with imperfect channel covariance information”. In: *Proc. ASILOMAR*.
- [58] Björnson, E., L. Sanguinetti, J. Hoydis, and M. Debbah. 2014d. “Designing multi-user MIMO for energy efficiency: When is massive MIMO the answer?” In: *Proc. IEEE WCNC*. 242–247.
- [59] Björnson, E., L. Sanguinetti, J. Hoydis, and M. Debbah. 2015c. “Optimal design of energy-efficient multi-user MIMO systems: Is massive MIMO the answer?” *IEEE Trans. Wireless Commun.* 14(6): 3059–3075.
- [60] Björnson, E., L. Sanguinetti, and M. Kountouris. 2016d. “Deploying dense networks for maximal energy efficiency: Small cells meet massive MIMO”. *IEEE J. Sel. Areas Commun.* 34(4): 832–847.
- [61] Björnson, E., R. Zakhour, D. Gesbert, and B. Ottersten. 2010. “Cooperative multicell precoding: Rate region characterization and distributed strategies with instantaneous and statistical CSI”. *IEEE Trans. Signal Process.* 58(8): 4298–4310.
- [62] Blandino, S., C. Desset, A. Bourdoux, L. V. der Perre, and S. Pollin. 2017. “Analysis of out-of-band interference from saturated power amplifiers in Massive MIMO”. In: *Proc. IEEE EuCNC*.
- [63] Boche, H. and M. Schubert. 2002. “A general duality theory for uplink and downlink beamforming”. In: *Proc. IEEE VTC-Fall*. 87–91.
- [64] Bock, F. and B. Ebstein. 1964. “Assignment of transmitter powers by linear programming”. *IEEE Trans. Electromagn. Compat.* 6(2): 36–44.
- [65] Boström, J. 2015. “Spectrum for mobile – A Swedish perspective for 2020 and beyond”. *Tech. rep.* Swedish Post and Telecom Authority (PTS). URL: <http://wireless.kth.se/wp-content/uploads/2015/02/KTH-Frekvenser-f%5C%22%7Bo%7Dr-4G-och-5G.pdf>.
- [66] Boyd, S., S.-J. Kim, L. Vandenberghe, and A. Hassibi. 2007. “A tutorial on geometric programming”. *Optimization and Engineering*. 8: 67–127.

- [67] Boyd, S. and L. Vandenberghe. 2004. *Convex Optimization*. Cambridge University Press.
- [68] Brennan, D. G. 1959. “Linear diversity combining techniques”. *Proc. IRE*. 43(6): 1975–1102.
- [69] Bussgang, J. J. 1952. “Crosscorrelation functions of amplitude-distorted Gaussian signals”. *Tech. rep.* No. 216. Research Laboratory of Electronics, Massachusetts Institute of Technology.
- [70] Cadambe, V. and S. Jafar. 2008. “Interference alignment and degrees of freedom of the K -user interference channel”. *IEEE Trans. Inf. Theory*. 54(8): 3425–3441.
- [71] Cai, D. W. H., T. Q. S. Quek, C. W. Tan, and S. H. Low. 2012. “Max-min SINR coordinated multipoint downlink transmission—Duality and algorithms”. *IEEE Trans. Signal Process.* 60(10): 5384–5395.
- [72] Caire, G. 2017. “On the Ergodic Rate Lower Bounds with Applications to Massive MIMO”. *CoRR*. abs/1705.03577. URL: <http://arxiv.org/abs/1705.03577>.
- [73] Caire, G., N. Jindal, M. Kobayashi, and N. Ravindran. 2010. “Multiuser MIMO achievable rates with downlink training and channel state feedback”. *IEEE Trans. Inf. Theory*. 56(6): 2845–2866.
- [74] Caire, G. and S. Shamai. 2003. “On the achievable throughput of a multiantenna Gaussian broadcast channel”. *IEEE Trans. Inf. Theory*. 49(7): 1691–1706.
- [75] Carvalho, E. D. and D.T.M. Slock. 1997. “Cramer-Rao bounds for semi-blind, blind and training sequence based channel estimation”. In: *Proc. IEEE SPAWC*. 129–132.
- [76] Carvalho, E. de, E. Björnson, J. H. Sørensen, P. Popovski, and E. G. Larsson. 2017. “Random access protocols for Massive MIMO”. *IEEE Commun. Mag.* 54(5): 216–222.
- [77] Chen, J. and V. Lau. 2014. “Two-Tier Precoding for FDD Multi-Cell Massive MIMO Time-Varying Interference Networks”. *IEEE J. Sel. Areas Commun.* 32(6): 1230–1238.

- [78] Chen, Z. and E. Björnson. 2017. “Channel Hardening and Favorable Propagation in Cell-Free Massive MIMO with Stochastic Geometry”. *CoRR*. abs/1710.00395. URL: <http://arxiv.org/abs/1710.00395>.
- [79] Chen, Z. N. and K.-M. Luk. 2009. *Antennas for base stations in wireless communications*. McGraw-Hill.
- [80] Cheng, H. V., E. Björnson, and E. G. Larsson. 2017. “Optimal pilot and payload power control in single-cell massive MIMO systems”. *IEEE Trans. Signal Process.*
- [81] Chiang, M., P. Hande, T. Lan, and C. Tan. 2008. “Power control in wireless cellular networks”. *Foundations and Trends in Networking*. 2(4): 355–580.
- [82] Chien, T. V., E. Björnson, and E. G. Larsson. 2016. “Joint power allocation and user association optimization for massive MIMO systems”. *IEEE Trans. Wireless Commun.* 15(9): 6384–6399.
- [83] Chizhik, D., J. Ling, P. W. Wolniansky, R. A. Valenzuela, N. Costa, and K. Huber. 2003. “Multiple-input-multiple-output measurements and modeling in Manhattan”. *IEEE J. Sel. Areas Commun.* 21(3): 321–331.
- [84] Choi, J., D. Love, and P. Bidigare. 2014. “Downlink Training Techniques for FDD Massive MIMO Systems: Open-Loop and Closed-Loop Training with Memory”. *IEEE J. Sel. Topics Signal Process.* 8(5): 802–814.
- [85] Chong, C.-C., C.-M. Tan, D. I. Laurenson, S. McLaughlin, M. A. Beach, and A. R. Nix. 2003. “A new statistical wideband spatio-temporal channel model for 5-GHz band WLAN systems”. *IEEE J. Sel. Areas Commun.* 21(2): 139–150.
- [86] Cisco. 2016. “Visual networking index: Global mobile data traffic forecast update, 2015 – 2020”. *Tech. rep.*
- [87] Clerckx, B., G. Kim, and S. Kim. 2008. “Correlated Fading in Broadcast MIMO Channels: Curse or Blessing?” In: *Proc. IEEE GLOBECOM*.
- [88] Clerckx, B. and C. Oestges. 2013. *MIMO wireless networks: Channels, techniques and standards for multi-antenna, multi-user and multi-cell systems*. Academic Press.

- [89] Coldrey, M. 2008. "Modeling and capacity of polarized MIMO channels". In: *Proc. IEEE VTC-Spring*. IEEE. 440–444.
- [90] Common Public Radio Interface (CPRI). 2015. "Interface specification". *Tech. rep.*
- [91] Cooper, M. 2010. "The Myth of Spectrum Scarcity". *Tech. rep.* DYNA llc. URL: <https://ecfsapi.fcc.gov/file/7020396128.pdf>.
- [92] Costa, E. and S. Pupolin. 2002. "M-QAM-OFDM system performance in the presence of a nonlinear amplifier and phase noise". *IEEE Trans. Commun.* 50(3): 462–472.
- [93] Couillet, R. and M. Debbah. 2011. *Random matrix methods for wireless communications*. Cambridge University Press.
- [94] Cover, T. M. and J. A. Thomas. 1991. *Elements of information theory*. Wiley.
- [95] Cui, S., A. Goldsmith, and A. Bahai. 2004. "Energy-efficiency of MIMO and cooperative MIMO techniques in sensor networks". *IEEE J. Sel. Areas Commun.* 22(6): 1089–1098.
- [96] Cupo, R. L., G. D. Golden, C. C. Martin, K. L. Sherman, N. R. Sollenberger, J. H. Winters, and P. W. Wolniansky. 1997. "A four-element adaptive antenna array for IS-136 PCS base stations". In: *Proc. IEEE VTC*. 1577–1581.
- [97] D. Gesbert, L. Pittman, and M. Kountouris. 2006. "Transmit Correlation-Aided Scheduling in multiuser MIMO networks". In: *Proc. IEEE ICASSP*. Vol. 4. 249–252.
- [98] D. Hammarwall, M. Bengtsson, and B. Ottersten. 2008. "Utilizing the Spatial Information Provided by Channel Norm Feedback in SDMA Systems". *IEEE Trans. Signal Process.* 56(7): 3278–3293.
- [99] Dabeer, O. and U. Madhow. 2010. "Channel estimation with low-precision analog-to-digital conversion". In: *Proc. IEEE ICC*.
- [100] Dahrouj, H. and W. Yu. 2010. "Coordinated beamforming for the multicell multi-antenna wireless system". *IEEE Trans. Wireless Commun.* 9(5): 1748–1759.
- [101] Demir, A., A. Mehrotra, and J. Roychowdhury. 2000. "Phase noise in oscillators: A unifying theory and numerical methods for characterization". *IEEE Trans. Circuits Syst. I*. 47(5): 655–674.

- [102] Dessel, C. and B. Debaillie. 2016. “Massive MIMO for energy-efficient communications”. In: *Proc. EuMC*. 138–141.
- [103] Dessel, C. and L. V. der Perre. 2015. “Validation of low-accuracy quantization in massive MIMO and constellation EVM analysis”. In: *Proc. IEEE EuCNC*.
- [104] Dhillon, H. S., M. Kountouris, and J. G. Andrews. 2013. “Downlink MIMO HetNets: Modeling, ordering results and performance analysis”. *IEEE Trans. Wireless Commun.* 12(10): 5208–5222.
- [105] Doukopoulos, X. G. and G. V. Moustakides. 2008. “Fast and stable subspace tracking”. *IEEE Trans. Signal Process.* 56(4): 4790–4807.
- [106] Duel-Hallen, A., J. Holtzman, and Z. Zvonar. 1995. “Multiuser Detection for CDMA Systems”. *IEEE Personal Commun.* 2(2): 46–58.
- [107] Durisi, G., A. Tarable, C. Camarda, R. Devassy, and G. Montorsi. 2014. “Capacity bounds for MIMO microwave backhaul links affected by phase noise”. *IEEE Trans. Commun.* 62(3): 920–929.
- [108] Erceg, V., P. Soma, D. S. Baum, and S. Catreux. 2004. “Multiple-input multiple-output fixed wireless radio channel measurements and modeling using dual-polarized antennas at 2.5 GHz”. *IEEE Trans. Wireless Commun.* 3(6): 2288–2298.
- [109] Ericsson. 2017. “Ericsson mobility report”. *Tech. rep.* URL: <http://www.ericsson.com/mobility-report>.
- [110] *Evolved Universal Terrestrial Radio Access (E-UTRA); Radio frequency (RF) system scenarios (Release 8)*. 2008. 3GPP TS 36.942.
- [111] Farhang, A., N. Marchetti, L. E. Doyle, and B. Farhang-Boroujeny. 2014. “Filter bank multicarrier for massive MIMO”. In: *Proc. IEEE VTC-Fall*.
- [112] *Feasibility study for further advancements for E-UTRA (Release 12)*. 2014. 3GPP TS 36.912.
- [113] Feng, D., C. Jiang, G. Lim, L. J. Cimini, G. Feng, and G. Y. Li. 2013. “A survey of energy-efficient wireless communications”. *IEEE Commun. Surveys Tuts.* 15(1): 167–178.

- [114] Fernandes, F., A. Ashikhmin, and T. Marzetta. 2013. "Inter-cell interference in noncooperative TDD large scale antenna systems". *IEEE J. Sel. Areas Commun.* 31(2): 192–201.
- [115] Flordelis, J., X. Gao, G. Dahman, F. Rusek, O. Edfors, and F. Tufvesson. 2015. "Spatial separation of closely-spaced users in measured massive multi-user MIMO channels". In: *Proc. IEEE ICC*. 1441–1446.
- [116] Frefkiel, R. H. 1970. "A high-capacity mobile radiotelephone system modelusing a coordinated small-zone approach". *IEEE Trans. Veh. Technol.* 19(2): 173–177.
- [117] Friis, H. T. and C. B. Feldman. 1937. "A multiple unit steerable antenna for short-wave reception". *Proc. IRE*. 25(7): 841–917.
- [118] Friis, H. T. 1946. "A note on a simple transmission formula". *Proc. IRE*. 34(5): 254–256.
- [119] *Further advancements for E-UTRA physical layer aspects (Release 9)*. 2010. 3GPP TS 36.814.
- [120] Gao, X., O. Edfors, F. Rusek, and F. Tufvesson. 2011. "Linear pre-coding performance in measured very-large MIMO channels". In: *Proc. IEEE VTC Fall*.
- [121] Gao, X., O. Edfors, F. Rusek, and F. Tufvesson. 2015a. "Massive MIMO performance evaluation based on measured propagation data". *IEEE Trans. Wireless Commun.* 14(7): 3899–3911.
- [122] Gao, X., O. Edfors, F. Tufvesson, and E. G. Larsson. 2015b. "Massive MIMO in real propagation environments: Do all antennas contribute equally?" *IEEE Trans. Commun.* 63(11): 3917–3928.
- [123] Gao, X., F. Tufvesson, and O. Edfors. 2013. "Massive MIMO channels—Measurements and models". In: *Proc. ASILOMAR*. 280–284.
- [124] Gauger, M., J. Hoydis, C. Hoek, H. Schlesinger, A. Pascht, and S. t. Brink. 2015. "Channel measurements with different antenna array geometries for massive MIMO systems". In: *Proc. of 10th Int. ITG Conf. on Systems, Commun. and Coding*. 1–6.

- [125] Gerlach, D. and A. Paulraj. 1994. "Adaptive transmitting antenna arrays with feedback". *IEEE Signal Process. Lett.* 1(10): 150–152.
- [126] Gesbert, D., S. Hanly, H. Huang, S. Shamai, O. Simeone, and W. Yu. 2010. "Multi-cell MIMO cooperative networks: A new look at interference". *IEEE J. Sel. Areas Commun.* 28(9): 1380–1408.
- [127] Gesbert, D., M. Kountouris, R. W. Heath, C.-B. Chae, and T. Sälzer. 2007. "Shifting the MIMO paradigm". *IEEE Signal Process. Mag.* 24(5): 36–46.
- [128] Ghosh, A., J. Zhang, J. G. Andrews, and R. Muhamed. 2010. *Fundamentals of LTE*. Prentice Hall.
- [129] Goldsmith, A., S. A. Jafar, N. Jindal, and S. Vishwanath. 2003. "Capacity limits of MIMO channels". *IEEE J. Sel. Areas Commun.* 21(5): 684–702.
- [130] Gonthier, G. 2008. "Formal proof—The four-color theorem". *Notices of the AMS.* 55(11): 1382–1393.
- [131] Gopalakrishnan, B. and N. Jindal. 2011. "An analysis of pilot contamination on multi-user MIMO cellular systems with many antennas". In: *Proc. IEEE SPAWC*.
- [132] Grant, M. and S. Boyd. 2011. "CVX: Matlab software for disciplined convex programming". <http://cvxr.com/cvx>.
- [133] Guillaud, M., D. Slock, and R. Knopp. 2005. "A practical method for wireless channel reciprocity exploitation through relative calibration". In: *Proc. ISSPA*. 403–406.
- [134] Guo, K. and G. Ascheid. 2013. "Performance analysis of multi-cell MMSE based receivers in MU-MIMO systems with very large antenna arrays". In: *Proc. IEEE WCNC*.
- [135] Guo, K., Y. Guo, G. Fodor, and G. Ascheid. 2014. "Uplink power control with MMSE receiver in multi-cell MU-massive-MIMO systems". In: *Proc. IEEE ICC*. 5184–5190.
- [136] Gustavsson, U., C. Sánchez-Perez, T. Eriksson, F. Athley, G. Durisi, P. Landin, K. Hausmair, C. Fager, and L. Svensson. 2014. "On the impact of hardware impairments on massive MIMO". In: *Proc. IEEE GLOBECOM*.

- [137] Haghghatshoar, S. and G. Caire. 2017. “Massive MIMO Pilot Decontamination and Channel Interpolation via Wideband Sparse Channel Estimation”. *IEEE Trans. Wireless Commun.*
- [138] Han, C., T. Harrold, S. Armour, I. Krikidis, S. Videv, P. M. Grant, H. Haas, J. S. Thompson, I. Ku, C. X. Wang, T. A. Le, M. R. Nakhai, J. Zhang, and L. Hanzo. 2011. “Green radio: Radio techniques to enable energy-efficient wireless networks”. *IEEE Commun. Mag.* 49(6): 46–54.
- [139] Harris, P. *et al.* 2016. “Serving 22 Users in Real-Time with a 128-Antenna Massive MIMO Testbed”. In: *Proc. IEEE International Workshop on Signal Processing Systems (SiPS)*.
- [140] Hasan, Z., H. Boostanimehr, and V. K. Bhargava. 2011. “Green cellular networks: a survey, some research issues and challenges”. *IEEE Commun. Surveys Tuts.* 13(4): 524–540.
- [141] Heath, R. W., N. Gonzalez-Prelcic, S. Rangan, W. Roh, and A. M. Sayeed. 2016. “An overview of signal processing techniques for millimeter wave MIMO systems”. *IEEE J. Sel. Topics Signal Process.* 10(3): 436–453.
- [142] Hochwald, B. M., T. L. Marzetta, and V. Tarokh. 2004. “Multiple-antenna channel hardening and its implications for rate feedback and scheduling”. *IEEE Trans. Inf. Theory.* 60(9): 1893–1909.
- [143] Hoeg, W. and T. Lauterbach. 2009. *Digital Audio Broadcasting: Principles and Applications of DAB, DAB+ and DMB*. John Wiley & Sons, Ltd.
- [144] Holma, H. and A. Toskala. 2011. *LTE for UMTS: Evolution to LTE-Advanced*. 2nd edition. Wiley.
- [145] Honig, M. L. and W. Xiao. 2001. “Performance of reduced-rank linear interference suppression”. *IEEE Trans. Inf. Theory.* 47(5): 1928–1946.
- [146] Hoorfar, A. and M. Hassani. 2008. “Inequalities on the Lambert W function and hyperpower function”. *J. Inequalities in Pure and Applied Math.* 9(2): 1–5.
- [147] Horlin, F. and A. Bourdoux. 2008. *Digital front-end compensation for emerging wireless systems*. John Wiley & Sons, Ltd.

- [148] Hoydis, J., S. ten Brink, and M. Debbah. 2013a. “Massive MIMO in the UL/DL of cellular networks: How many antennas do we need?” *IEEE J. Sel. Areas Commun.* 31(2): 160–171.
- [149] Hoydis, J., M. Debbah, and M. Kobayashi. 2011. “Asymptotic moments for interference mitigation in correlated fading channels”. In: *Proc. IEEE ISIT*.
- [150] Hoydis, J., C. Hoek, T. Wild, and S. ten Brink. 2012. “Channel measurements for large antenna arrays”. In: *Proc. IEEE ISWCS*.
- [151] Hoydis, J., K. Hosseini, S. t. Brink, and M. Debbah. 2013b. “Making smart use of excess antennas: Massive MIMO, small cells, and TDD”. *Bell Labs Technical Journal.* 18(2): 5–21.
- [152] Hu, D., L. He, and X. Wang. 2016. “Semi-blind pilot decontamination for massive MIMO systems”. *IEEE Trans. Wireless Commun.* 15(1): 525–536.
- [153] Huang, Y., C. Desset, A. Bourdoux, W. Dehaene, and L. V. der Perre. 2017. “Massive MIMO processing at the semiconductor edge: Exploiting the system and circuit margins for power savings”. In: *Proc. IEEE ICASSP.* 3474–3478.
- [154] Huh, H., G. Caire, H. Papadopoulos, and S. Ramprasad. 2012. “Achieving “Massive MIMO” spectral efficiency with a not-so-large number of antennas”. *IEEE Trans. Wireless Commun.* 11(9): 3226–3239.
- [155] Ingemarsson, C. and O. Gustafsson. 2015. “On fixed-point implementation of symmetric matrix inversion”. In: *Proc. ECCTD.* 1–4.
- [156] Irmer, R., H. Droste, P. Marsch, M. Grieger, G. Fettweis, S. Brueck, H.-P. Mayer, L. Thiele, and V. Jungnickel. 2011. “Coordinated multipoint: Concepts, performance, and field trial results”. *IEEE Commun. Mag.* 49(2): 102–111.
- [157] Isheden, C., Z. Chong, E. Jorswieck, and G. Fettweis. 2012. “Framework for link-level energy efficiency optimization with informed transmitter”. *IEEE Trans. Wireless Commun.* 11(8): 2946–2957. DOI: 10.1109/TWC.2012.060412.111829.

- [158] Jacobsson, S., G. Durisi, M. Coldrey, T. Goldstein, and C. Studer. 2016. “Quantized precoding for massive MU-MIMO”. <https://arxiv.org/abs/1610.07564>.
- [159] Jaeckel, S., L. Raschkowski, K. Börner, L. Thiele, F. Burkhardt, and E. Eberlein. 2016. “QuaDRiGa - Quasi deterministic radio channel generator, user manual and documentation”. *Tech. rep.* v1.4.8-571. Fraunhofer Heinrich Hertz Institute.
- [160] Jamsa, T., P. Kyosti, and K. Kusume. 2015. *D1.4: METIS Channel Models*. ICT-317669-METIS.
- [161] Jiang, Z., A. F. Molisch, G. Caire, and Z. Niu. 2015. “Achievable rates of FDD Massive MIMO systems with spatial channel correlation”. *IEEE Trans. Wireless Commun.* 14(5): 2868–2882.
- [162] Jindal, N. 2006. “MIMO broadcast channels with finite-rate feedback”. *IEEE Trans. Inf. Theory.* 52(11): 5045–5060.
- [163] Jindal, N., S. Vishwanath, and A. Goldsmith. 2004. “On the Duality of Gaussian Multiple-Access and Broadcast Channels”. *IEEE Trans. Inf. Theory.* 50(5): 768–783.
- [164] Joham, M., W. Utschick, and J. Nossek. 2005. “Linear transmit processing in MIMO communications systems”. *IEEE Trans. Signal Process.* 53(8): 2700–2712.
- [165] Johnson, C. 2012. *Long Term Evolution IN BULLETS*. CreateSpace Independent Publishing Platform.
- [166] Jorswieck, E. and H. Boche. 2007. “Majorization and matrix-monotone functions in wireless communications”. *Foundations and Trends in Communications and Information Theory.* 3(6): 553–701.
- [167] Jorswieck, E. and E. Larsson. 2008. “The MISO interference channel from a game-theoretic perspective: A combination of selfishness and altruism achieves Pareto optimality”. In: *Proc. IEEE ICASSP*. 5364–5367.
- [168] Jorswieck, E. and H. Boche. 2004. “Optimal transmission strategies and impact of correlation in multiantenna systems with different types of channel state information”. *IEEE Trans. Signal Process.* 52(12): 3440–3453.

- [169] Jose, J., A. Ashikhmin, T. L. Marzetta, and S. Vishwanath. 2011. "Pilot contamination and precoding in multi-cell TDD systems". *IEEE Trans. Commun.* 10(8): 2640–2651.
- [170] Josse, N. L., C. Laot, and K. Amis. 2008. "Efficient series expansion for matrix inversion with application to MMSE equalization". *IEEE Commun. Lett.* 12(1): 35–37.
- [171] Joung, H., H.-S. Jo, C. Mun, and J.-G. Yook. 2014. "Capacity loss due to polarization-mismatch and space-correlation on MISO channel". *IEEE Trans. Wireless Commun.* 13(4): 2124–2136.
- [172] Kahn, L. R. 1954. "Ratio squarer". *Proc. IRE.* 42(11): 1704.
- [173] Kammoun, A., A. Müller, E. Björnson, and M. Debbah. 2014. "Linear precoding based on polynomial expansion: Large-scale multi-cell MIMO systems". *IEEE J. Sel. Topics Signal Process.* 8(5): 861–875.
- [174] Kang, D., D. Kim, Y. Cho, J. Kim, B. Park, C. Zhao, and B. Kim. 2011. "1.6 - 2.1 GHz broadband Doherty power amplifiers for LTE handset applications". In: *Proc. IEEE MTT-S.* 1–4.
- [175] Kay, S. M. 1993. *Fundamentals of statistical signal processing: Estimation theory*. Prentice Hall.
- [176] Kelly, F., A. Maulloo, and D. Tan. 1997. "Rate control for communication networks: Shadow prices, proportional fairness and stability". *J. Operational Research Society.* 49(3): 237–252.
- [177] Kermaal, J., L. Schumacher, K. I. Pedersen, P. Mogensen, and F. Frederiksen. 2002. "A stochastic MIMO radio channel model with experimental validation". *IEEE J. Sel. Areas Commun.* 20(6): 1211–1226.
- [178] Khansefid, A. and H. Minn. 2014. "Asymptotically optimal power allocation for massive MIMO uplink". In: *Proc. IEEE GlobalSIP.* 627–631.
- [179] Khanzadi, M. R., G. Durisi, and T. Eriksson. 2015. "Capacity of SIMO and MISO phase-noise channels with common/separate oscillators". *IEEE Trans. Commun.* 63(9): 3218–3231.
- [180] Ko, K. and J. Lee. 2012. "Multiuser MIMO user selection based on chordal distance". *IEEE Trans. Commun.* 60(3): 649–654.

- [181] Korb, M. and T. G. Noll. 2010. "LDPC decoder area, timing, and energy models for early quantitative hardware cost estimates". In: *Proc. IEEE SOCC*. 169–172.
- [182] Kotecha, J. and A. Sayeed. 2004. "Transmit signal design for optimal estimation of correlated MIMO channels". *IEEE Trans. Signal Process.* 52(2): 546–557.
- [183] Krishnamoorthy, A. and D. Menon. 2013. "Matrix inversion using Cholesky decomposition". In: *Proc. Alg. Arch. Arrangements Applicat.* 70–72.
- [184] Krishnan, N., R. D. Yates, and N. B. Mandayam. 2014. "Uplink linear receivers for multi-cell multiuser MIMO with pilot contamination: large system analysis". *IEEE Trans. Wireless Commun.* 13(8): 4360–4373.
- [185] Kumar, R. and J. Gurugubelli. 2011. "How green the LTE technology can be?" In: *Proc. Wireless VITAE*.
- [186] Lahiri, K., A. Raghunathan, S. Dey, and D. Panigrahi. 2002. "Battery-driven system design: A new frontier in low power design". In: *Proc. ASP-DAC/VLSI*. 261–267.
- [187] Lakshminaryana, S., J. Hoydis, M. Debbah, and M. Assaad. 2010. "Asymptotic analysis of distributed multi-cell beamforming". In: *Proc. IEEE PIMRC*. IEEE. 2105–2110.
- [188] Lapidoth, A. 2002. "On phase noise channels at high SNR". In: *Proc. IEEE ITW*.
- [189] Ledoit, O. and M. Wolf. 2004. "A well-conditioned estimator for large-dimensional covariance matrices". *J. Multivariate Anal.* 88(2): 365–411.
- [190] Lei, Z. and T. Lim. 1998. "Simplified polynomial-expansion linear detectors for DS-CDMA systems". *Electronics Lett.* 34(16): 1561–1563.
- [191] Li, L., A. Ashikhmin, and T. Marzetta. 2013a. "Pilot contamination precoding for interference reduction in large scale antenna systems". In: *Allerton*. 226–232.
- [192] Li, M., S. Jin, and X. Gao. 2013b. "Spatial orthogonality-based pilot reuse for multi-cell massive MIMO transmission". In: *Proc. WCSP*.

- [193] Li, X., E. Björnson, E. G. Larsson, S. Zhou, and J. Wang. 2017. “Massive MIMO with multi-cell MMSE processing: Exploiting all pilots for interference suppression”. *EURASIP J. Wirel. Commun. Netw.* (117).
- [194] Li, X., E. Björnson, S. Zhou, and J. Wang. 2016. “Massive MIMO with multi-antenna users: When are additional user antennas beneficial?” In: *Proc. IEEE ICT*.
- [195] Liu, Y., T. Wong, and W. Hager. 2007. “Training signal design for estimation of correlated MIMO channels with colored interference”. *IEEE Trans. Signal Process.* 55(4): 1486–1497.
- [196] Löfberg, J. 2004. “YALMIP: A Toolbox for modeling and optimization in MATLAB”. In: *Proc. IEEE CACSD*. 284–289.
- [197] Lopez-Perez, D., M. Ding, H. Claussen, and A. H. Jafari. 2015. “Enhanced intercell interference coordination challenges in heterogeneous networks”. *IEEE Commun. Surveys Tuts.* 17(4): 2078–2101.
- [198] López-Pérez, D., M. Ding, H. Claussen, and A. H. Jafari. 2015. “Towards 1 Gbps/UE in cellular systems: Understanding ultra-dense small cell deployments”. *IEEE Commun. Surveys Tuts.* 17(4): 2078–2101.
- [199] Love, R. and V. Nangia. 2009. “Uplink physical channel structure”. In: *LTE - The UMTS Long Term Evolution: From Theory to Practice*. Ed. by S. Sesia, I. Toufik, and M. Baker. Wiley. Chap. 17. 377–403.
- [200] Lu, W. and M. D. Renzo. 2015. “Stochastic Geometry Modeling of Cellular Networks: Analysis, Simulation and Experimental Validation”. In: *ACM International Conference on Modeling, Analysis and Simulation of Wireless and Mobile Systems*.
- [201] Luo, Z.-Q. and S. Zhang. 2008. “Dynamic spectrum management: Complexity and duality”. *IEEE J. Sel. Topics Signal Process.* 2(1): 57–73.
- [202] Lupas, R. and S. Verdu. 1989. “Linear multiuser detectors for synchronous code-division multiple-access channels”. *IEEE Trans. Inf. Theory.* 35(1): 123–136.

- [203] Ma, J. and L. Ping. 2014. “Data-aided channel estimation in large antenna systems”. *IEEE Trans. Signal Process.* 62(12): 3111–3124.
- [204] MacDonald, V. H. 1979. “The cellular concept”. *Bell System Technical Journal.* 58(1): 15–41.
- [205] Madhow, U. and M. L. Honig. 1994. “MMSE interference suppression for direct-sequence spread-spectrum CDMA”. *IEEE Trans. Commun.* 42(12): 3178–3188.
- [206] Marks, B. R. and G. P. Wright. 1978. “A general inner approximation algorithm for nonconvex mathematical programs”. *Operations Research.* 26(4): 681–683.
- [207] Martinez, A. O., E. De Carvalho, and J. O. Nielsen. 2014. “Towards very large aperture massive MIMO: A measurement based study”. In: *Proc. IEEE GLOBECOM Workshops.* 281–286.
- [208] Marzetta, T. L. 2010. “Noncooperative cellular wireless with unlimited numbers of base station antennas”. *IEEE Trans. Wireless Commun.* 9(11): 3590–3600.
- [209] Marzetta, T. L. 2015. “Massive MIMO: An introduction”. *Bell Labs Technical Journal.* 20: 11–22.
- [210] Marzetta, T. L., E. G. Larsson, H. Yang, and H. Q. Ngo. 2016. *Fundamentals of Massive MIMO.* Cambridge University Press.
- [211] Marzetta, T. L., G. H. Tucci, and S. H. Simon. 2011. “A random matrix-theoretic approach to handling singular covariance estimates”. *IEEE Trans. Inf. Theory.* 57(9): 6256–6271.
- [212] Marzetta, T. and A. Ashikhmin. 2011. “MIMO system having a plurality of service antennas for data transmission and reception and method thereof”. US Patent. 8594215.
- [213] Mathecken, P., T. Riihonen, S. Werner, and R. Wichman. 2011. “Performance analysis of OFDM with Wiener phase noise and frequency selective fading channel”. *IEEE Trans. Commun.* 59(5): 1321–1331.
- [214] Medard, M. 2000. “The effect upon channel capacity in wireless communications of perfect and imperfect knowledge of the channel”. *IEEE Trans. Inf. Theory.* 46(3): 933–946.

- [215] Mehrpouyan, H., A. Nasir, S. Blostein, T. Eriksson, G. Karagiannis, and T. Svensson. 2012. "Joint estimation of channel and oscillator phase noise in MIMO systems". *IEEE Trans. Signal Process.* 60(9): 4790–4807.
- [216] Meshkati, F., H. V. Poor, S. C. Schwartz, and N. B. Mandayam. 2005. "An energy-efficient approach to power control and receiver design in wireless data networks". *IEEE Trans. Commun.* 53(11): 1885–1894.
- [217] Mestre, X. 2008. "Improved Estimation of Eigenvalues and Eigenvectors of Covariance Matrices Using Their Sample Estimates". *IEEE Trans. Inf. Theory.* 54(11): 5113–5129.
- [218] Mezghani, A. and J. A. Nossek. 2007. "On ultra-wideband MIMO systems with 1-bit quantized outputs: Performance analysis and input optimization". In: *Proc. IEEE ISIT*. 1286–1289.
- [219] Mezghani, A. and J. A. Nossek. 2011. "Power efficiency in communication systems from a circuit perspective". In: *Proc. IEEE ISCAS*. 1896–1899.
- [220] Mo, J. and R. W. Heath. 2015. "Capacity analysis of one-bit quantized MIMO systems with transmitter channel state information". *IEEE Trans. Signal Process.* 63(20): 5498–5512.
- [221] Mo, J. and J. Walrand. 2000. "Fair end-to-end window-based congestion control". *IEEE/ACM Trans. Netw.* 8(5): 556–567.
- [222] Mo, J. and R. W. Heath. 2014. "High SNR capacity of millimeter wave MIMO systems with one-bit quantization". In: *Proc. IEEE ITA*. IEEE. 1–5.
- [223] Moghadam, N. N., P. Zetterberg, P. Händel, and H. Hjalmarsson. 2012. "Correlation of distortion noise between the branches of MIMO transmit antennas". In: *Proc. IEEE PIMRC*.
- [224] Mohammed, S. 2014. "Impact of transceiver power consumption on the energy efficiency of zero-forcing detector in massive MIMO systems". *IEEE Trans. Commun.* 62(11): 3874–3890.
- [225] Molisch, A. F. 2007. *Wireless communications*. John Wiley & Sons.

- [226] Mollén, C., J. Choi, E. G. Larsson, and R. W. Heath. 2017. “Uplink performance of wideband Massive MIMO with one-bit ADCs”. *IEEE Trans. Wireless Commun.* 16(1): 87–100.
- [227] Mollén, C., U. Gustavsson, T. Eriksson, and E. G. Larsson. 2016a. “Out-of-band radiation measure for MIMO arrays with beamformed transmission”. In: *Proc. IEEE ICC*.
- [228] Mollén, C., E. G. Larsson, and T. Eriksson. 2016b. “Waveforms for the massive MIMO Downlink: Amplifier Efficiency, Distortion and Performance”. *IEEE Trans. Commun.* 64(12): 5050–5063.
- [229] Moshavi, S., E. G. Kanterakis, and D. L. Schilling. 1996. “Multi-stage linear receivers for DS-CDMA systems”. *Int. J. Wireless Information Networks.* 3(1): 1–17.
- [230] Motahari, A. S. and A. K. Khandani. 2009. “Capacity bounds for the Gaussian interference channel”. *IEEE Trans. Inf. Theory.* 55(2): 620–643.
- [231] Müller, A., A. Kammoun, E. Björnson, and M. Debbah. 2016. “Linear precoding based on polynomial expansion: Reducing complexity in massive MIMO”. *EURASIP J. Wirel. Commun. Netw.*
- [232] Müller, R., L. Cottatellucci, and M. Vehkaperä. 2014. “Blind pilot decontamination”. *IEEE J. Sel. Topics Signal Process.* 8(5): 773–786.
- [233] Muller, R. and S. Verdú. 2001. “Design and analysis of low-complexity interference mitigation on vector channels”. *IEEE J. Sel. Areas Commun.* 19(8): 1429–1441.
- [234] Al-Naffouri, T. Y., M. Sharif, and B. Hassibi. 2009. “How much does transmit correlation affect the sum-rate scaling of MIMO Gaussian broadcast channels?” *IEEE Trans. Commun.* 57(2): 562–572.
- [235] Nam, J., A. Adhikary, J.-Y. Ahn, and G. Caire. 2014. “Joint spatial division and multiplexing: Opportunistic beamforming, user grouping and simplified downlink scheduling”. *IEEE J. Sel. Topics Signal Process.* 8(5): 876–890.
- [236] Nayebi, E., A. Ashikhmin, T. L. Marzetta, and H. Yang. 2015. “Cell-Free Massive MIMO Systems”. In: *Proc. Asilomar*.

- [237] Nayebi, E., A. Ashikhmin, T. L. Marzetta, H. Yang, and B. D. Rao. 2017. "Precoding and Power Optimization in Cell-Free Massive MIMO Systems". *IEEE Trans. Wireless Commun.* 16(7): 4445–4459.
- [238] Neumann, D., M. Joham, and W. Utschick. 2014. "Suppression of pilot-contamination in massive MIMO systems". In: *Proc. IEEE SPAWC*. 11–15.
- [239] Neumann, D., M. Joham, and W. Utschick. 2017. "On MSE Based Receiver Design for Massive MIMO". In: *Proc. SCC*.
- [240] Ngo, H. Q., A. E. Ashikhmin, H. Yang, E. G. Larsson, and T. L. Marzetta. 2015. "Cell-free massive MIMO: Uniformly great service for everyone". In: *Proc. IEEE SPAWC*.
- [241] Ngo, H. Q., A. Ashikhmin, H. Yang, E. G. Larsson, and T. L. Marzetta. 2017. "Cell-Free Massive MIMO Versus Small Cells". *IEEE Trans. Wireless Commun.* 16(3): 1834–1850.
- [242] Ngo, H. Q. and E. Larsson. 2012. "EVD-based channel estimations for multicell multiuser MIMO with very large antenna arrays". In: *Proc. IEEE ICASSP*.
- [243] Ngo, H. Q. and E. G. Larsson. 2017. "No Downlink Pilots Are Needed in TDD Massive MIMO". *IEEE Trans. Wireless Commun.* 16(5): 2921–2935.
- [244] Ngo, H. Q., E. G. Larsson, and T. L. Marzetta. 2013. "Energy and spectral efficiency of very large multiuser MIMO systems". *IEEE Trans. Commun.* 61(4): 1436–1449.
- [245] Ngo, H. Q., E. G. Larsson, and T. L. Marzetta. 2014a. "Aspects of favorable propagation in massive MIMO". In: *Proc. EUSIPCO*.
- [246] Ngo, H. Q., M. Matthaiou, and E. G. Larsson. 2012. "Performance analysis of large scale MU-MIMO with optimal linear receivers". In: *Proc. IEEE Swe-CTW*. 59–64.
- [247] Ngo, H. Q., M. Matthaiou, and E. G. Larsson. 2014b. "Massive MIMO with optimal power and training duration allocation". *IEEE Commun. Lett.* 3(6): 605–608.

- [248] Nishimori, K., K. Cho, Y. Takatori, and T. Hori. 2001. "Automatic calibration method using transmitting signals of an adaptive array for TDD systems". *IEEE Trans. Veh. Technol.* 50(6): 1636–1640.
- [249] Oestges, C., B. Clerckx, M. Guillaud, and M. Debbah. 2008. "Dual-polarized wireless communications: From propagation models to system performance evaluation". *IEEE Trans. Wireless Commun.* 7(10): 4019–4031.
- [250] Palomar, D. and M. Chiang. 2006. "A tutorial on decomposition methods for network utility maximization". *IEEE J. Sel. Areas Commun.* 24(8): 1439–1451.
- [251] Palomar, D. and Y. Jiang. 2006. "MIMO transceiver design via majorization theory". *Foundations and Trends in Communications and Information Theory.* 3(4-5): 331–551.
- [252] Park, J. and B. Clerckx. 2014. "Multi-polarized multi-user massive MIMO: Precoder design and performance analysis". In: *Proc. EUSIPCO*. IEEE. 326–330.
- [253] Park, J. and B. Clerckx. 2015. "Multi-user linear precoding for multi-polarized Massive MIMO system under imperfect CSIT". *IEEE Trans. Wireless Commun.* 14(5): 2532–2547.
- [254] Paulraj, A. and C. Papadias. 1997. "Space-time processing for wireless communications". *IEEE Signal Process. Mag.* 14(6): 49–83.
- [255] Paulraj, A., R. Nabar, and D. Gore. 2003. *Introduction to space-time wireless communications*. Cambridge University Press.
- [256] Pedersen, K. I., P. E. Mogensen, and B. H. Fleury. 1997. "Power azimuth spectrum in outdoor environments". *Electronics Lett.* 33(18): 1583–1584.
- [257] Peterson, H. O., H. H. Beverage, and J. B. Moore. 1931. "Diversity telephone receiving system of R.C.A. communications, Inc." *Proc. IRE.* 19(4): 562–584.
- [258] Petrovic, D., W. Rave, and G. Fettweis. 2007. "Effects of phase noise on OFDM systems with and without PLL: Characterization and compensation". *IEEE Trans. Commun.* 55(8): 1607–1616.

- [259] Pi, Z. and F. Khan. 2011. “An introduction to millimeter-wave mobile broadband systems”. *IEEE Commun. Mag.* 49(6): 101–107.
- [260] Pillai, S. U., T. Suel, and S. Cha. 2005. “The Perron-Frobenius theorem: Some of its applications”. *IEEE Signal Process. Mag.* 22(2): 62–75.
- [261] Pinsker, M. S., V. V. Prelov, and E. C. van der Meulen. 1998. “Information Transmission over Channels with Additive-Multiplicative Noise”. In: *Proc. IEEE ISIT*. 239.
- [262] Pitarokoilis, A., E. Björnson, and E. G. Larsson. 2016. “Performance of the massive MIMO uplink with OFDM and phase noise”. *IEEE Wireless Commun. Lett.* 20(8): 1595–1598.
- [263] Pitarokoilis, A., E. Björnson, and E. G. Larsson. 2017. “On the Effect of Imperfect Timing Synchronization on Pilot Contamination”. In: *Proc. IEEE ICC*.
- [264] Pitarokoilis, A., S. K. Mohammed, and E. G. Larsson. 2012. “On the optimality of single-carrier transmission in large-scale antenna systems”. *IEEE Wireless Commun. Lett.* 1(4): 276–279.
- [265] Pitarokoilis, A., S. K. Mohammed, and E. G. Larsson. 2015. “Uplink performance of time-reversal MRC in massive MIMO systems subject to phase noise”. *IEEE Trans. Wireless Commun.* 14(2): 711–723.
- [266] Pizzo, A., D. Verenzuela, L. Sanguinetti, and E. Björnson. 2017. “Network Deployment for Maximal Energy Efficiency in Uplink with Zero-Forcing”. In: *Proc. IEEE GLOBECOM*.
- [267] Polyanskiy, Y., H. Poor, and S. Verdú. 2010. “Channel coding rate in the finite blocklength regime”. *IEEE Trans. Inf. Theory.* 56(5): 2307–2359.
- [268] Poon, A. S. Y., R. W. Brodersen, and D. N. C. Tse. 2005. “Degrees of freedom in multiple-antenna channels: A signal space approach”. *IEEE Trans. Inf. Theory.* 51(2): 523–536.
- [269] Qian, L. P., Y. J. Zhang, and J. Huang. 2009. “MAPEL: Achieving global optimality for a non-convex wireless power control problem”. *IEEE Trans. Wireless Commun.* 8(3): 1553–1563.

- [270] Qiao, D., S. Choi, and K. G. Shin. 2002. "Goodput analysis and link adaptation for IEEE 802.11 a Wireless LANs". *IEEE Trans. Mobile Comp.* 1(4): 278–292.
- [271] Qualcomm. 2012. "Rising to meet the 1000x mobile data challenge". *Tech. rep.* Qualcomm Incorporated.
- [272] Rangan, S., T. S. Rappaport, and E. Erkip. 2014. "Millimeter-wave cellular wireless networks: Potentials and challenges". *Proc. IEEE.* 102(3): 366–385.
- [273] Rao, X. and V. Lau. 2014. "Distributed compressive CSIT estimation and feedback for FDD multi-user massive MIMO systems". *IEEE J. Sel. Areas Commun.* 62(12): 3261–3271.
- [274] Rappaport, T. S., R. W. Heath Jr, R. C. Daniels, and J. N. Murdock. 2014. *Millimeter wave wireless communications*. Pearson Education.
- [275] Rappaport, T. S., S. Sun, R. Mayzus, H. Zhao, Y. Azar, K. Wang, G. N. Wong, J. K. Schulz, M. Samimi, and F. Gutierrez. 2013. "Millimeter wave mobile communications for 5G cellular: It will work!" *IEEE Access.* 1: 335–349.
- [276] Rashid-Farrokhi, F., L. Tassiulas, and K. J. R. Liu. 1998. "Joint optimal power control and beamforming in wireless networks using antenna arrays". *IEEE Trans. Commun.* 46(10): 1313–1324.
- [277] Ring, D. H. 1947. "Mobile Telephony - Wide Area Coverage". *Bell Laboratories Technical Memorandum*.
- [278] Rockafellar, R. 1993. "Lagrange multipliers and optimality". *SIAM Review.* 35(2): 183–238.
- [279] Rogalin, R., O. Y. Bursalioglu, H. Papadopoulos, G. Caire, A. F. Molisch, A. Michaloliakos, V. Balan, and K. Psounis. 2014. "Scalable synchronization and reciprocity calibration for distributed multiuser MIMO". *IEEE Trans. Wireless Commun.* 13(4): 1815–1831.
- [280] Roy, R. H. and B. Ottersten. 1991. "Spatial division multiple access wireless communication systems". US Patent. 5515378.

- [281] Rusek, F., D. Persson, B. K. Lau, E. G. Larsson, T. L. Marzetta, O. Edfors, and F. Tufvesson. 2013. "Scaling up MIMO: Opportunities and challenges with very large arrays". *IEEE Signal Process. Mag.* 30(1): 40–60.
- [282] Sadek, M., A. Tarighat, and A. Sayed. 2007. "A leakage-based precoding scheme for downlink multi-user MIMO channels". *IEEE Trans. Wireless Commun.* 6(5): 1711–1721.
- [283] Saleh, A. A. and R. A. Valenzuela. 1987. "A statistical model for indoor multipath propagation". *IEEE J. Sel. Areas Commun.* 5(2): 128–137.
- [284] Salz, J. and J. H. Winters. 1994. "Effect of fading correlation on adaptive arrays in digital mobile radio". *IEEE Trans. Veh. Technol.* 43(4): 1049–1057.
- [285] Sanguinetti, L., R. Couillet, and M. Debbah. 2016a. "Large system analysis of base station cooperation for power minimization". *IEEE Trans. Wireless Commun.* 15(8): 5480–5496.
- [286] Sanguinetti, L., A. A. D'Amico, M. Morelli, and M. Debbah. 2016b. "Random access in uplink massive MIMO systems: how to exploit asynchronicity and excess antennas". In: *Proc. GLOBE-COM*.
- [287] Sarkar, T. K., Z. Ji, K. Kim, A. Medouri, and M. Salazar-Palma. 2003. "A survey of various propagation models for mobile communication". *IEEE Antennas Propag. Mag.* 45(3): 51–82.
- [288] Saxena, V., G. Fodor, and E. Karipidis. 2015. "Mitigating pilot contamination by pilot reuse and power control schemes for massive MIMO systems". In: *Proc. IEEE VTC-Spring*.
- [289] Sayeed, A. 2002. "Deconstructing multiantenna fading channels". *IEEE Trans. Signal Process.* 50(10): 2563–2579.
- [290] Schenk, T. 2008. *RF imperfections in high-rate wireless systems: Impact and digital compensation*. Springer.
- [291] Schulte, H. J. and W. A. Cornell. 1960. "A high-capacity mobile radiotelephone system model using a coordinated small-zone approach". *IEEE Trans. Veh. Technol.* 9(1): 49–53.

- [292] Sessler, G. and F. Jondral. 2005. “Low complexity polynomial expansion multiuser detector for CDMA systems”. *IEEE Trans. Veh. Technol.* 54(4): 1379–1391.
- [293] Shafi, M., M. Zhang, A. L. Moustakas, P. J. Smith, A. F. Molisch, F. Tufvesson, and S. H. Simon. 2006. “Polarized MIMO channels in 3-D: Models, measurements and mutual information”. *IEEE J. Sel. Areas Commun.* 24(3): 514–527.
- [294] Shamai, S. and B. M. Zaidel. 2001. “Enhancing the cellular downlink capacity via co-processing at the transmitting end”. In: *Proc. IEEE VTC-Spring*. Vol. 3. 1745–1749.
- [295] Shang, X., B. Chen, G. Kramer, and H. V. Poor. 2011. “Noisy-interference sum-rate capacity of parallel Gaussian interference channels”. *IEEE Trans. Inf. Theory.* 57(1): 210–226.
- [296] Shang, X., G. Kramer, B. Chen, and H. V. Poor. 2009. “A new outer bound and the noisy-interference sum-rate capacity for Gaussian interference channels”. *IEEE Trans. Inf. Theory.* 55(2): 689–699.
- [297] Shannon, C. E. 1948. “A mathematical theory of communication”. *Bell System Technical Journal.* 27: 379–423, 623–656.
- [298] Shannon, C. E. 1949. “Communication in the presence of noise”. *Proc. IRE.* 37(1): 10–21.
- [299] Shariati, N., E. Björnson, M. Bengtsson, and M. Debbah. 2014. “Low-complexity polynomial channel estimation in large-scale MIMO with arbitrary statistics”. *IEEE J. Sel. Topics Signal Process.* 8(5): 815–830.
- [300] Shepard, C., H. Yu, N. Anand, L. Li, T. Marzetta, R. Yang, and L. Zhong. 2012. “Argos: Practical many-antenna base stations”. In: *Proc. ACM MobiCom*.
- [301] Shiu, D., G. Foschini, M. Gans, and J. Kahn. 2000. “Fading correlation and its effect on the capacity of multielement antenna systems”. *IEEE Trans. Commun.* 48(3): 502–513.
- [302] Sifaou, H., A. Kammoun, L. Sanguinetti, M. Debbah, and M. S. Alouini. 2017. “Max-min SINR in large-scale single-cell MU-MIMO: Asymptotic analysis and low-complexity transceivers”. *IEEE Trans. Signal Process.* 65(7): 1841–1854.

- [303] Simeone, O., N. Levy, A. Sanderovich, O. Somekh, B. M. Zaidel, H. V. Poor, and S. Shamai. 2012. “Cooperative wireless cellular systems: An information-theoretic view”. *Foundations and Trends in Communications and Information Theory*. 8(1-2): 1–177.
- [304] Somekh, O. and S. Shamai. 2000. “Shannon-theoretic approach to a Gaussian cellular multiple-access channel with fading”. *IEEE Trans. Inf. Theory*. 46(4): 1401–1425.
- [305] Sørensen, J. H., E. de Carvalho, C. Stefanovic, and P. Popovski. 2016. “Coded pilot access: A random access solution for massive MIMO systems”. *CoRR*. abs/1605.05862. URL: <http://arxiv.org/abs/1605.05862>.
- [306] Studer, C. and G. Durisi. 2016. “Quantized massive MU-MIMO-OFDM uplink”. *IEEE Trans. Commun.* 64(6): 2387–2399.
- [307] Sturm, J. 1999. “Using SeDuMi 1.02, a MATLAB toolbox for optimization over symmetric cones”. *Optimization Methods and Software*. 11-12: 625–653.
- [308] Swales, S. C., M. A. Beach, D. J. Edwards, and J. P. McGeehan. 1990. “The performance enhancement of multibeam adaptive base-station antennas for cellular land mobile radio systems”. *IEEE Trans. Veh. Technol.* 39(1): 56–67.
- [309] Tomatis, F. and S. Sesia. 2009. “Synchronization and cell search”. In: *LTE - The UMTS Long Term Evolution: From Theory to Practice*. Ed. by S. Sesia, I. Toufik, and M. Baker. Wiley. Chap. 7. 141–157.
- [310] Tomba, L. 1998. “On the effect of Wiener phase noise in OFDM systems”. *IEEE Trans. Commun.* 46(5): 580–583.
- [311] Tombaz, S., K. W. Sung, and J. Zander. 2012. “Impact of densification on energy efficiency in wireless access networks”. In: *Proc. IEEE GLOBECOM Workshop*. 57–62.
- [312] Tombaz, S., A. Västberg, and J. Zander. 2011. “Energy- and cost-efficient ultra-high-capacity wireless access”. *IEEE Wireless Commun.* 18(5): 18–24.

- [313] Trump, T. and B. Ottersten. 1996. “Estimation of nominal direction of arrival and angular spread using an array of sensors”. *Signal Processing*. 50(1-2): 57–69.
- [314] Tse, D. and P. Viswanath. 2005. *Fundamentals of wireless communications*. Cambridge University Press.
- [315] Tulino, A. M. and S. Verdú. 2004. “Random matrix theory and wireless communications”. *Foundations and Trends in Communications and Information Theory*. 1(1): 1–182.
- [316] Tütüncü, R., K. Toh, and M. Todd. 2003. “Solving semidefinite-quadratic-linear programs using SDPT3”. *Mathematical Programming*. 95(2): 189–217.
- [317] Tuy, H. 2000. “Monotonic optimization: Problems and solution approaches”. *SIAM J. Optim.* 11(2): 464–494.
- [318] Tuy, H., F. Al-Khayyal, and P. Thach. 2005. “Monotonic optimization: Branch and cut methods”. In: *Essays and Surveys in Global Optimization*. Ed. by C. Audet, P. Hansen, and G. Savard. Springer US.
- [319] Upadhyya, K., S. A. Vorobyov, and M. Vehkaperä. 2017a. “Downlink Performance of Superimposed Pilots in Massive MIMO systems”. *CoRR*. abs/1606.04476. URL: <http://arxiv.org/abs/1606.04476>.
- [320] Upadhyya, K., S. A. Vorobyov, and M. Vehkaperä. 2017b. “Superimposed Pilots Are Superior for Mitigating Pilot Contamination in Massive MIMO”. *IEEE Trans. Signal Process.* 65(11): 2917–2932.
- [321] Va, V., J. Choi, and R. W. Heath. 2017. “The Impact of Beamwidth on Temporal Channel Variation in Vehicular Channels and its Implications”. *IEEE Trans. Veh. Technol.*
- [322] Valkama, M. 2011. “RF impairment compensation for future radio systems”. In: *Multi-Mode/Multi-Band RF Transceivers for Wireless Communications*. Ed. by G. Hueber and R. B. Staszewski. John Wiley & Sons, Inc. 453–496.
- [323] Vaughan, R. G. 1990. “Polarization diversity in mobile communications”. *IEEE Trans. Veh. Technol.* 39(3): 177–186.

- [324] Veen, B. D. V. and K. M. Buckley. 1988. “Beamforming: a versatile approach to spatial filtering”. *IEEE ASSP Mag.* 5(2): 4–24.
- [325] Venkatesan, S., A. Lozano, and R. Valenzuela. 2007. “Network MIMO: Overcoming intercell interference in indoor wireless systems”. In: *Proc. IEEE ACSSC*. 83–87.
- [326] Verdú, S. 1990. “On channel capacity per unit cost”. *IEEE Trans. Inf. Theory.* 36(5): 1019–1030.
- [327] Verenzuela, D., E. Björnson, and M. Matthaiou. 2016. “Hardware design and optimal ADC resolution for uplink massive MIMO systems”. In: *Proc. SAM Workshop*.
- [328] Verenzuela, D., E. Björnson, and L. Sanguinetti. 2017. “Spectral and Energy Efficiency of Superimposed Pilots in Uplink Massive MIMO”. *CoRR*. abs/1709.07722. URL: <http://arxiv.org/abs/1709.07722>.
- [329] Vieira, J., S. Malkowsky, K. Nieman, Z. Miers, N. Kundargi, L. Liu, I. C. Wong, V. Öwall, O. Edfors, and F. Tufvesson. 2014a. “A flexible 100-antenna testbed for massive MIMO”. In: *Proc. IEEE GLOBECOM Workshop*. 287–293.
- [330] Vieira, J., F. Rusek, O. Edfors, S. Malkowsky, L. Liu, and F. Tufvesson. 2017. “Reciprocity Calibration for Massive MIMO: Proposal, Modeling, and Validation”. *IEEE Trans. Wireless Commun.* 16(5): 3042–3056.
- [331] Vieira, J., R. Rusek, and F. Tufvesson. 2014b. “Reciprocity calibration methods for massive MIMO based on antenna coupling”. In: *Proc. IEEE GLOBECOM*.
- [332] Viering, I., H. Hofstetter, and W. Utschick. 2002. “Spatial long-term variations in urban, rural and indoor environments”. In: *COST273 5th Meeting, Lisbon, Portugal*.
- [333] Vinogradova, J., E. Björnson, and E. G. Larsson. 2016a. “Detection and mitigation of jamming attacks in massive MIMO systems using random matrix theory”. In: *Proc. IEEE SPAWC*.
- [334] Vinogradova, J., E. Björnson, and E. G. Larsson. 2016b. “On the separability of signal and interference-plus-noise subspaces in blind pilot decontamination”. In: *Proc. IEEE ICASSP*.

- [335] Viswanath, P. and D. N. C. Tse. 2003. "Sum capacity of the vector Gaussian broadcast channel and uplink-downlink duality". *IEEE Trans. Inf. Theory*. 49(8): 1912–1921.
- [336] Wagner, S., R. Couillet, M. Debbah, and D. Slock. 2012. "Large system analysis of linear precoding in MISO broadcast channels with limited feedback". *IEEE Trans. Inf. Theory*. 58(7): 4509–4537.
- [337] Wallace, J. W. and M. A. Jensen. 2001. "Measured characteristics of the MIMO wireless channel". In: *Proc. IEEE VTC-Fall*. Vol. 4. 2038–2042.
- [338] Wallace, J. W. and M. A. Jensen. 2002. "Modeling the indoor MIMO wireless channel". *IEEE Trans. Antennas Propag.* 50(5): 591–599.
- [339] Wallis, J. S. 1976. "On the existence of Hadamard matrices". *Journal of Combinatorial Theory*. 21(2): 188–195.
- [340] Wang, H., P. Wang, L. Ping, and X. Lin. 2009. "On the impact of antenna correlation in multi-user MIMO systems with rate constraints". *IEEE Commun. Lett.* 13(12): 935–937.
- [341] Weeraddana, P., M. Codreanu, M. Latva-aho, A. Ephremides, and C. Fischione. 2012. "Weighted sum-rate maximization in wireless networks: A review". *Foundations and Trends in Networking*. 6(1-2): 1–163.
- [342] Weingarten, H., Y. Steinberg, and S. Shamai. 2006. "The capacity region of the Gaussian multiple-input multiple-output broadcast channel". *IEEE Trans. Inf. Theory*. 52(9): 3936–3964.
- [343] Wen, C.-K., S. Jin, K.-K. Wong, C.-J. Wang, and G. Wu. 2015. "Joint channel-and-data estimation for large-MIMO systems with low-precision ADCs". In: *Proc. IEEE ISIT*. 1237–1241.
- [344] Wenk, M. 2010. *MIMO-OFDM testbed: Challenges, implementations, and measurement results. Series in microelectronics*. Hartung-Gorre.
- [345] Wiesel, A., Y. Eldar, and S. Shamai. 2006. "Linear precoding via conic optimization for fixed MIMO receivers". *IEEE Trans. Signal Process.* 54(1): 161–176.

- [346] Wiesel, A., Y. Eldar, and S. Shamai. 2008. “Zero-forcing precoding and generalized inverses”. *IEEE Trans. Signal Process.* 56(9): 4409–4418.
- [347] WINNER II Channel Models. 2008. “Deliverable 1.1. 2 v. 1.2”. *Tech. rep.*
- [348] Winters, J. H. 1984. “Optimum combining in digital mobile radio with cochannel interference”. *IEEE J. Sel. Areas Commun.* 2(4): 528–539.
- [349] Winters, J. H. 1987. “Optimum combining for indoor radio systems with multiple users”. *IEEE Trans. Commun.* 35(11): 1222–1230.
- [350] Winters, J. H. 1998. “Smart antennas for wireless systems”. *IEEE Personal Commun.* 5(1): 23–27.
- [351] Wu, J., Y. Zhang, M. Zukerman, and E. K. N. Yung. 2015. “Energy-efficient base-stations sleep-mode techniques in green cellular networks: A survey”. *IEEE Commun. Surveys Tuts.* 17(2): 803–826.
- [352] Wu, M., B. Yin, G. Wang, C. Dick, J. R. Cavallaro, and C. Studer. 2014. “Large-scale MIMO detection for 3GPP LTE: Algorithms and FPGA implementations”. *IEEE J. Sel. Topics Signal Process.* 8(5): 916–929.
- [353] Wyner, A. D. 1994. “Shannon-theoretic approach to a Gaussian cellular multiple-access channel”. *IEEE Trans. Inf. Theory.* 40(6): 1713–1727.
- [354] Xiao, H., Y. Chen, Y.-N. R. Li, and Z. Lu. 2015. “CSI feedback for massive MIMO system with dual-polarized antennas”. In: *Proc. IEEE PIMRC*. IEEE. 2324–2328.
- [355] Xiao, M., S. Mumtaz, Y. Huang, L. Dai, Y. Li, M. Matthaiou, G. K. Karagiannidis, E. Björnson, K. Yang, C.-L. I, and A. Ghosh. 2017. “Millimeter Wave Communications for Future Mobile Networks”. *IEEE J. Sel. Areas Commun.* 35(9): 1909–1935.
- [356] Xu, J., W. Xu, and F. Gong. 2017. “On Performance of Quantized Transceiver in Multiuser Massive MIMO Downlinks”. *IEEE Wireless Commun. Lett.*

- [357] Yang, H. and T. L. Marzetta. 2013a. “Performance of conjugate and zero-forcing beamforming in large-scale antenna systems”. *IEEE J. Sel. Areas Commun.* 31(2): 172–179.
- [358] Yang, H. and T. L. Marzetta. 2013b. “Total energy efficiency of cellular large scale antenna system multiple access mobile networks”. In: *Proc. IEEE Online GreenComm.* 27–32.
- [359] Yang, H. and T. L. Marzetta. 2014. “A macro cellular wireless network with uniformly high user throughputs”. In: *Proc. IEEE VTC-Fall.*
- [360] Yates, R. 1995. “A framework for uplink power control in cellular radio systems”. *IEEE J. Sel. Areas Commun.* 13(7): 1341–1347.
- [361] Ye, Q., O. Y. Bursalioglu, H. C. Papadopoulos, C. Caramanis, and J. G. Andrews. 2016. “User Association and Interference Management in Massive MIMO HetNets”. *IEEE Trans. Commun.* 64(5): 2049–2064.
- [362] Yin, H., L. Cottatellucci, D. Gesbert, R. R. Müller, and G. He. 2016. “Robust Pilot Decontamination Based on Joint Angle and Power Domain Discrimination”. *IEEE Trans. Signal Process.* 64(11): 2990–3003.
- [363] Yin, H., D. Gesbert, M. Filippou, and Y. Liu. 2013. “A coordinated approach to channel estimation in large-scale multiple-antenna systems”. *IEEE J. Sel. Areas Commun.* 31(2): 264–273.
- [364] Young, W. R. 1979. “Advanced mobile phone service: Introduction, background, and objectives”. *Bell System Technical Journal.* 58(1): 1–14.
- [365] Yu, K., M. Bengtsson, B. Ottersten, D. McNamara, P. Karlsson, and M. Beach. 2004. “Modeling of wide-band MIMO radio channels based on NLoS indoor measurements”. *IEEE Trans. Veh. Technol.* 53(3): 655–665.
- [366] Yu, W. 2006. “Uplink-downlink duality via minimax duality”. *IEEE Trans. Inf. Theory.* 52(2): 361–374.
- [367] Yu, W. and T. Lan. 2007. “Transmitter optimization for the multi-antenna downlink with per-antenna power constraints”. *IEEE Trans. Signal Process.* 55(6): 2646–2660.

- [368] Zakhour, R. and D. Gesbert. 2009. “Coordination on the MISO interference channel using the virtual SINR framework”. In: *Proc. ITG Workshop on Smart Antennas (WSA)*.
- [369] Zander, J. 1992. “Performance of optimum transmitter power control in cellular radio systems”. *IEEE Trans. Veh. Technol.* 41(1): 57–62.
- [370] Zander, J. and M. Frodigh. 1994. “Comment on “Performance of optimum transmitter power control in cellular radio systems””. *IEEE Trans. Veh. Technol.* 43(3): 636.
- [371] Zappone, A. and E. Jorswieck. 2015. “Energy Efficiency in Wireless Networks via Fractional Programming Theory”. *Foundations and Trends in Communications and Information Theory*. 11(3-4): 185–396.
- [372] Zarei, S., W. Gerstacker, R. R. Müller, and R. Schober. 2013. “Low-complexity linear precoding for downlink large-scale MIMO systems”. In: *Proc. IEEE PIMRC*.
- [373] Zetterberg, P. and B. Ottersten. 1995. “The spectrum efficiency of a base station antenna array system for spatially selective transmission”. *IEEE Trans. Veh. Technol.* 44(3): 651–660.
- [374] Zetterberg, P. 2011. “Experimental investigation of TDD reciprocity-based zero-forcing transmit precoding”. *EURASIP J. Adv. Signal Process.* (137541).
- [375] Zhang, H., N. Mehta, A. Molisch, J. Zhang, and H. Dai. 2008. “Asynchronous interference mitigation in cooperative base station systems”. *IEEE Trans. Wireless Commun.* 7(1): 155–165.
- [376] Zhang, J., Y. Wei, E. Björnson, Y. Han, and X. Li. 2017. “Spectral and Energy Efficiency of Cell-Free Massive MIMO Systems with Hardware Impairments”. In: *Proc. WCSP*.
- [377] Zhang, W. 2012. “A general framework for transmission with transceiver distortion and some applications”. *IEEE Trans. Commun.* 60(2): 384–399.
- [378] Zhu, X., Z. Wang, L. Dai, and C. Qian. 2015. “Smart pilot assignment for Massive MIMO”. *IEEE Commun. Lett.* 19(9): 1644–1647.